US Army Corps of Engineers
Waterways Experiment Station

AD-A285 367

Technical Report ITL-94-4
September 1994

Computer-Aided Structural Engineering (CASE) Project

Dynamics of Intake Towers and Other MDOF Structures Under Earthquake Loads: A Computer-Aided Approach

by Samuel E. French, University of Tennessee at Martin
Robert M. Ebeling, WES
Ralph Strom, North Pacific Division

Prepared for Headquarters, U.S. Army Corps of Engineers

This is the second report in a series of Computer-Aided Structural Engineering (CASE) Project reports on structural dynamics. The previous reports in this series are:

Ebeling, R. M. (1992). "Introduction to the Computation of Response Spectrum for Earthquake Loading," Technical Report ITL-92-4, U.S. Army Engineer Waterways Experiment Station, Vicksburg, MS.

Computer-Aided Structural Engineering (CASE) Project

Technical Report ITL-94-4
September 1994

Dynamics of Intake Towers and Other MDOF Structures Under Earthquake Loads: A Computer-Aided Approach

by Samuel E. French

University of Tennessee at Martin
Martin, TN 38237

Robert M. Ebeling

U.S. Army Corps of Engineers
Waterways Experiment Station
3909 Halls Ferry Road
Vicksburg, MS 39180-6199

Ralph Strom

U.S. Army Engineer Division, North Pacific
Portland, OR 97208-2870

Final report

Approved for public release; distribution is unlimited

Prepared for U.S. Army Corps of Engineers
Washington, DC 20314-1000

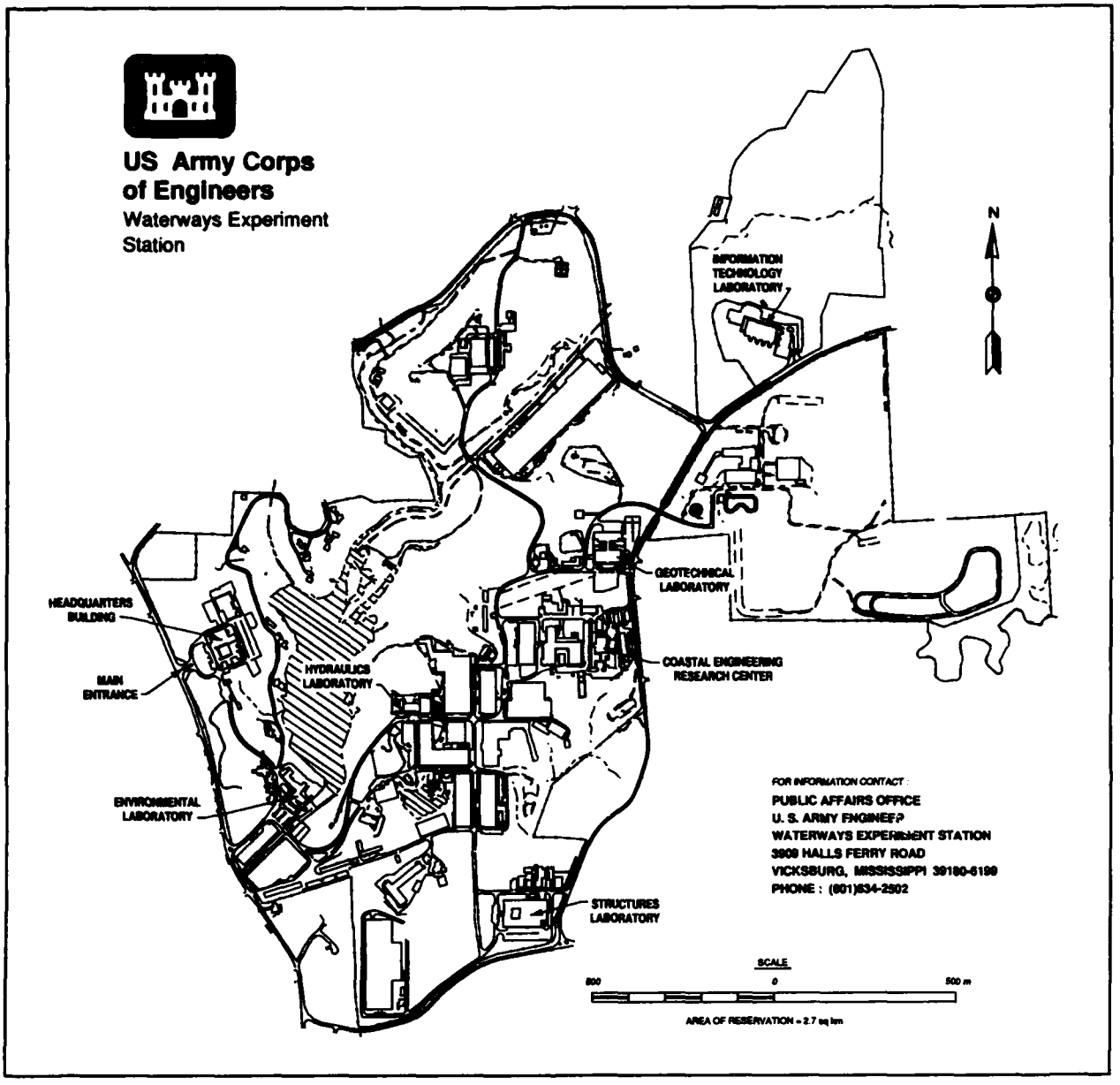

Waterways Experiment Station Cataloging-In-Publication Data

French, Samuel E., 1930-
Dynamics of intake towers and other MDOF structures under earthquake loads : A computer-aided approach / by Samuel E. French, Robert M. Ebeling, Ralph Strom ; prepared for U.S. Army Corps of Engineers.
95 p. : ill. ; 28 cm. — (Technical report ; ITL-94-4)
Includes bibliographic references.
1. Intakes (Hydraulic engineering) 2. Earthquake resistant design. 3. Structural dynamics — Data processing. 4. Hydraulic structures — Vibration. I. Ebeling, Robert M., 1954- II. Strom, Ralph. III. United States. Army. Corps of Engineers. IV. U.S. Army Engineer Waterways Experiment Station. V. Information Technology Laboratory (U.S. Army Corps of Engineers, Waterways Experiment Station) VI. Computer-aided Structural Engineering Project. VII. Title. VIII. Series: Technical report (U.S. Army Engineer Waterways Experiment Station) ; ITL-94-4.
TA7 W34 no.ITL-94-4

Contents

Preface

This report is a primer on the subject of structural dynamics, oriented toward the analysis of the intake structures that fall under the authority of the U.S. Army Corps of Engineers. It is a part of the work sponsored by the Computer-Aided Structural Engineering Program sponsored by the Directorate, Headquarters, U.S. Army Corps of Engineers (HQUSACE) under the Structural Engineering Research Program. Funds for publication of the report were provided from those available for the Computer-Aided Structural Engineering (CASE) project managed by the Information Technology Laboratory (ITL) at the U.S. Army Corps of Engineers Waterways Experiment Station (WES) at Vicksburg, MS. H. Wayne Jones is the CASE project manager. Technical monitor for the project is Mr. Lucien Guthrie, HQUSACE.

The work was performed at WES under the direction of Dr. Robert M. Ebeling, Interdisciplinary Research Group, Computer-Aided Engineering Division (CAED), ITL. The report was prepared by Professor Samuel E. French of the University of Tennessee at Martin, Dr. Ebeling, and Mr. Ralph Strom, North Pacific Division, U.S. Army Corps of Engineers. This report is part of a general development of design manuals intended for use primarily by district personnel whose background does not include advanced dynamics. The work was accomplished under the general direction of Dr. Reed L. Mosher, Acting Chief, CAED, and the general supervision of Dr. N. Radhakrishnan, Director, ITL.

At the time of publication of this report, Director of WES was Dr. Robert W. Whalin. Commander was COL Bruce K. Howard, EN.

Conversion Factors, Non-SI to SI Units of Measurement

Non-SI units of measurement used in this report can be converted to SI (*Systeme Internationale*) units by applying the following factors:

Multiply	By	To Obtain
angular degrees	0.01745329	radians
cycles per second	1.000	Hertz
cycles per second	6.28318531	radians per second
feet	0.3048	meters
feet per second per second	30.4838	centimeters per second per second
gravitational acceleration	980.665	centimeters per second per second
gravitational acceleration	32.174	feet per second per second
gravitational acceleration	386.086	inches per second per second
inches	2.54	centimeters
pounds	4.4822	Newtons
tons	8.896	kilonewtons

1 Single-Degree-of-Freedom Systems

Introduction

This report presents the fundamental concepts of the dynamics of intake towers. The theory is quite general, however, and will apply to multiple-degree-of-freedom (MDOF) systems other than intake towers. The ultimate purpose is to present the computer-aided analysis of distributed-mass towers such as the step-tapered tower shown in Figure 1i. The development of the theory therefore becomes slanted toward distributed-mass towers as it progresses. In this chapter of the report systems having a single degree of freedom (SDOF systems) are discussed. The single lumped-mass systems depicted in Figure 1 are typical examples of such SDOF systems.

The primary source of dynamic excitation of structures is earthquake motion. A brief summary of earthquake loading as it is characterized in terms of response spectra is presented in Chapter 2 of this report. Distributed-mass systems such as towers are presented in Chapter 3 as an application of the Rayleigh method. While the distributed-mass systems of Chapter 3 are recognized as MDOF systems, the Rayleigh method allows them to be examined one degree of freedom at a time. Multistory lumped-mass systems are presented in Chapter 4. Such systems are MDOF systems that can also be examined one degree of freedom at a time.

The lumped-mass systems (but not the distributed-mass systems) shown in Figure 1 can oscillate in only one way, that is, the motion of the single mass can be only a back-and-forth motion across its initial at-rest position. Figure 2 is a sketch of such an oscillating system. The position of the mass at any point in time in the system is entirely predictable.

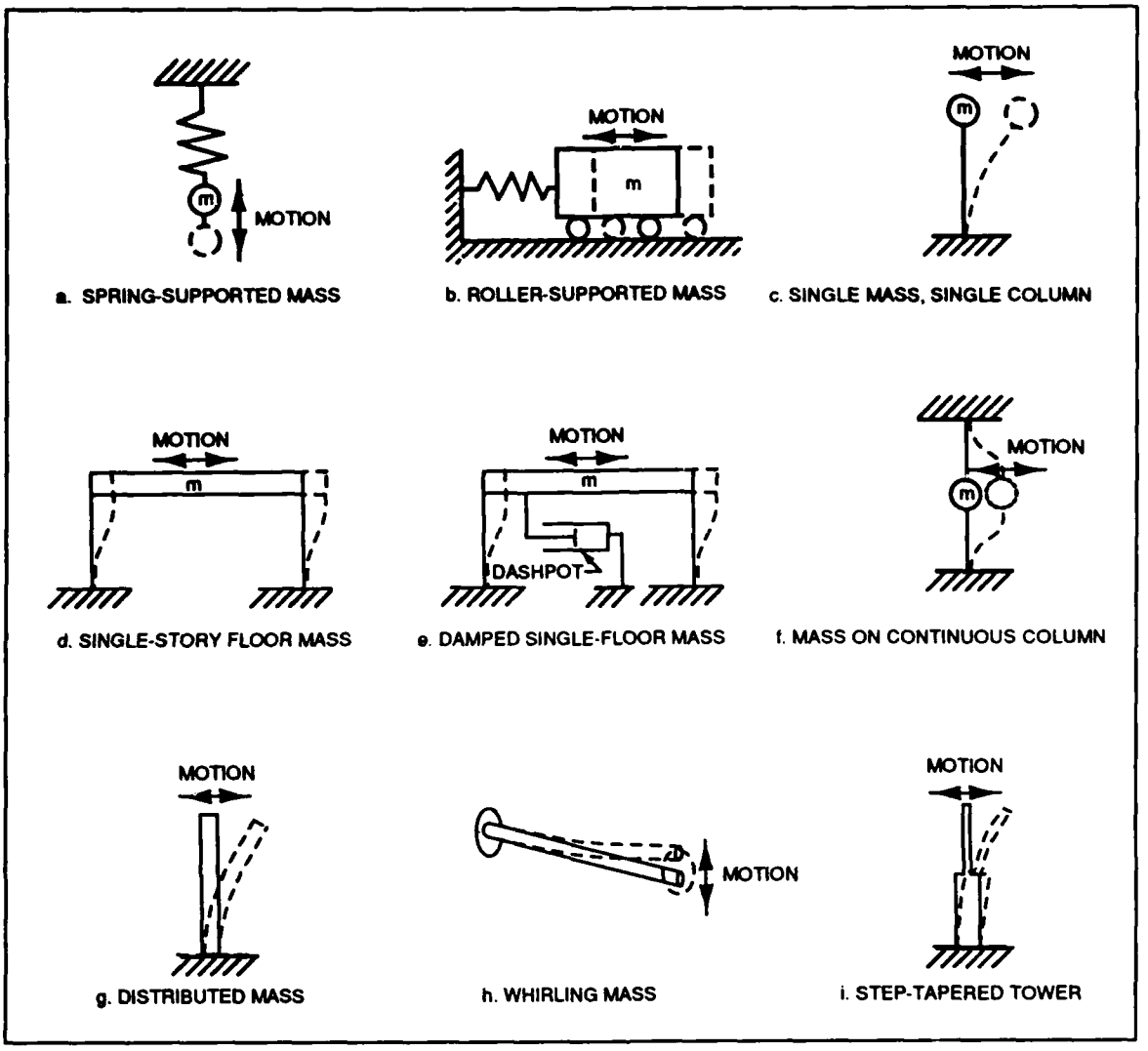

Figure 1. Common types of oscillating systems

Figure 1 shows several common types of single- and distributed-mass oscillating systems. If any one of these systems is given an initial displacement of *amplitude* u_0[1] and then released, it will oscillate at its *natural frequency*, continuing to oscillate with ever-decreasing amplitude (and ever-decreasing energy) until it finally returns to its at-rest state.

The causes of the decrease in amplitude might be such things as hysteresis losses, inelastic behavior, or any one of many other sources of energy dissipation. The cause could also include man-made shock absorbers deliberately placed to reduce oscillations. Taken together, these losses in

---

[1] For convenience, symbols and abbreviations are listed in the notation (Appendix B).

energy are called *damping effects*; without damping, the mass could theoretically oscillate forever with no loss in amplitude. Shown schematically, damping effects are usually lumped together and shown as a viscous shock absorber called a *dashpot*, such as that shown in Figure 1e.

Figure 3 shows the displacement of an oscillating mass both with and without damping. The damping will affect only the force resulting from the *velocity* of the mass in motion. Damping effects are greatest when the mass is at its highest velocity. As velocities decrease, the damping also decreases, resulting in an asymptotic decrease in amplitude as shown.

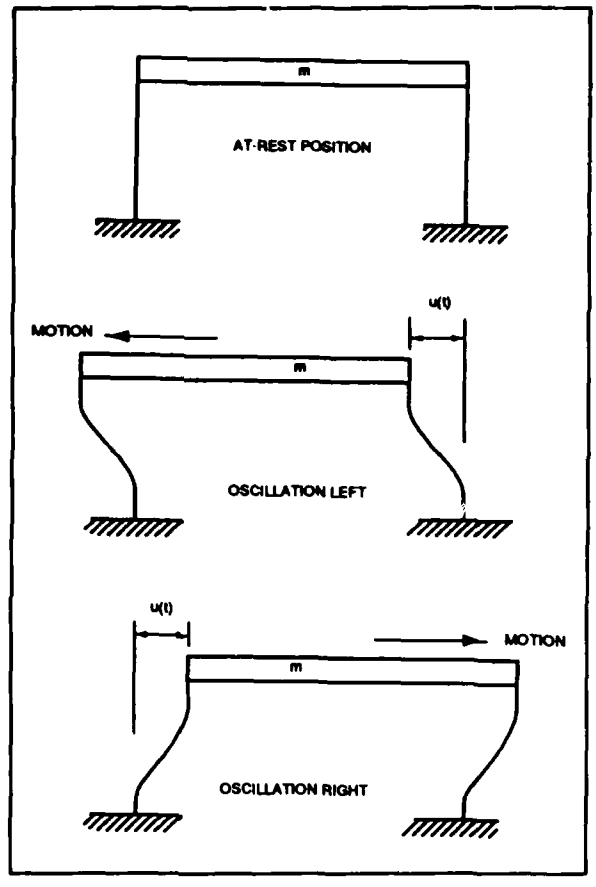

Figure 2. Oscillations of a lumped-mass system

Figure 3 also indicates the *period* of oscillation, T. The period is the time in seconds for the mass to complete one full oscillation, or cycle. The *frequency* of oscillation f is another commonly used property; the frequency is the number of cycles completed in one second (Hz). Mathematically, frequency is the reciprocal of the period T. The rotational speed ω is another commonly used property and is the *angular velocity* in radians per second where there are 2π radians in one complete cycle.

$$f \text{ in cycles/second} = \frac{1}{T \text{ seconds}} \tag{1}$$

$$\omega \text{ in radians/second} = \frac{2\pi \text{ radians/cycle}}{T \text{ seconds}} \tag{2}$$

Figure 3 shows that the period of oscillation T for this structure is essentially the same for both damped and undamped oscillations. At very high levels of damping, there will in fact be a slight elongation in the period T ($T_{DAMPED} > T_{UNDAMPED}$), but for ordinary structures working at elastic levels of stress, the level of damping is so low that any such

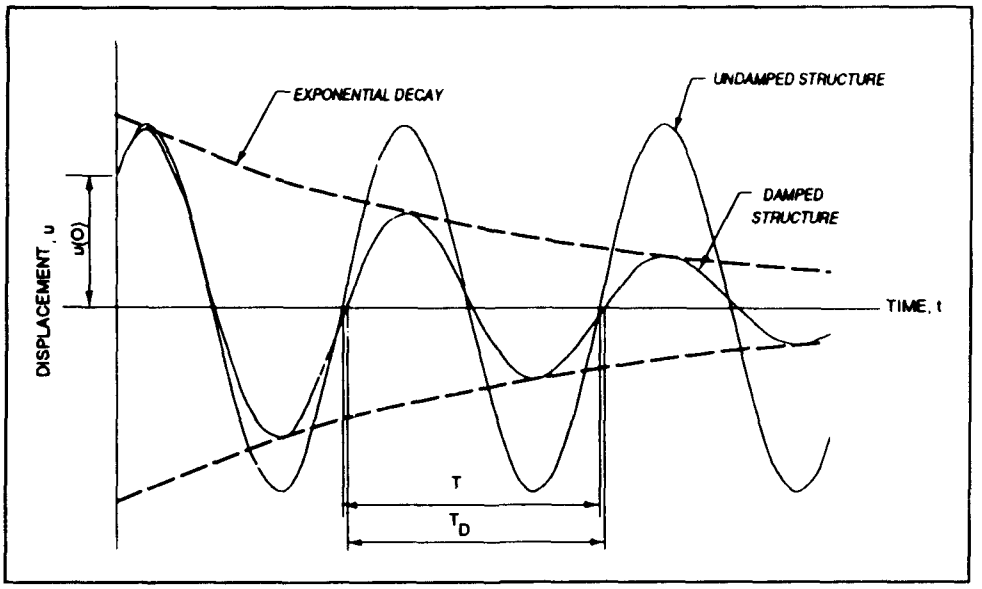

Figure 3. Damped oscillations

difference can be safely ignored. The dominant effect of damping is to reduce the velocity of oscillation, thereby producing the asymptotic reduction in amplitude shown in Figure 3.

The angular velocity ω does not always appear physically in an oscillating system, but the symbol ω usually does. Figure 4, in which an imaginary wheel is added to a laterally oscillating system, shows a means to visualize a rotational velocity when none actually exists. The rotational velocity of the imaginary wheel is ω.

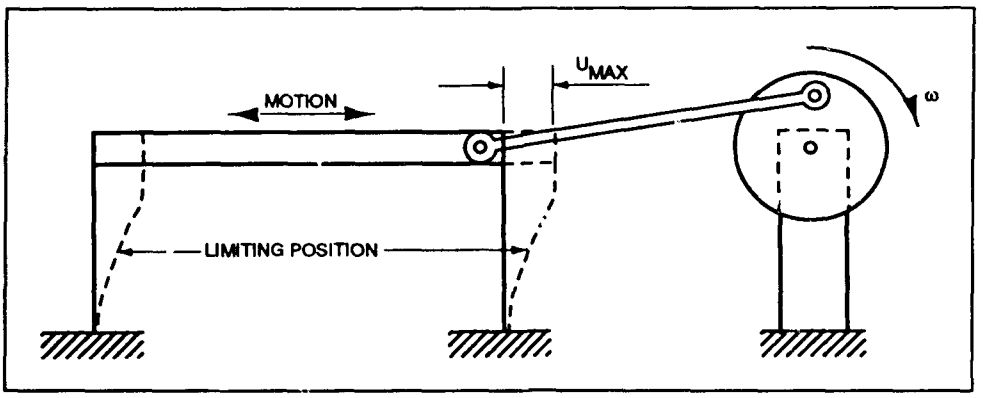

Figure 4. Rotational velocity for a linear oscillation

Equation of Motion

The equation of motion for lumped-mass systems having a single degree of freedom (termed SDOF systems) is derived from Newton's second law, force = mass times acceleration. Consider the system shown in Figure 5 in which the oscillating mass has been removed as a free body at some instant in time t. An externally applied dynamic force p(t) is acting on the system. The force p(t) varies with time and is called a *forcing function*.

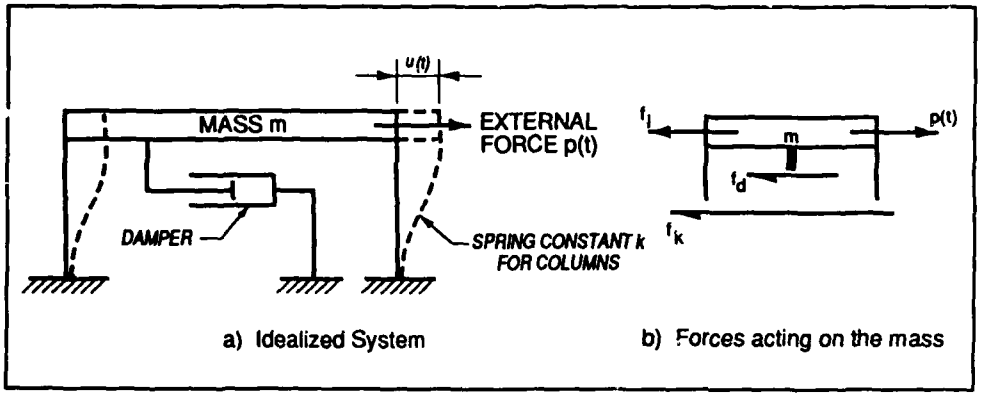

Figure 5. Common SDOF oscillating system

The free body shown in Figure 5 is subject to four forces, each one varying with time.

a. The inertial force ($f_i = m\ddot{u}$) is given by D'Alembert's principle to be a force acting through the center of mass, opposite in direction to the imposed motion.

b. The restoring force ($f_k = ku$) is the stiffness k (in pounds of force per unit of displacement) times the displacement u.

c. The damping force ($f_d = c\dot{u}$) is the damping constant c (in pounds of force per unit of velocity) times the velocity $\dot{u}$ at any time t.

d. The fourth force is that of the forcing function [p(t)], which may or may not exist at any given time.

The sum of forces yields the equation of basic force equilibrium:

$$-f_i - f_k - f_d + p(t) = 0 \qquad (3)$$

All of these forces may be expressed in terms of the displacement u, where, as noted earlier:

$$f_i = m\ddot{u} \tag{4a}$$

$$f_d = c\dot{u} \tag{4b}$$

$$f_k = ku \tag{4c}$$

Substituting Equations 4a, b, and c into Equation 3 yields the basic equation of motion for an SDOF system subjected to an externally applied forcing function:

$$m\ddot{u} + c\dot{u} + ku = p(t) \tag{5}$$

This same equation applies equally to all of the SDOF systems shown in Figure 1. For the rotational oscillations of Figure 1h, rotational displacement ω would have to be substituted for lateral displacement u.

In all of the lumped-mass systems of Figure 1, the mass of the system is understood to be rigid. Consider, for example, the idealized one-story, single-bay building frame of Figure 1d. Under the indicated displacement, it is assumed that the rigid mass does not undergo any bending; only the columns will experience bending. Therefore, all of the restoring force f_k in this system must come from bending in the columns.

The equation of motion (Equation 5) for the systems of Figure 1 includes a forcing function p(t) applied to the mass m. An earthquake, however, does not produce such a tangible force acting on the system. Rather, an earthquake will produce displacements of the foundations of the structure. It is these displacements, rather than tangible forces, which the earthquake imposes on the system.

The results of such earthquake-induced displacements are shown in the free body of Figure 6. The earthquake ground motions are shown as $u_g(t)$, which are random motions in time. The total displacement of the mass relative to its at-rest position, $u_t(t)$, is shown in Figure 6a. The displacement u again represents the displacement of the structural mass relative to the base of the structure at any time t. The geometry of Figure 6a shows that the total displacement $u_t(t)$ is given by

$$u_t(t) = u_g(t) + u(t) \tag{6}$$

Figure 6b shows the forces associated with the free body of Figure 6a. In this case, however, the inertial force f_i created by the total acceleration $\ddot{u}_t(t)$ becomes:

$$f_i = m\ddot{u}_t(t) = m\ddot{u}_g(t) + m\ddot{u} \tag{7}$$

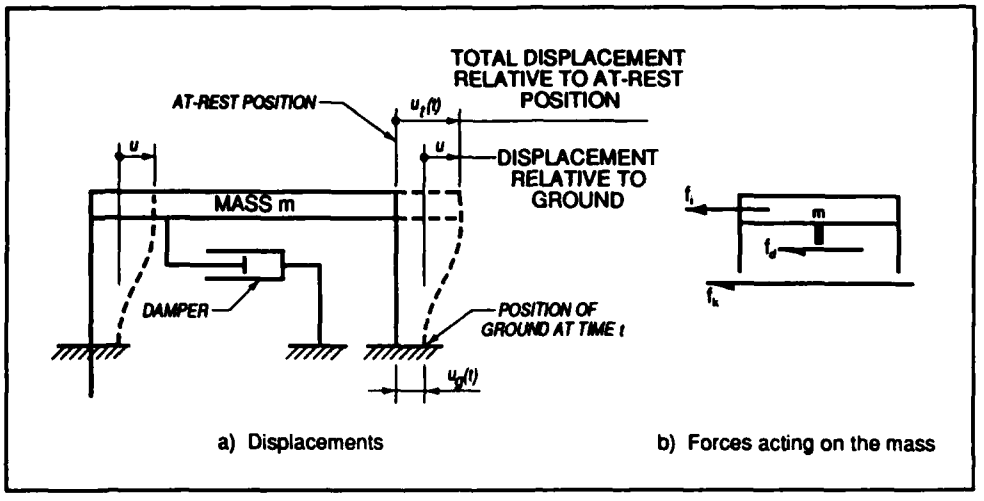

Figure 6. Relative displacements of SDOF systems

Forces are summed as before, yielding the equation of force equilibrium:

$$f_i + f_d + f_k = 0 \tag{8}$$

where

$$f_d = c\dot{u}$$

$$f_k = ku$$

These values of displacements are substituted into Equation 8, yielding:

$$m\ddot{u}_g(t) + m\ddot{u} + c\dot{u} + ku = 0 \tag{9}$$

Rearranging terms produces the final form of the equation of motion for a structure subjected to earthquake displacements at its base:

$$m\ddot{u} + c\dot{u} + ku = -m\ddot{u}_g(t) \tag{10}$$

Equation 10 is essentially the same as Equation 5, with the forcing function being the effective force $-m\ddot{u}_g(t)$. The amount of force exerted on a structure is therefore a function of the mass of the structure itself. Lightweight steel or timber structures will experience much less force from earthquake motions than will heavier concrete or masonry structures.

Equation 10 is the general equation of motion for a single-mass structure subjected to a dynamic forcing function such as an earthquake. A typical example of such a structure is shown schematically in Figure 7. Figure 7 shows that under the actual excitation, the earth is moving relative

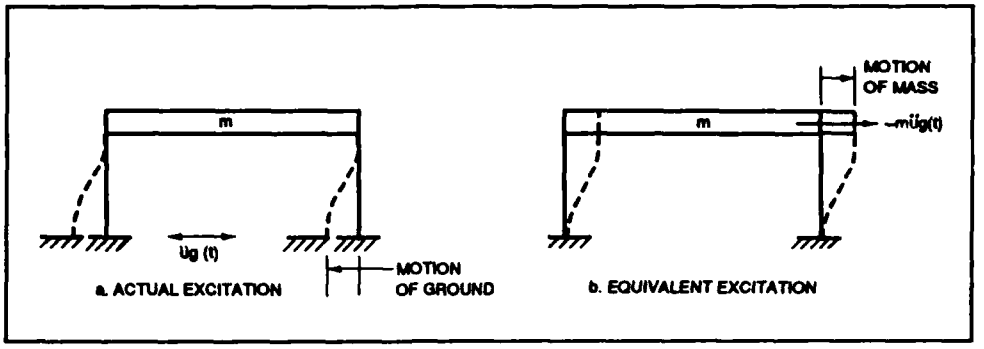

Figure 7. SDOF system under earthquake forcing function

to the mass whereas under the equivalent excitation, the mass is moving relative to the earth.

The major part of this report is devoted to the solution of Equation 10. As with any differential equation, the solution of Equation 10 consists of two parts:

a. The general solution of the homogeneous equation, that is, a solution with the forcing function $\ddot{u}_g(t) = 0$ and the structure undergoing unforced (free) oscillations.

b. A particular solution of the general equation, that is, a solution with the forcing function in place and the structure being forced to undergo the same displacements as the forcing function, but with a time lag.

The solution for the unforced free oscillations will be developed first.

Undamped Free Oscillations

The equation of motion given by the homogeneous portion of Equation 10 will be solved first without any damping. Damping will then be added, and the final form of the solution will be developed.

At some instant $t = t_O$, an SDOF system is assumed to have a known displacement u_0 and a known velocity $\dot{u}_0$. Thereafter, the system is allowed to oscillate freely without any further forcing function being applied. The equation of motion for the undamped free oscillations is then given by:

$$m\ddot{u} + ku = 0 \tag{11a}$$

or,

$$\ddot{u} + (k/m)u = 0 \tag{11b}$$

The solution of this ordinary differential equation is:

$$u = A \sin(\omega t) + B \cos(\omega t) \tag{12}$$

where ω is the constant circular frequency of the solution in radians per second and A and B are the constants of integration.

The circular frequency ω is found from the solution as:

$$\omega = \sqrt{k/m} \tag{13}$$

The natural period of oscillation T can now be determined, even before the constants of integration have been evaluated:

$$T = 2\pi \sqrt{m/k} \tag{14}$$

Equation 14 shows that the natural period of oscillation of an undamped SDOF system is dependent only on the mass of the system and the stiffness of the system. No boundary conditions or any other factors affect the undamped natural period T.

The constants of integration A and B can be found as usual by evaluating the boundary conditions:

At time $t = 0$, $u = u_0 = A \sin[\omega(0)] + B \cos[\omega(0)]$

$$u_0 = B \tag{15}$$

The velocity $\dot{u}$ at any time t is given by:

$$\dot{u} = A\omega \cos(\omega t) - B\omega \sin(\omega t)$$

At time $t = 0$, $\dot{u} = \dot{u}_0 = A\omega$

$$\dot{u}_0/\omega = A \tag{16}$$

The final solution is then given by:

$$u = u_0 \cos(\omega t) + (\dot{u}_0/\omega) \sin(\omega t) \tag{17}$$

The maximum amplitude given by Equation 17 will occur when the derivative of the amplitude (the velocity) is zero:

$$\dot{u} = 0 = -u_0\omega \sin(\omega t) + (\dot{u}_0/\omega)\, \omega \cos(\omega t)$$

or,

$$0 = -\dot{u}_0 \sin(\omega t) + (\dot{u}_0/\omega) \cos(\omega t) \tag{18}$$

Equation 18 is squared:

$$0 = u_0^2 \sin^2(\omega t) - (2u_0\dot{u}_0/\omega)\sin(\omega t)\cos(\omega t) + (\dot{u}_0/\omega)^2 \cos^2(\omega t) \tag{19}$$

Equation 17 is squared:

$$u^2 = u_0^2 \cos^2(\omega t) + (2u_0\dot{u}_0/\omega)\sin(\omega t)\cos(\omega t) + (\dot{u}_0/\omega)^2 \sin^2(\omega t) \tag{20}$$

Equations 19 and 20 are summed to yield the maximum amplitude u_{max} that can be produced by the motions of Equation 17.

$$u_{max} = \sqrt{u_0^2 + \dot{u}_0^2/\omega^2} \tag{21}$$

The motion described by Equation 17 for an undamped, unforced SDOF system is summarized schematically in Figure 8.

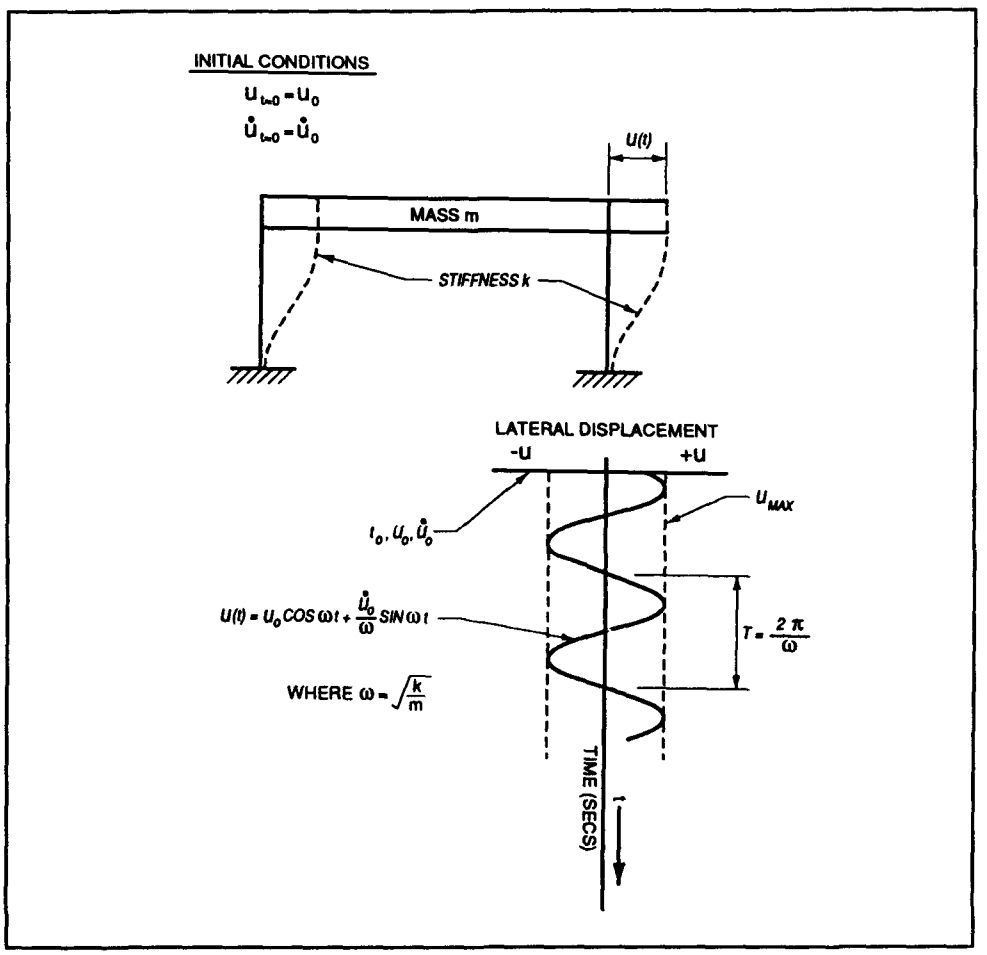

Figure 8. Undamped, unforced oscillations

Damped Free Oscillations

The foregoing solution for free oscillations did not include damping. When damping is included (still without a forcing function), the homogeneous part of Equation 10 becomes:

$$m\ddot{u} + c\dot{u} + ku = 0 \tag{22}$$

The equation is divided by m to put it in standard form:

$$\ddot{u} + 2\beta\omega\dot{u} + \omega^2 u = 0 \tag{23a}$$

where the constant

$$\beta = c/2m\omega \tag{23b}$$

For $\beta < 1$, the solution of Equation 23a is:

$$u = e^{-\beta\omega t}\left(u_0 \cos \omega_D t + \frac{\dot{u} + \beta\omega u_0}{\omega_D} \sin \omega_D t\right) \tag{24}$$

The motion described by Equation 24 for $\beta < 1$ is summarized in Figure 9. It is a periodic function having an exponentially decaying amplitude and a damped circular frequency ω_D:

$$\omega_D = \omega\sqrt{1 - \beta^2} = \sqrt{k(1 - \beta^2)/m} \tag{25}$$

where ω is, as usual, the circular frequency of the undamped system.

The damped period for the motion of Equation 24 is found from Equation 25:

$$T_D = T/\sqrt{1 - \beta^2} \tag{26}$$

where T is, as previously defined, the natural period of oscillation of the undamped system.

If the factor β in Equation 26 could be made equal to 1, the natural period of the damped system would become infinite. Such a system would simply return to its original at-rest position following a displacement, i.e., there would be no oscillations. For the case in which $\beta = 1$, the damping coefficient c as given by Equation 23 is its value of *critical damping*:

$$c = c_{critical} = 2m\omega \tag{27}$$

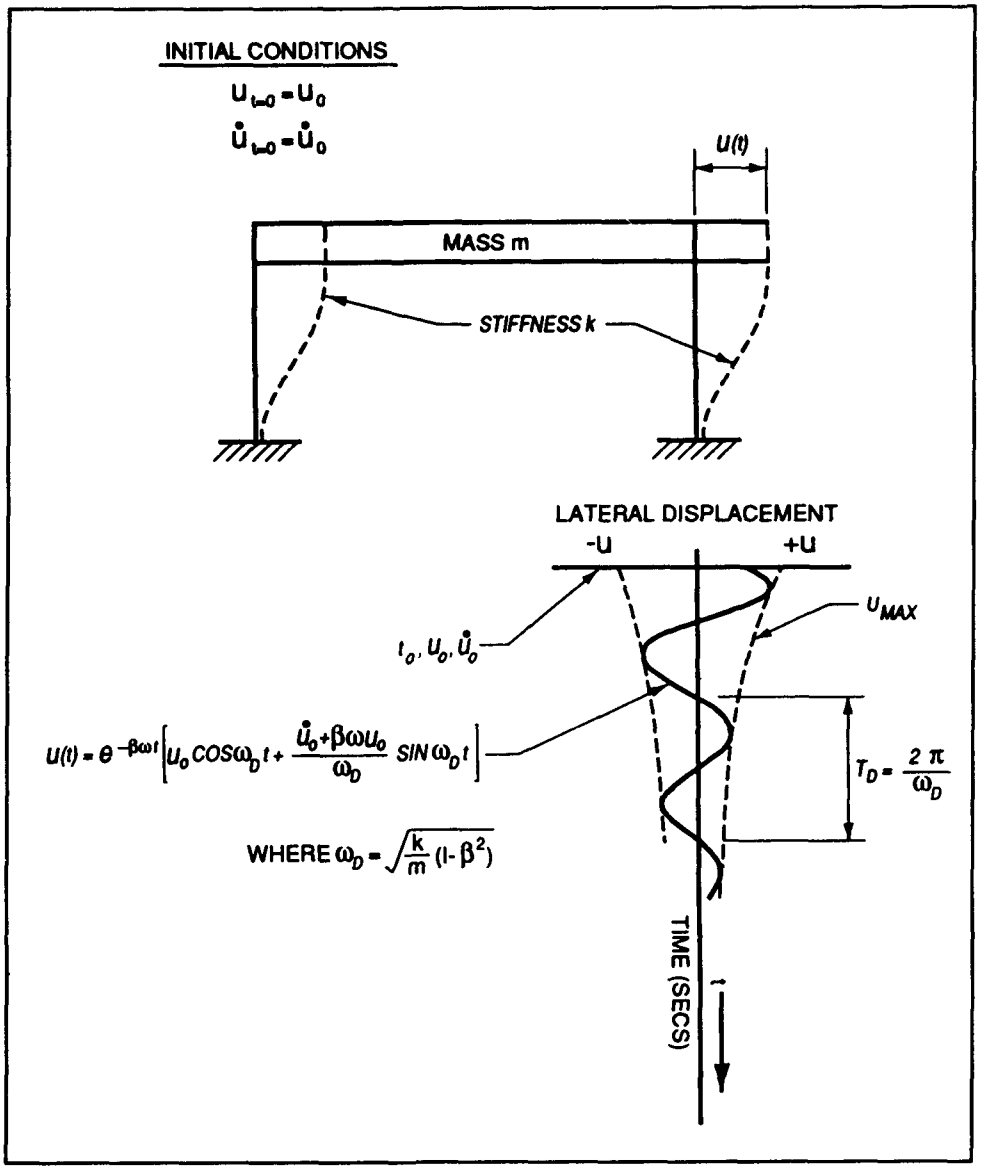

Figure 9. Damped, unforced oscillations

Further examination of Equation 23a reveals that the factor β may be regarded as the fraction of critical damping in a system, i.e.:

$$\beta = c/2m\omega = c/c_{critical} \tag{28}$$

For typical structures working in their elastic ranges, the factor β has been found to be less than 0.1, or, stated another way, the maximum amount of damping in a typical structure will normally be less than 10 percent of its critical damping. Substitution of this maximum value of $\beta = 0.1$ into Equation 26 indicates that for typical structures, the effects of damping on the period of oscillation are indeed negligible and can be ignored, i.e.:

$$T = T_D \tag{29}$$

Forced Oscillations with a Dynamic Forcing Function

As stated earlier, the intended solution of Equation 10 would consist of the general solution of the homogeneous equation, both with and without damping, plus a particular solution of the general equation, both with and without damping. Equations 17 and 24 satisfy the first part of this solution. They are the required general solutions of the homogeneous equation. It remains now to find a particular solution of Equation 10, both with and without damping, when the system is subjected to a dynamic forcing function.

When a forcing function is included, Equation 10 takes its most general form:

$$m\ddot{u} + c\dot{u} + ku = -m\ddot{u}_g(t) \tag{10}$$

The forcing function $m\ddot{u}_g(t)$ is the mass of the structure times the ground acceleration; physically, the result is a force. The nature of this force has yet to be defined.

Two cases of dynamic forcing functions will be considered for examination, one being a harmonic variation and the other being the random variation produced by an earthquake. The first case considers a forcing function that has a harmonic variation similar to that of the natural oscillations of the structure. The forcing function, however, is assumed to have some frequency which is not necessarily the same as the natural frequency of the structure:

$$-m\ddot{u} = p_0 \sin \bar{\omega}t \tag{30}$$

where p_0 is the maximum magnitude of the forcing function.

When a harmonic forcing function such as that of Equation 30 is applied to a damped SDOF structure, the response of the structure will consist of two parts, as noted earlier. The first part, the free oscillation part, is that given by Equation 24. This free oscillation soon decays, however, leaving only the second part. The second part is the continuous steady-state response that is being imposed on the system by the forcing function. This steady-state response is the particular solution of Equation 10. The forcing function is physically forcing the SDOF system to follow the motions of the forcing function.

However, the forcing function is not acting on the oscillating mass. The forcing function acts at the base of the columns as shown earlier in Figure 7. The motion of the mass is being created by a back-and-forth ground motion at the base of the columns. At any time t, the force imparted to the columns is that given by Equation 30.

The displacements of the mass will follow the same harmonic displacements as the ground motion. There will be a lag in time, however, between the motion of the ground and the motion of the mass. The lag occurs as the columns develop enough lateral force to produce (or to change) the motion in the mass. It is well to note also that the amplitude of motion of the mass need not be equal to the amplitude of motion of the ground. Such a difference is indicated in Figure 10.

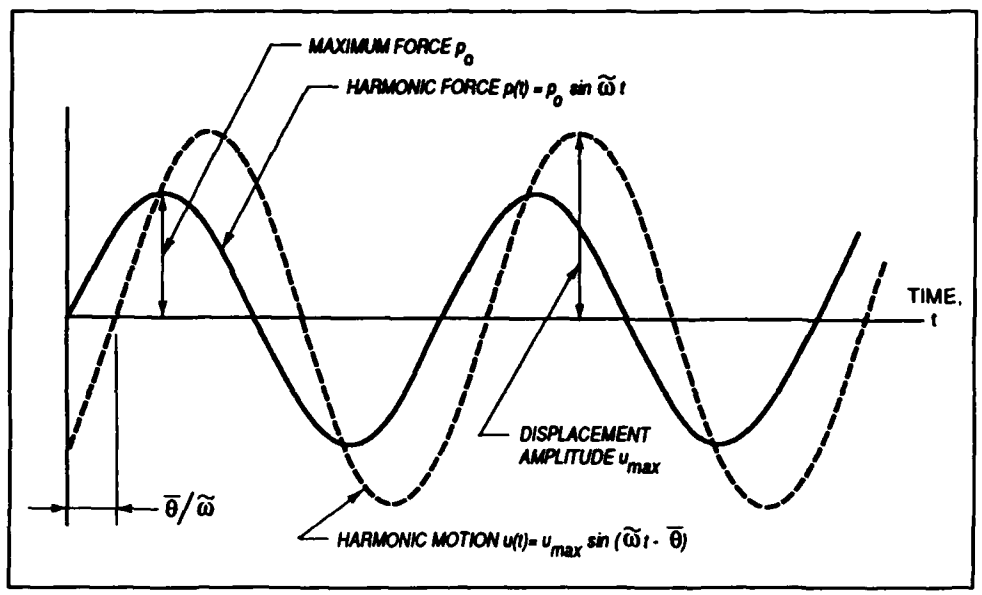

Figure 10. Steady-state response due to harmonic ground motion

The displacement u of the oscillating mass at any time t is:

$$u = u_{max} \sin(\bar{\omega}t - \bar{\theta}) \tag{31}$$

where $\bar{\theta}$ is the lagging phase angle between the motion of the ground and the motion of the mass.

The solution for the response of the system to various excitation frequencies $\bar{\omega}$ is mathematically quite complex, far beyond the scope of an elementary treatment such as this (see Paz, Structural Dynamics 1991). The end result of the solution, however, is relatively simple. The displacement u at any time t is given by the solution as:

$$u = u_{max} \sin(\bar{\omega}t - \bar{\theta}) \tag{32a}$$

where

$$\frac{u_{max}}{u_{st}} = \frac{1}{\sqrt{[1 - (\tilde{\omega}/\omega)^2]^2 + [2\beta(\tilde{\omega}/\omega)]^2}} \tag{32b}$$

and the lagging phase angle $\bar{\theta}$ is given by

$$\bar{\theta} = \tan^{-1} \frac{2\beta(\tilde{\omega}/\omega)}{1 - (\tilde{\omega}/\omega)^2} \tag{32c}$$

In Equations 32a and 32b, the displacement u_{st} is the displacement that the maximum force p_0 would produce if the force were to be applied as a static force (i.e., $u_{st} = p_0/k$). All other symbols in Equations 32a, b, and c were introduced and defined earlier.

Equation 32b reveals that there are two primary variables. The first variable is u_{max}/u_{st}, which indicates the relative level of magnification of displacement at various forcing frequencies $\tilde{\omega}$. The second variable is $\tilde{\omega}/\omega$, which is the ratio of the forcing frequency $\tilde{\omega}$ to the natural frequency ω. (The third variable β, the ratio of critical damping, can be assigned whatever value the physical conditions warrant.)

Figure 11 presents a graph of Equation 32b for various levels of damping. The most significant feature of the graph is, of course, the sharp increase in displacement as the frequency of the forcing function approaches the natural frequency of the system. A second significant feature of the graph is the effect of the damping. A large amount of damping is required if a pronounced reduction in the peaking effect is required.

Figure 11 reveals the phenomenon of *resonance*. The peak value of displacement given by Equation 32b occurs when the forcing frequency $\tilde{\omega}$ is:

$$\tilde{\omega}_{peak} = \omega\sqrt{1 - 2\beta^2} \tag{33}$$

In comparison, the damped natural frequency ω is:

$$\omega_D = \omega\sqrt{1 - \beta^2} \tag{34}$$

The resonant frequency is therefore not exactly equal to the damped natural frequency of the system, but for low values of damping, the difference is quite small. In general, this small difference is ignored, and the resonant frequency is taken to be essentially equal to the natural frequency.

Insofar as the structural design is concerned, it is considered prudent to keep the natural frequency of a structure as far away as possible from the frequency $\tilde{\omega}$ of any known dynamic loading. Since the natural frequency of the structure is a function only of stiffness and mass:

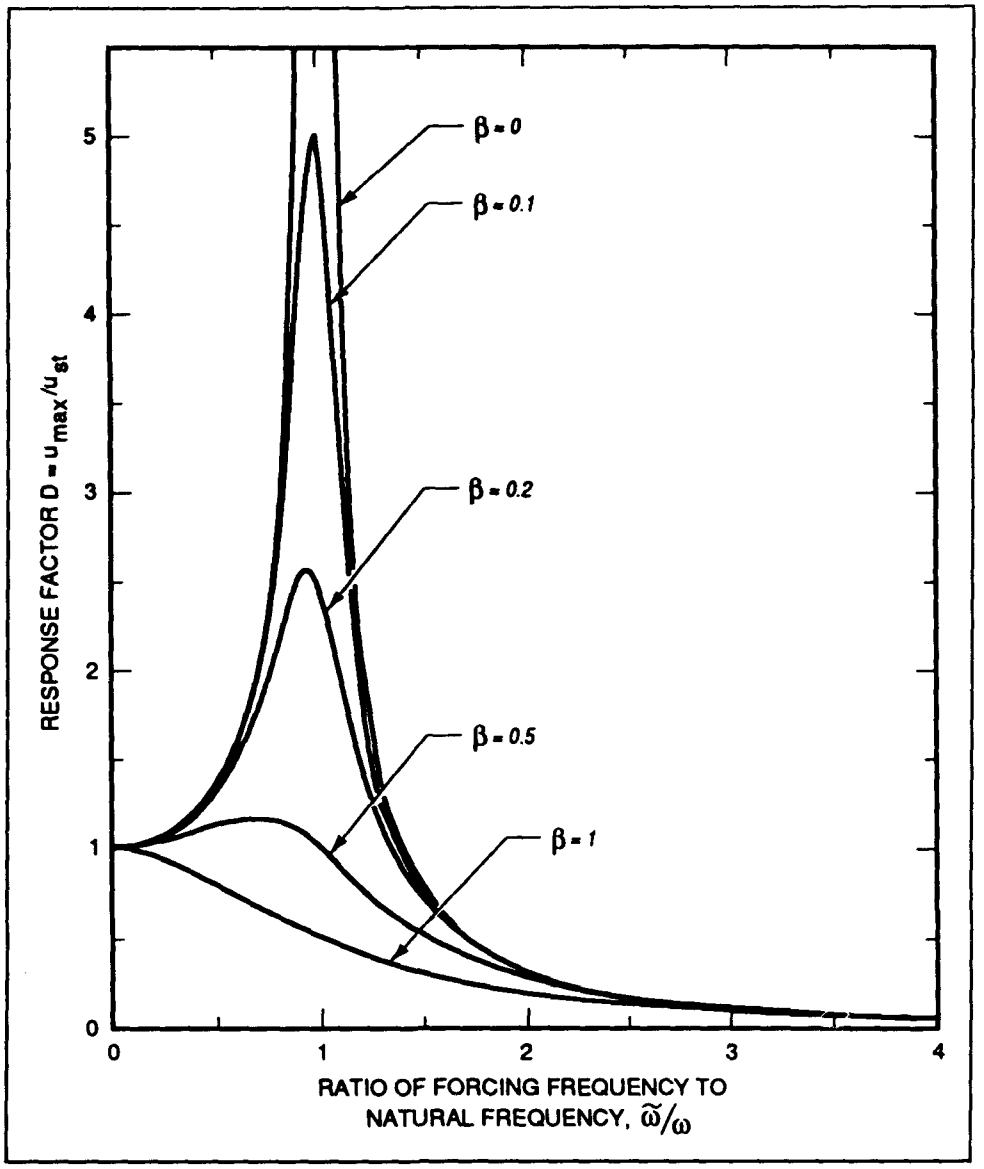

Figure 11. SDOF system with a harmonic forcing function

$$\omega = \sqrt{k/m} \tag{13}$$

a designer might deliberately alter the structural stiffness or the structural mass in order to change the natural frequency and decrease any chance of accidental resonance.

In the case of earthquakes, however, the motion is irregular, i.e., there is no single value for $\tilde{\omega}$. Therefore, the structural design should include some reasonable amplification of load over a broad range of forcing frequencies. This point is discussed further in Chapter 2.

Forced Oscillations Under Earthquake Ground Motions

For the general case of loading in which the forcing function is that of random earthquake motions, the equation of motion, Equation 10, remains in its most general form:

$$m\ddot{u} + c\dot{u} + ku = -m\ddot{u}_g(t) \tag{10}$$

In its standard integrable form, Equation 10 becomes:

$$\ddot{u} + 2\beta\omega\dot{u} + \omega^2 u = -\ddot{u}_g(t) \tag{35}$$

The problem of a damped SDOF system shaken by a time-varying ground acceleration is equivalent to the problem of a damped SDOF system resting on a fixed base and being subjected to a time-dependent force p(t) of magnitude $-m \cdot \ddot{u}_g(t)$, as shown in Figure 12.

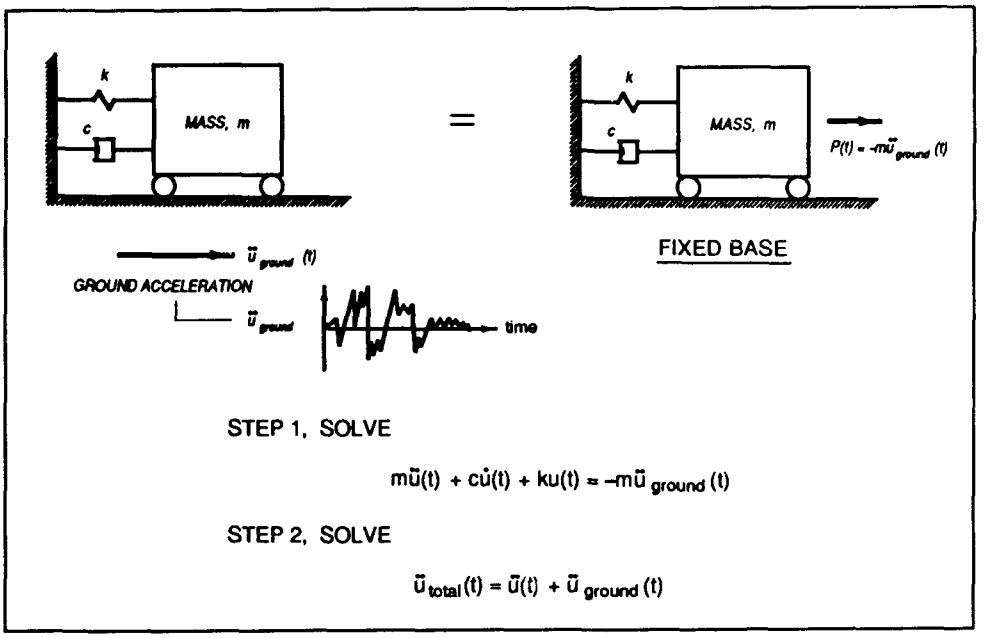

Figure 12. Equivalent dynamic SDOF system problems

The total dynamic response of the SDOF system problem is computed in two steps:

Step 1) Solve for the relative response of the damped SDOF system as governed by the ordinary differential equation, Equation 35.

Step 2) Sum the relative response with the motion of the ground to obtain the total response.

Step 1 assumes that the contribution of the general solution is negligible compared with the contribution of the particular solution.

For simple harmonic ground accelerations, e.g., [$\ddot{u}_g$ = *constant* · sin ($\omega_d t$)], closed-form solutions to Equation 35 are available in numerous textbooks on both mechanical vibrations and structural dynamics. This procedure is impractical for solving earthquake engineering problems due to the irregular nature of ground acceleration/time histories.

A second procedure used to solve for the relative displacement of the SDOF system involves the representation of the load/time history $p(t) = -m \cdot \ddot{u}_g(t)$ as a series of impulse loadings P(τ) applied to the SDOF system for infinitesimal time intervals dτ. Duhamel's integral for a damped SDOF system is given by:

$$u(t) = -(1/\omega_D) \int_0^t \ddot{u}_g(\tau)\, e^{-\beta\omega(t-\tau)} \sin [\omega_D (t - \tau)]\, d\tau \qquad (36)$$

where

ω_D = the damped angular frequency of vibration.

ω = the undamped angular frequency of vibration.

β = the fraction of critical damping.

The irregular forms of acceleration/time histories require numerical solutions to be used to solve Duhamel's integral (e.g., Paz 1991, or Clough and Penzien 1993).

In usual applications to earthquake engineering problems, numerical methods are used to solve Equations 35 and 36 for the relative displacement of the SDOF mass because of the irregular nature of ground acceleration/time histories. In general, there are two categories of numerical methods used for solving the dynamic equilibrium equation: 1) direct integration methods, and 2) frequency domain methods. The reader is referred to books on structural dynamics, e.g., Paz 1991, Clough and Penzien 1993, or Ebeling 1992 for a description of these two methods.

The solution of Duhamel's equation with $\beta = 0$ yields a useful relationship between displacement, velocity, and acceleration (Appendix A, Ebeling 1992).

$$\dot{u} = \omega u \qquad (37a)$$

$$\ddot{u} = \omega^2 u \tag{37b}$$

It is important to recognize that the relationships given by Equations 37a and b are exact only when damping is zero. The velocity $\dot{u}$ computed from Equation 37a is called *pseudovelocity* and the acceleration ü computed from Equation 37b is called *pseudoacceleration*. Equations 37a and b define the interrelationship between spectral displacement u, pseudovelocity $\dot{u}$, and pseudoacceleration ü, three terms to be discussed in detail in Chapter 2.

2 Design Response Spectra

Introduction

Earthquake loading is typically represented in a dynamic analysis either by a ground acceleration/time history or by a response spectrum. A response spectrum is a graphical relationship of maximum values of acceleration, velocity, and displacement response of SDOF systems having a natural frequency f. The graph is drawn over the usual range of frequencies for elastic SDOF systems.

To prepare such a response spectrum, Equation 35 is evaluated for the relative accelerations ü of an SDOF system during a particular earthquake excitation. The evaluation is made for the frequency f (or period T) of the SDOF system and its level of damping β. As indicated in Figure 13, the absolute acceleration response spectrum SA is then computed as the maximum absolute value of the sum of this computed relative acceleration/time history for the SDOF system plus the ground acceleration/time history from step 2 of Figure 12.

Also indicated in Figure 13, the solution is then searched over the entire time history for the maximum absolute acceleration SA of the SDOF system, which is found and recorded. The corresponding value of pseudoacceleration S_A is also computed and recorded, where $S_A = \omega^2 S_D$. The procedure is performed repeatedly at close intervals of frequency. The resulting sets of values for frequency f and pseudoacceleration S_A are then plotted as the spectra of responses for the various SDOF systems. A key feature of a response spectrum is that it has been made independent of time.

As more recordings of earthquake acceleration/time histories became available during the 1970's, statistical analyses of response spectra of earthquake ground motions were conducted by several groups of earthquake engineers and seismologists. The results of some of the early ground motion studies are summarized in Seed, Ugas, and Lysmer (1976), Mohraz (1976), and Newmark and Hall (1982). Their studies showed that the spectral frequency contents of the recorded accelerograms were dependent on the earthquake magnitude, distance from causative fault to site,

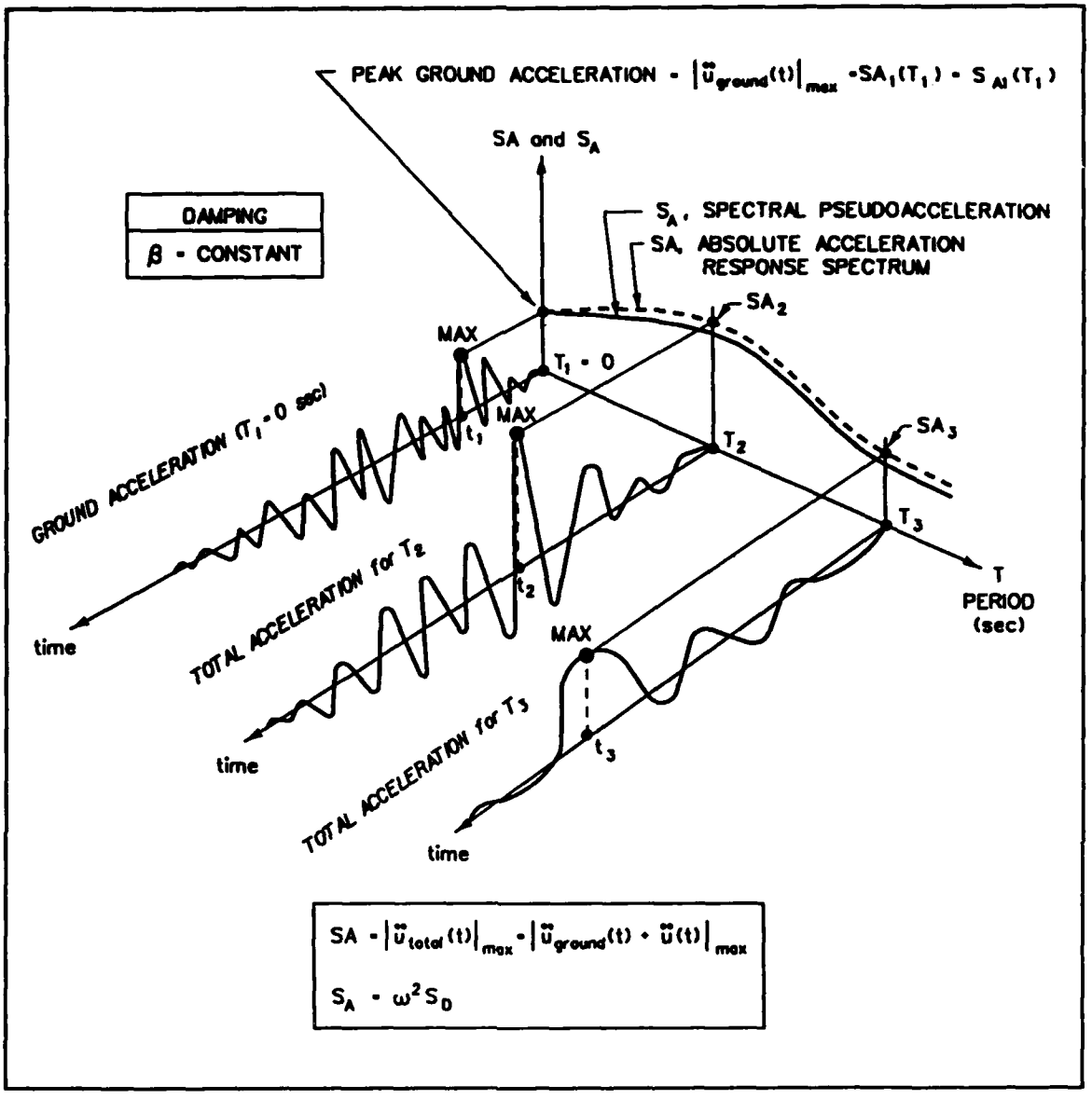

Figure 13. Absolute accelerations and pseudoaccelerations for elastic SDOF systems (Ebeling 1992)

the type of substratum on which the recording station was founded (i.e., rock, shallow alluvium, or deep alluvium), and the tectonic environment (i.e., strike-slip faulting, normal faulting, thrust faulting, subduction zones, etc.). A summary of the studies of Seed, Ugas, Lysmer, Mohraz, Newmark and Hall is presented in EM 1110-2-6050.

The response spectra developed and plotted from such studies are quite rough and jagged, but a general form can be readily deduced. Figure 14 shows an example of such a plot for a hypothetical plot of accelerations from three earthquake records. The overall average value of pseudoacceleration is a smoothed line as shown, drawn manually between

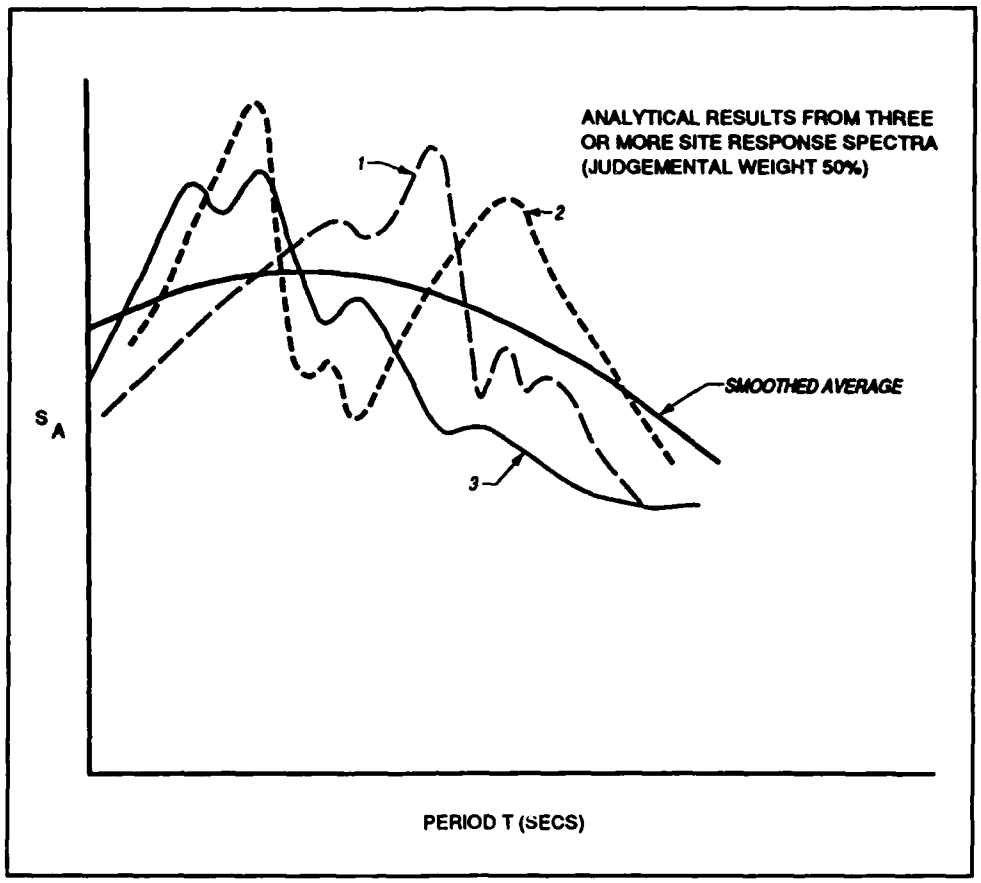

Figure 14. Smoothing of raw response data

the peak values. The overall accuracy increases, of course, as the number of records increases.

With an adequate number of records (see the appendix of EM 1110-2-6050), such smooth curves can be developed well within the range of accuracy of the earthquake projections themselves. All of the smooth-shaped spectra are drawn using this technique.

Smooth-Shaped, Broad-Band Design Response Spectra

Early ground motion studies identified the factors affecting the response spectra for earthquake motions, characterizing shape or the frequency content of the earthquake spectrum for the category under study and developing smooth, broad-band spectra for use in the design of structures for earthquake loadings. A broad-band spectrum ensures that sufficient seismic energy is delivered to all frequencies.

There are two smooth-shaped, broad-band response spectra now in wide use by dynamicists and structural engineers:

- The Newmark and Hall response spectra.
- The Applied Technology Council ATC 3-06 response spectra.

Both spectra are nonsite-specific and both can be applied in general structural applications.

Newmark and Hall Response Spectra

In the Newmark and Hall approach for developing design response spectra, it is necessary first to identify the peak ground acceleration (PGA), peak ground velocity (PGV), and peak ground displacement (PGD) for the design earthquake. These peak values are then multiplied by appropriate spectral amplification factors to obtain the corresponding displacements, velocities, and accelerations of SDOF systems throughout a range of natural frequencies. The results are presented graphically in a particular type of graph called a tripartite graph. Figure 15 is an example of such a design response spectrum adapted from Newmark and Hall 1982.

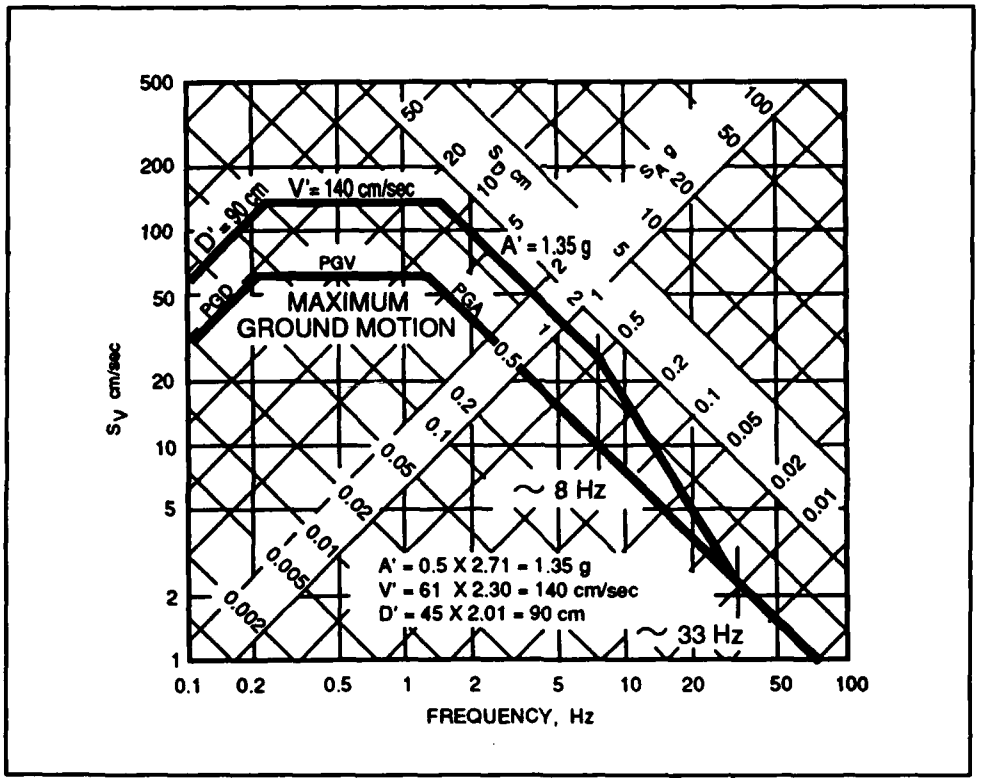

Figure 15. Newmark and Hall design response spectrum for a site having a stiff soil

There are four logarithmic scales used in Figure 15 to show the following three quantities as functions of the frequency f.

- D′ is the maximum relative displacement between the ground and the mass of an SDOF system having a natural frequency f, at whatever point in time it occurs.

- V′ is the maximum pseudovelocity $\omega D'$ of the SDOF mass.

- A′ is the maximum pseudoacceleration $\omega^2 D'$ of the SDOF mass.

Since all four quantities are interrelated, the tripartite plot provides a convenient means to show the entire interrelationship in a single curve. It can be shown (Hudson 1979 or Ebeling 1992) that for low levels of damping, the pseudovelocity and the pseudoacceleration are nearly equal to the maximum relative velocity and maximum relative acceleration. This approximation applies over most of the usual frequency range, with the pseudoacceleration being more accurate than the pseudovelocity. (For additional details regarding these issues, see Ebeling 1992.)

For reference, the maximum ground motion is shown in dashed lines on the graph of Figure 15. The ground motion shows only values of PGD, PGV, and PGA without regard to time.

In order to draw a SDOF response curve, a ground motion curve must be established, which means that the values of PGD, PGV, and PGA must be established. To establish these peak values of ground motion, it is necessary first to adopt a *design basis earthquake*. There are two *minimum* design basis earthquakes in use by the Army Corps of Engineers for intake towers (ER 1110-2-1806 and EM 1110-2-2401):

- *Operational Basis Earthquake (OBE)*: The OBE is the level of ground motion for which the structure is expected to remain functional with little or no damage. Ordinarily, the OBE is defined as a ground motion having a 50 percent probability of exceedance during the design life of 100 years (a 144-year return period). The associated performance level is normally the requirement that the structure will function within the elastic range with little or no damage and without interruption of function. Because the purpose of the OBE is to protect against economic losses from damage or loss of service, alternative choices of return period for the OBE may be made on the basis of an economic analysis. The OBE is normally based on a probabilistic site hazard analysis (PSHA).

- *Maximum Design Earthquake (MDE)*: The MDE is the maximum level of ground motion for which the structure is designed or evaluated. The associated performance level is the requirement that the structure perform without catastrophic failure, such as uncontrolled release of a reservoir, although severe damage or economic loss may be tolerated. For critical structures (refer to

ER 1110-2-1806), the MDE is the same as the maximum credible earthquake (MCE). For noncritical structures (refer to ER 1110-2-1806), the MDE may be chosen as a lesser earthquake than the MCE to provide economical designs meeting appropriate safety standards. For noncritical structures, the MDE can be determined by a PSHA.

The maximum credible earthquake (MCE) is defined as the greatest earthquake that can reasonably be expected to be generated by a specific source, on the basis of seismological and geological evidence. Since a project site may be affected by earthquakes generated by various sources, each with its own fault mechanism, maximum earthquake magnitude, and distance from the site, multiple MCE's may be defined for the site, each with characteristic ground motion parameters and spectral shape. The MCE is determined by a Deterministic Seismic Hazard Analysis (DSHA).

Moderate levels of damage may be acceptable in existing intake towers if it can be demonstrated that the structure will continue to function following an OBE event. The acceptance of a higher level of damage in existing intake towers will depend on the cost of retrofitting to preclude damage versus the cost of repairs following an OBE event.

There are two special cases for defining the MDE to be the same as the MCE. In the special case in which failure of the tower due to an earthquake can lead to failure of the dam and loss of the reservoir, the MDE should be the maximum credible earthquake (MCE).

The other special case in which the MDE is defined as the MCE occurs when the intake tower is required to operate after a severe earthquake. The tower may be damaged but its ability to function is not impaired by damage sustained during ground motions in excess of the *minimum* design basis earthquake. The MDE is the MCE for this case so that the postearthquake functionality of the intake structure can be demonstrated.

When site-specific information is not available, Newmark and Hall recommend that a v/a ratio of 48 in/sec/g (122 cm/sec/g) be used for a competent (stiff) soil. For rock, they recommend a v/a ratio of 36 in/sec/g (91 cm/sec/g). To ensure that the spectrum includes an adequate band width of frequencies, they recommend that ad/v^2 be taken at 6. (In these recommendations, a, v, and d are the values of the peak ground acceleration, peak ground velocity, and peak ground displacement, respectively.) From these recommended values, the value of d/a is found to be 90 cm/g for competent soil and 51 cm/g for rock.

The smooth elastic design spectrum shown in Figure 12 is an 84^{th} percentile spectrum developed for a site located on a competent soil with an estimated PGA value of a = 0.5g. In the spectrum of Figure 15, a value of 122 cm/sec/g is used for v/a, and a value of 90 is used for d/a. For a value of a = 0.5g, the corresponding value for velocity v is 61 cm/sec and for displacement d is 45 cm.

In an earlier paper, Newmark and Hall (1978) provided values of amplification factors for the different parts of the spectrum. These spectrum amplification factors are shown in Table 1 for various damping ratios. For the MDE, the spectrum amplification factors at 5 percent damping are 2.71, 2.30, and 2.01 for acceleration A, velocity V, and displacement D, respectively, of the SDOF system.

Table 1
Spectrum Amplification Factors for Horizontal Elastic Response (Source: Adapted from Newmark and Hall 1982)

Damping percent critical	One sigma (84.1%)			Median (50%)		
	A	V	D	A	V	D
0.5	5.10	3.84	3.04	3.68	2.59	2.01
1.0	4.38	3.38	2.73	3.21	2.31	1.82
2.0	3.66	2.92	2.42	2.74	2.03	1.63
3.0	3.24	2.64	2.24	2.46	1.86	1.52
5.0	2.71	2.30	2.01	2.12	1.65	1.39
7.0	2.36	2.08	1.85	1.89	1.51	1.29
10.0	1.99	1.84	1.69	1.64	1.37	1.20
20.0	1.26	1.37	1.38	1.17	1.08	1.01

For these amplification factors, the following bounds for the response spectrum are computed:

$$A' = A \times PGA = 2.71 \times 0.5g = 1.35g$$

$$V' = V \times PGV = 2.30 \times 61\ cm/sec = 140\,cm/sec$$

$$D' = D \times PGD = 2.01 \times 45\ cm = 90\,cm$$

The resulting elastic response spectrum is that shown in Figure 15. As shown there, Newmark and Hall (1982) connect the SDOF acceleration at 8 cps to the peak ground acceleration at 33 cps, thereby completing the high-frequency portion of the spectrum. They do not, however, specify at what frequency the SDOF displacement should be connected to the peak ground displacement to complete the low-frequency portion of the spectrum.

ATC 3-06 Response Spectra

In studies and analyses separate from those of Newmark and Hall, the Applied Technology Council (ATC) developed another form of the broad-band, smooth-shaped response spectra. The results of their analyses are presented in publication ATC 3-06, dated 1978.

The ATC 3-06 broad-band, smooth-shaped spectra were based on the smoothed mean spectral shapes from the study by Seed, Ugas, and Lysmer (1976) shown in Figure 16. These average spectra are based on 104 records mostly from earthquakes from the western part of the United States and having a Richter magnitude range of 5.25 to 7.5.

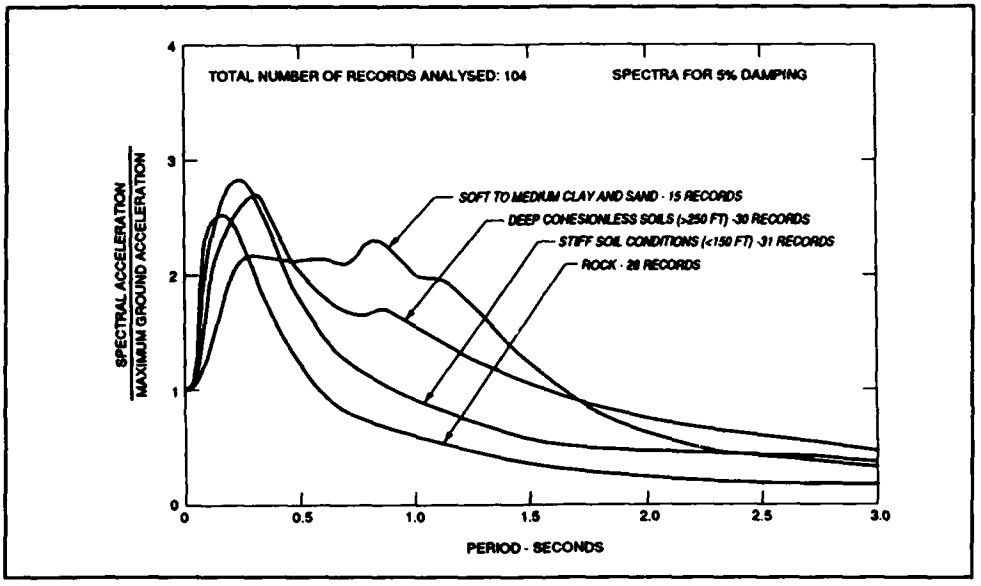

Figure 16. Average acceleration spectra (Seed, Ugas, Lysmer 1976)

Like the Newmark and Hall analysis, the end product of the ATC analysis is a graph. The ATC graph is a linear graph on which the periods of SDOF systems are plotted against the normalized spectral acceleration (pseudoacceleration divided by the peak ground acceleration). An example of the ATC 3-06 response spectra, drawn for 5 percent damping, is shown in Figure 17; a distinct advantage of the ATC response spectra is that the various soil conditions are included directly with the spectra.

In Figure 17, the nonsite-specific response spectra appropriate for use at a given site are distinguished between the three site classifications given in Table 2.

The ordinate of the ATC 3-06 response spectra of Figure 17 is normalized, that is, it is the ratio of peak SDOF pseudoacceleration to peak ground acceleration. Note also that Figure 17 is a linear plot rather than a log plot.

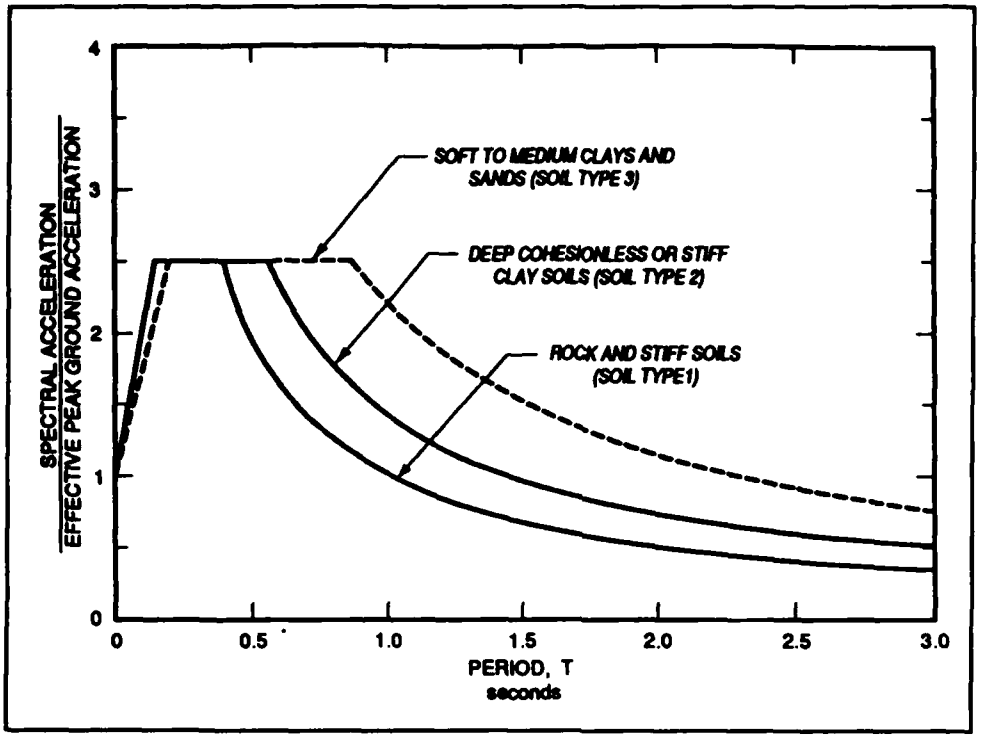

Figure 17. ATC 3-06 response spectra, 5 percent damping

Table 2
Soil Types

Type	Descriptions
1	A soil profile with either: a. A rock-like material characterized by a shear wave velocity greater than 2,500 fps or by other suitable means of classification. or b. Stiff or dense soil condition where the soil depth is less than 200 ft.
2	A soil profile with dense or stiff soil conditions, where the soil depth exceeds 200 ft.
3	A soil profile 70 ft or more in depth and containing more than 20 ft of soft to medium-stiff clay but not more than 40 ft of soft clay.

For SDOF systems founded on rock or stiff soils (Type 1 soils), the maximum normalized value of 2.5 occurs in SDOF systems having a natural period between 0.2 to 0.4 sec. For SDOF systems founded on Type 1 soils but which have periods longer than 0.4 sec, the normalized values decrease in amplitude inversely proportional to the period T, as indicated in Figure 17 (recall that T = 1/f).

For soils softer than Type 1 soils, the peak normalized acceleration is elongated significantly, extending to periods of 0.6 sec for Type 2 soils and to 0.9 sec for Type 3 soils. Even when acceleration does start to decrease in Types 2 and 3 soils, the rate of decrease is less than that in stiffer soils. Such long periods are more characteristic of flexible structural systems than rigid structural systems, indicating that when soils are soft, spectral accelerations are likely to be high for both flexible and rigid structural systems.

The greatest dynamic amplification of ground motion occurs in structures when the fundamental period of the structure is close to the characteristic period of the ground motions. This means that flexible or long-period structures on soft sites will respond more to earthquake ground motions than flexible structures on stiff sites. The ATC 3-06 standard spectra for various site conditions attempts to capture this phenomenon.

As a matter of interest, the smoothed plot for rock foundations as it was proposed in the Seed, Ugas, Lysmer study is shown in Figure 18. It has already been noted that the ATC curves evolved from this study. Shown also for comparison are the plot as it was finally adopted for the ATC 3-06 curve and the corresponding plot taken from a Newmark and Hall response spectra for the same rock foundation.

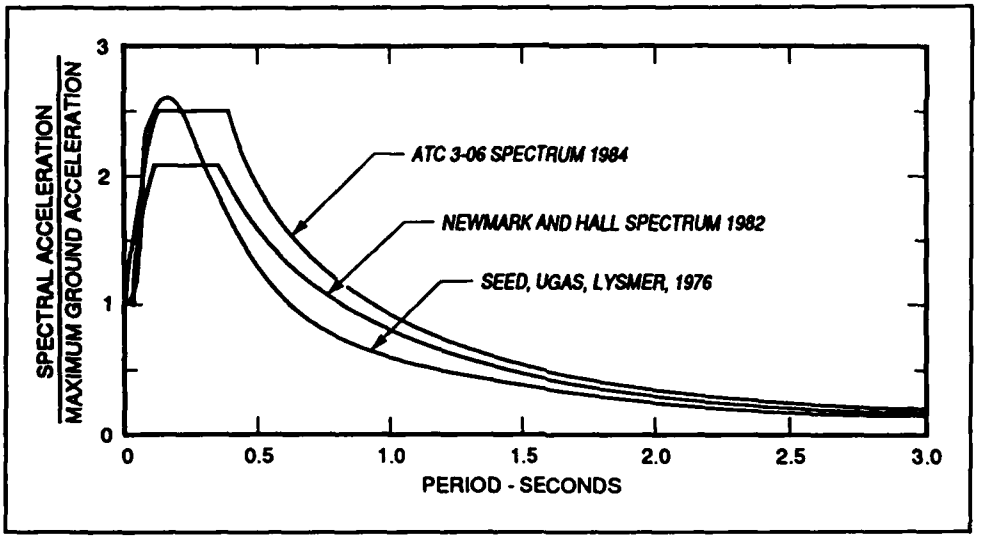

Figure 18. Comparison of design response spectra for rock foundations

Comparing the ATC curve with the Seed curve (a "mean" curve) shows that ATC truncated Seed's peak normalized acceleration at 2.5. This maximum of 2.5 is applied to all soils in the ATC spectra (see Figure 17), not just rock. Also, ATC more than tripled the range of periods which would experience the maximum normalized acceleration of 2.5.

Comparing the two major response spectra of Newmark and Hall and ATC 3-06 shows that the maximum magnitude of the ATC response is

significantly higher than that of Newmark and Hall (a "median" curve), and remains higher for all values of T. It is concluded that the ATC 3-06 spectrum is somewhat more conservative than the Newmark and Hall spectrum for all frequencies.

The ATC 3-06 spectra also appear in the 1991 Uniform Building Code as a general nonsite-specific design requirement. They are included as well in the recommended Lateral Force Requirements of the Structural Engineers Association of California (SEAOC) and are also used in the tri-services manual TM 5-809-10-1, SEISMIC DESIGN MANUAL FOR ESSENTIAL BUILDINGS. The ATC 3-06 Type 1 response spectra are used in EM 1110-2-2401 intake tower example problems.

Standard spectra, such as ATC 3-06, are intended to be used only for preliminary structural evaluations when site-specific response spectra are not yet available for the site. Another procedure for developing standard spectra to be used in preliminary structural evaluations is described in ER 1110-2-1806.

3 Distributed-Mass Systems

Period of Oscillation of Distributed-Mass Systems

A true SDOF system is one in which only one deflection pattern can occur. All of the lumped-mass systems shown in Figure 1 are such SDOF systems. In solutions to SDOF systems there was never any need to consider multiple patterns of oscillations.

A distributed-mass system such as the tower shown in Figure 19 is not an SDOF system. The tower could have a number of patterns of oscillations as shown, and it could also oscillate in two or more of these patterns at the same time. The distributed-mass system of Figure 19 is, in fact, a multiple-degree-of-freedom (MDOF) system with an infinite number of degrees of freedom.

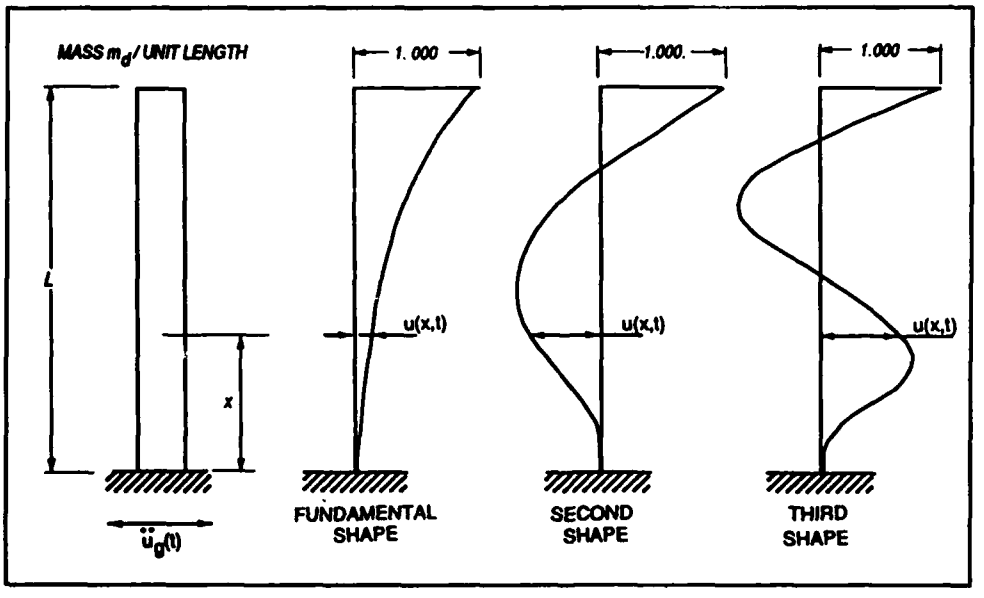

Figure 19. Distributed-mass system

If, however, it is assumed that the tower oscillates in only a single deflection shape at any one time, the system could be analyzed as an SDOF system. Such an assumption is the basis of analysis of distributed-mass systems, i.e., that the system can in fact be limited to a single pattern of deflections at a particular time. The *Rayleigh method* provides such an analysis of distributed-mass systems.

In the Rayleigh method, it is assumed that the deflection u(x,t) is limited to a single shape and that the single shape can be expressed as variables separable:

$$u(x,t) = \psi(x)\upsilon(t) \tag{38}$$

Inherently, the variables-separable solution uncouples the solution for displacements from the solution for frequency; each can be solved independently of the other. The *time function* $\upsilon(t)$ defines only the magnitude of the horizontal displacement at some reference level r at any time t. The displacement function ψ becomes only a *shape function*, defining the relative shape of the tower at any point x along its height as shown in Figure 20.

For the sake of simplicity, the reference level r in this report is always taken at the top of the cantilever, that is, x in Equation 38 equals L.

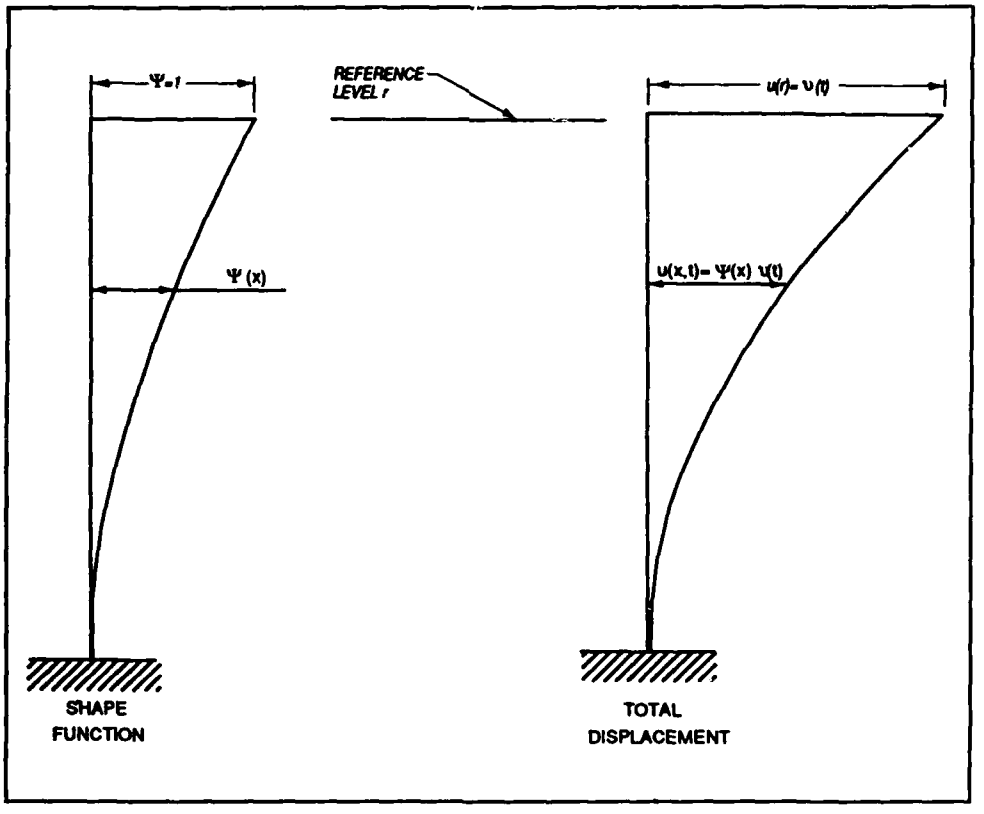

Figure 20. Shape function

The kinetic energy KE of the SDOF system of Figure 20 is given by:

$$KE = \tfrac{1}{2} m \dot{u}^2$$

$$= \tfrac{1}{2} \int_0^L m(x)\ [\dot{u}(x,t)]^2\, dx \tag{39}$$

The stored potential energy PE in the system is the strain energy due to flexure:

$$PE = \tfrac{1}{2} \int_0^L M\,\theta dx \tag{40}$$

where M is the moment on the cross section and θ is the rotation of the cross section about the neutral axis. The rotation θ is given by the Bernoulli equation:

$$\theta = \frac{1}{\rho} = \frac{M}{EI} = \frac{d^2 u}{dx^2} \tag{41}$$

The final form of the PE equation is then:

$$PE = \tfrac{1}{2} \int_0^L EI(x)\ [u''(x,t)]^2\, dx \tag{42}$$

An important observation is appropriate at this point. Note that the potential energy used in the Rayleigh solution is limited to the flexural moment-times-rotation strain energy. Shear deformations, axial deformations, and torsional rotations are all ignored. The Rayleigh solution is, therefore, most accurate in those applications in which the flexural energy dominates all other strain energy sources to such an extent that they may be safely ignored.

It should be noted that for squat towers the shear displacement can be a significant part of the total lateral displacement (flexural and shear). Intake towers with height-to-width aspect ratios of 3 or less should be designed for earthquake ground motions using procedures that include shear stiffness capability.

The variation in KE at any time interval must be equal and opposite to the variation in the PE over the same interval since there is no damping in this conservative system. The resulting solutions of Equations 39 and 42 are rather complicated solutions in the calculus of variations (Paz 1991) which yields the Rayleigh solution:

$$m^* \ddot{v}(t) + k^* v(t) = p_{eff}^*(t) \tag{43}$$

where

$$m^* = \int_0^L m(x)\,\psi^2\,dx = \textit{generalized mass} \tag{44a}$$

$$k^* = \int_0^L EI(x)\,[\psi'']^2\,dx = \textit{generalized stiffness} \tag{44b}$$

$$p_{eff}^*(t) = -\ddot{u}_g \int_0^L m(x)\,\psi dx = \textit{generalized load} \tag{44c}$$

In Equations 43 and 44, the asterisks denote that the functions are *generalized* functions which occur at the reference level r at the top of the cantilever.

A careful examination of Equations 43 and 44 reveals that the Rayleigh solution is actually a solution for a lumped-mass system rather than for a distributed-mass system. Such an equivalent system is shown in Figure 21.

As indicated in Figure 21, the Rayleigh solution given by Equation 43 is an equivalent solution for the oscillations of a generalized mass m* at the reference level r with respect only to time. The solution for $\upsilon(t)$ is no longer a function of the height x. This indicates that the Rayleigh solution transforms an MDOF distributed-mass system into an equivalent SDOF lumped-mass system at the reference level r.

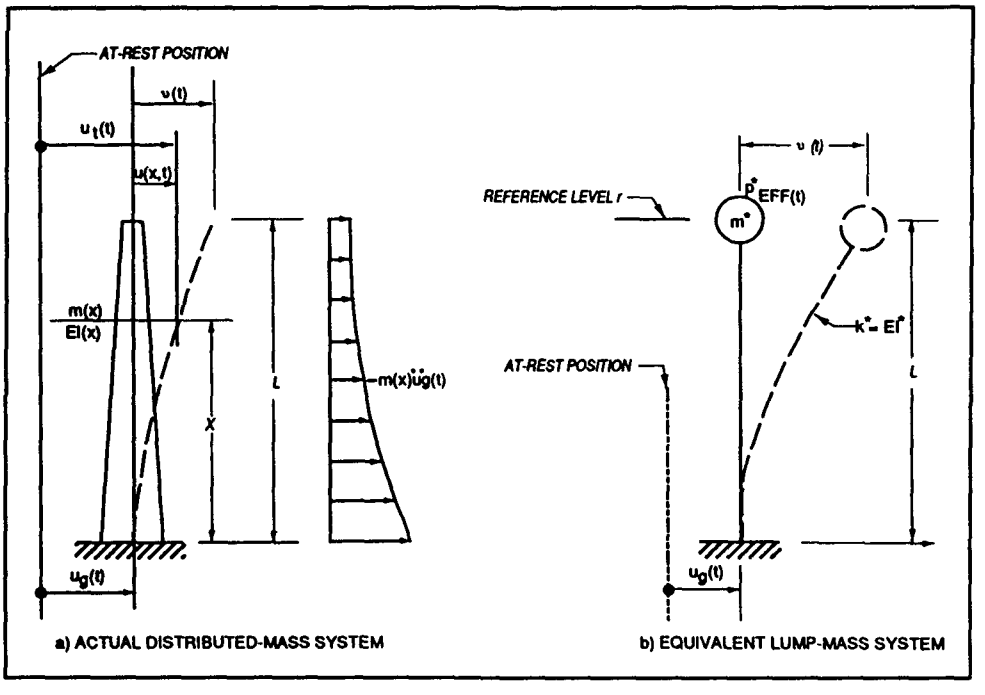

Figure 21. Equivalent Rayleigh lumped-mass system

Equation 43 does not include damping, i.e., there is no loss of energy anywhere in the system. It was shown earlier, however, that the natural period of oscillation is not affected by damping (for low levels of damping), so the period computed by use of Equation 43 will still be correct.

The solution of Equation 43 takes the form:

$$\ddot{\upsilon}(t) + k^*/m^*\upsilon(t) = -(L_n/m^*)\,\ddot{u}_g(t) \tag{45}$$

where

$$L_n = \int_0^L m(x)\psi dx \tag{46}$$

The natural frequency of this system remains, of course, the unforced frequency. Again, the unforced solution for $\upsilon(t)$ is harmonic, i.e.,

$$\upsilon(t) = \upsilon_0 \sin \omega t \tag{47}$$

and

$$u(x,t) = \psi(x)\upsilon_0 \sin \omega t \tag{48}$$

where υ_0 is the maximum value of displacement at the reference level r.

With no damping, the energy in this conservative system remains constant. The sum of KE (Equation 39) and PE (Equation 42) is therefore a constant. At maximum amplitude, the velocity is zero, and all the energy in the system at that time is in the form of PE:

$$PE = \tfrac{1}{2} \int_0^L EI(x)\ [u'']^2\, dx \tag{42}$$

Equation 48 is substituted, yielding:

$$PE = \tfrac{1}{2}\,\upsilon_0^2 \int_0^L EI(x)\,[\psi'']^2\, dx \tag{49a}$$

or

$$PE = \tfrac{1}{2}\,\upsilon_0^2\, k^* \tag{49b}$$

where υ_0 is the displacement at the reference level r.

Similarly, when displacement u(x,t) is zero, all of the energy in the system is in the form of KE:

$$KE = \tfrac{1}{2} \int_0^L m(x)\ [\dot{u}(x,t)]^2\, dx \tag{39}$$

Equation 48 is substituted, where, with $\cos(\omega t) = 1$ when $\dot{u}(x,t)$ is at its maximum:

$$KE = \tfrac{1}{2} v_0^2 \omega^2 \int_0^L m(x)\ [\psi(x)]^2\, dx \tag{50a}$$

or

$$KE = \tfrac{1}{2} v_0^2\, \omega^2 m^* \tag{50b}$$

Equations 49 and 50 must be equal in a conservative system. Equating them produces the result:

$$\omega^2 = k^*/m^* \tag{51a}$$

or equivalently,

$$T = 2\pi \sqrt{m^*/k^*} \tag{51b}$$

When Equation 51a is substituted into Equation 45, the result is the final form of the Rayleigh solution:

$$\ddot{v}(t) + \omega^2 v(t) = -(L_n/m^*)\, \ddot{u}_g(t) \tag{52}$$

where the natural period T and the circular frequency ω are those given by Equations 51a and b.

The factor L_n/m^* on the right-hand side of Equation 52 is an important feature of the Rayleigh solution. It is a dimensionless number, a multiplier that is applied to the ground acceleration $\ddot{u}_g(t)$. As such, it becomes a part of the forcing function and, consequently, it automatically becomes the same multiplier of the spectral quantities S_D, S_V, and S_A (to be discussed later).

Equation 52 shows that the factor L_n by itself is the "normalization" factor between the actual ground acceleration $\ddot{u}_g(t)$ and the response $\ddot{v}$ by the generalized mass m^*. When divided by m^*, the entire factor L_n/m^* becomes the normalization ratio factor between $\ddot{u}_g(t)$ and $\ddot{v}$ per unit of generalized mass.

Equation 51a has more than one solution. The only requirement for a solution is that the strain energy stored in a given deformation shape be exactly equal to the work done by the mass in moving into that shape. For a distributed mass, there are an infinite number of shape functions that will satisfy all the energy relations and thus be a solution to Equation 51a.

Each such shape function will have its own corresponding circular frequency ω and period T.

In order to compute the period of the structure from Equation 51b, it is necessary to know the mass m(x) and its distribution, the stiffness EI(x) and its distribution, and the shape function ψ. Where EI is constant or varies in discrete steps, it is known from the Bernoulli equation that the restoring force on the system is the fourth derivative of the displacement function ψ:

$$\frac{d^4\psi}{dx^4} = \frac{d^2}{dx^2}\left(\frac{M}{EI}\right) = \frac{-p}{EI} \tag{53}$$

This restoring force at any point is equal to the spring constant k times the deflection ψ, with the direction of the force always opposite to the direction of the deflection ψ:

$$k\psi = -p \tag{54}$$

Equating these two values for p yields an equation of the form:

$$\psi'''' = (constant)\ (\psi) \tag{55a}$$

or,

$$\psi'''' - (constant)\ (\psi) = 0 \tag{55b}$$

The solution of an equation of this form is given by:

$$\psi = A \sin(az) + B \cos(az) + C \sinh(az) + D \cosh(az) \tag{56}$$

where z = x/L and a is a constant involving the rotational frequency ω ($a^4 = m_d\omega^2/EI$, Clough and Penzien 1993).

There are only four constants of integration in the solution, which limits the boundary conditions to four. There are five unknowns, however, since a is also unknown. Therefore, a fifth condition is required. One way to develop the fifth condition is to assign some arbitrary value (such as unity) to ψ at the reference level r (at the top of the cantilever, see Figure 21). The solution will then be a reference solution, or *normalized* solution, in terms of unit displacement at r.

An example will illustrate the format of the solution. The first three shape functions for the cantilever of Figure 22 will be found. The four boundary conditions for the cantilever are:

1) The deflection at the base of the cantilever is zero

at z = 0, $\psi = 0$

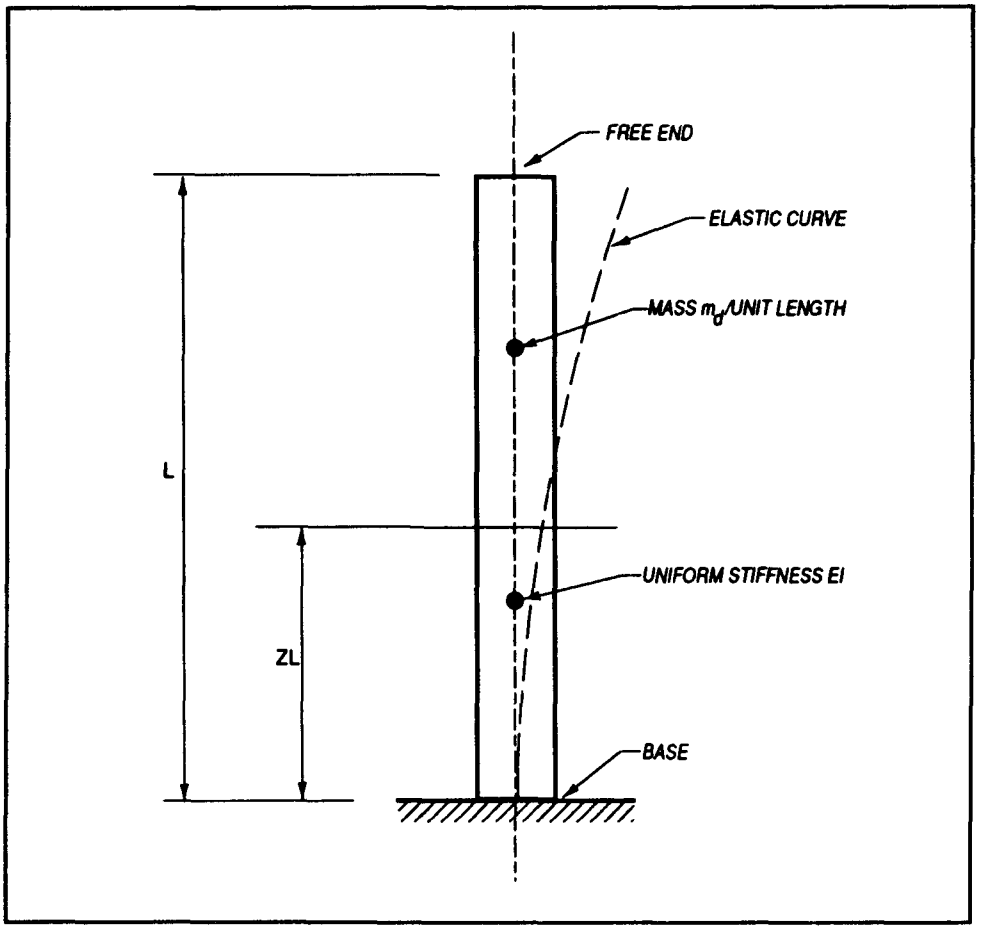

Figure 22. Typical distributed-mass cantilever

2) The slope of the elastic curve at the base is zero

at $z = 0$, $\psi' = 0$

3) The moment at the free end is zero

at $z = 1$, $\psi'' = 0$

4) The shear at the free end is zero

at $z = 1$, $\psi''' = 0$

The derivative forms of Equation 56 are:

$$\psi = A \sin(az) + B \cos(az) + C \sinh(az) + D \cosh(az)$$

$$\psi' = a A \cos(az) - aB \sin(az) + aC \cosh(az) + aD \sinh(az)$$

$$\psi'' = -a^2 A \sin(az) - a^2 B \cos(az) + a^2 C \sinh(az) + a^2 D \cosh(az)$$

$$\psi''' = -a^3 A \cos(az) + a^3 B \sin(az) + a^3 C \cosh(az) + a^3 D \sinh(az)$$

$$\psi'''' = a^4 A \sin(az) + a^4 B \cos(az) + a^4 C \sinh(az) + a^4 D \cosh(az)$$

These are substituted into the boundary conditions to find:

$$\text{At } z = 0,\ \psi = 0 = B + D$$

$$\text{At } z = 0,\ \psi' = 0 = A + C$$

$$\text{At } z = 1,\ \psi'' = 0 = -A \sin(a) - B \cos(a) + C \sinh(a) + D \cosh(a)$$

$$\text{At } z = 1,\ \psi''' = 0 = -A \cos(a) + B \sin(a) + C \cosh(a) + D \sinh(a)$$

A fifth condition is now imposed to obtain the required fifth equation. The value of ψ at the free end of the cantilever (reference level r) is assigned a value of unity, yielding:

$$\text{At } z = 1,\ \psi = 1 = A \sin(a) + B \cos(a) + C \sinh(a) + D \cosh(a)$$

A set of equations such as these five, having a variable coefficient in the matrix, is called a *characteristic problem* or an *eigenproblem*. A solution will exist only for particular values of the variable a; these values of a are called the *characteristic values* or the *eigenvalues*.

There are an infinite number of values of a in any distributed-mass system. Each value of a corresponds to a shape function; the lowest value of a corresponding to the first shape function, the next lowest value of a corresponding to the second shape function, and so on. For the sake of brevity, only three shape functions are presented here.

These five simultaneous equations are solved using conventional computer software (e.g., Maple, MathCAD, Matlab, Mathematica, etc.), though there are also specialized hand-held calculators available (e.g., HP 48S, TI 81, TI 85, etc.) that could solve such a set of equations. The first three solutions are:

a = 1.87510	a = 4.69409	a = 7.85476
A = +0.36705	A = -0.50923	A = +0.49961
B = -0.50000	B = +0.50000	B = -0.50000
C = -0.36705	C = +0.50923	C = -0.49961
D = +0.50000	D = -0.50000	D = +0.50000

Depending upon the particular software, the trial values of a are entered interactively by the engineer. The lowest value of a for which a solution can be obtained will yield the first shape function. The next lowest value of a will yield the second shape function, and so on. It is recommended

that the graphics capability of the software be used to verify each shape function so obtained. The number of curvatures corresponds to the number of the shape function (see Figure 23).

Therefore, the equations of the first three shape functions are:

$$\psi_1 = 0.367 \sin(1.875z) - 0.500 \cos(1.875z) - 0.367 \sinh(1.875z) + 0.500 \cosh(1.875z)$$

$$\psi_2 = -0.509 \sin(4.694z) + 0.500 \cos(4.694z) + 0.509 \sinh(4.694z) - 0.500 \cosh(4.694z)$$

$$\psi_3 = 0.500 \sin(7.855z) - 0.500 \cos(7.855z) - 0.500 \sinh(7.855z) + 0.500 \cosh(7.855z)$$

The configurations of the shape functions ψ corresponding to these first three solutions are shown in Figure 23.

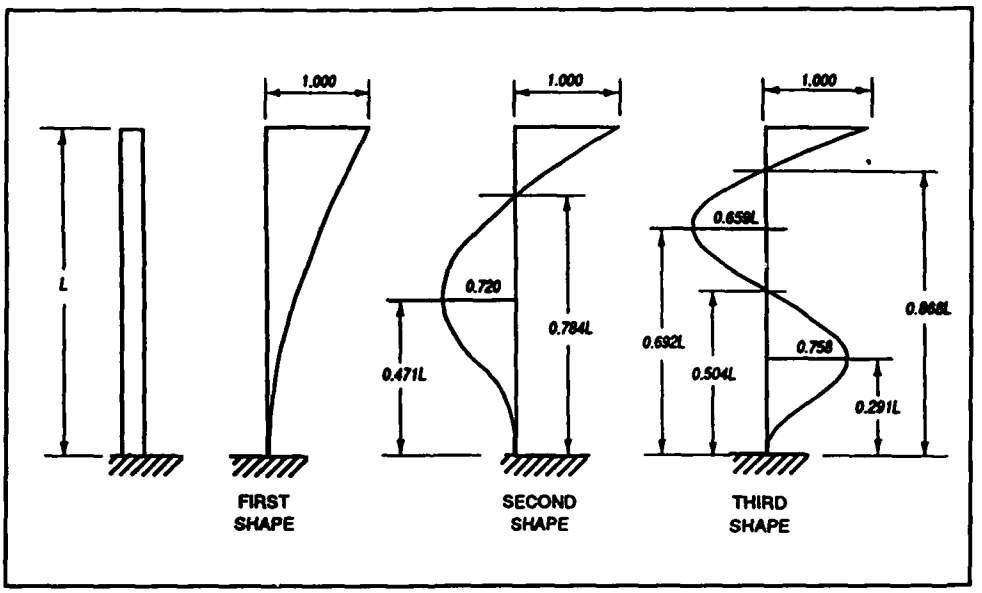

Figure 23. Shape functions for a cantilever having a uniformly distributed mass

The three equations for ψ are now used to evaluate the generalized functions for m*, k*, and L_n given by the integrals of Equations 44a and b and Equation 46 (or, equivalently, 44c). The integrals may be evaluated by conventional software or by specialized hand-held calculators. The generalized values for the three shape functions of Figure 20 are listed in Table 3, along with the rotational frequencies and the natural periods.

Table 3
Generalized Values for a Distributed Mass Cantilever

Shape Function 1	Shape Function 2	Shape Function 3
$m^* = 0.25000\ m_d L$	$m^* = 0.24998\ m_d L$	$m^* = 0.25019\ m_d L$
$k^* = 3.09055\ EI/L^3$	$k^* = 121.3693\ EI/L^3$	$k^* = 952.3417\ EI/L^3$
$L_n = 0.39149\ m_d L$	$L_n = -0.21701\ m_d L$	$L_n = 0.12758\ m_d L$
$L_n/m^* = 1.56599$	$L_n/m^* = -0.86811$	$L_n/m^* = 0.50995$
$\omega^2 = 12.36\ (EI/m_d L^4)$	$\omega^2 = 485.5\ (EI/m_d L^4)$	$\omega^2 = 3806\ (EI/m_d L^4)$
$T = 2\pi/\omega$	$T = 2\pi/\omega$	$T = 2\pi/\omega$

Flexural Stiffness EI for OBE and MDE

The value of k* given in Table 3 is a function of the modulus of elasticity E and the moment of inertia I. For concrete structures under the OBE, the value of EI is taken conservatively as that of the uncracked concrete section. The uncracked value of EI is used for determination of both the accelerations and displacements under an OBE earthquake.

For the maximum design earthquake, it is recognized that the worst-case values of acceleration and velocity will occur if the section does not crack since the higher the stiffness, the higher the structural system frequency and corresponding spectral acceleration and velocity. The uncracked section is, therefore, used when calculating accelerations and velocities under the MDE. For displacements, however, the largest displacements will occur when the concrete cracks, resulting in a reduction in stiffness which increases the period of the structure and its corresponding spectral displacement. Under the MDE, therefore, the uncracked value of EI is used to determine accelerations. To determine displacements, a flexural stiffness equal to half the gross section flexural stiffness is generally used. This value is considered an approximate typical effective stiffness for reinforced concrete structures loaded to yield levels.

Combined Effects in Distributed-Mass Systems

The values of the period T found from the Rayleigh solution are used to find the spectral values of S_D, S_V, and S_A, either from standard spectra such as Newmark and Hall or ATC 3-06 or from a design response spectra developed for the specific site. There will, of course, be three sets of spectral values, one for each shape function. Since the cantilever can experience all three (or even more) of the oscillation shapes at the same time,

the spectral values must now be combined. A means to combine the spectral values from several shape functions is presented in this section.

Finding a rational means to combine several shape functions is a major consideration if a set of SDOF solutions is to be taken as the solution to an MDOF problem. Because a system may oscillate in more than one frequency at any one time, a combination of SDOF shapes will undoubtedly occur in any MDOF oscillating system. For each of these participating shapes, a spectral maximum displacement S_D can be found, along with its corresponding spectral maximum pseudovelocity S_V and its spectral maximum pseudoacceleration S_A. The spectral values are the maximum values for each frequency. Since it is unlikely that all these maxima will occur at the same time, some reasonable basis for combining these maximum values is obviously needed.

There are two methods in common use for combining several SDOF solutions to obtain a single MDOF solution:

- square root of the sum of the squares (SRSS), and
- complete quadratic combination (CQC)

The older and more universal of these two methods is the SRSS method, which is an approximate method. Any number of spectral values can be combined by SRSS, but the usual number is three. When combined using SRSS, the spectral values for n SDOF solutions are:

$$S_D = \sqrt{S_{D1}^2 + S_{D2}^2 + S_{D3}^2 + \ldots\ldots S_{Dn}^2} \tag{57a}$$

$$S_V = \sqrt{S_{V1}^2 + S_{V2}^2 + S_{V3}^2 + \ldots\ldots S_{Vn}^2} \tag{57b}$$

$$S_A = \sqrt{S_{A1}^2 + S_{A2}^2 + S_{A3}^2 + \ldots\ldots S_{An}^2} \tag{57c}$$

The more recent CQC method is based on random vibration theory and it accounts for the interaction between two shape functions that have periods relatively close to each other. The method uses a cross-function coefficient ρ_{ij}, where i and j are any two shape functions and where $r = T_j/T_i$:

$$\rho_{ij} = \frac{8\beta^2 (1 + r)\, r^{1.5}}{(1 - r^2)^2 + 4\beta^2 r (1 + r)^2} \tag{58}$$

Figure 24 shows a graph of ρ_{ij}. For values of damping less than 5 percent, the periods must be within about 25 percent of each other for significant cross-function interaction to occur.

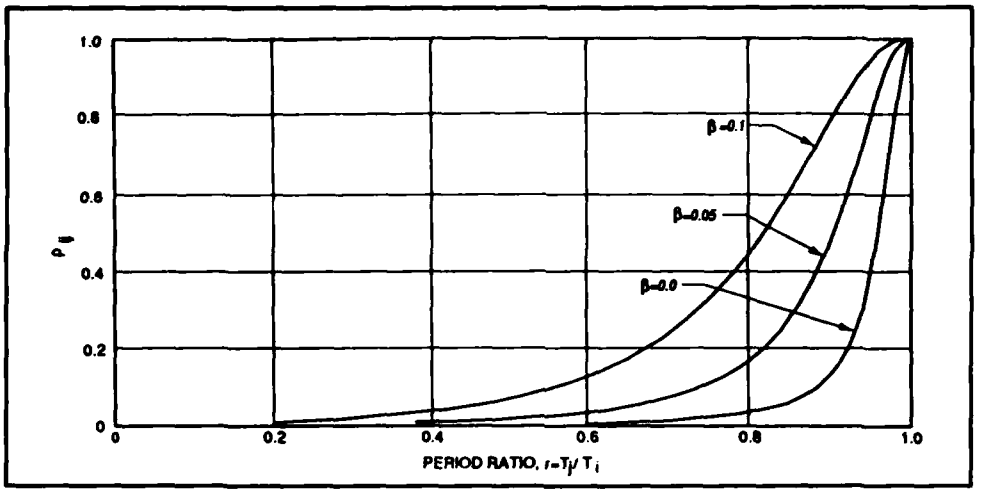

Figure 24. Cross-function coefficient ρ_{ij}

The spectral values for a CQC combination are given by:

$$S_D = \sqrt{\sum_{i=1}^{n} \sum_{j=1}^{n} S_{Di} \rho_{ij} S_{Dj}} \tag{59a}$$

$$S_V = \sqrt{\sum_{i=1}^{n} \sum_{j=1}^{n} S_{Vi} \rho_{ij} S_{Vj}} \tag{59b}$$

$$S_A = \sqrt{\sum_{i=1}^{n} \sum_{j=1}^{n} S_{Ai} \rho_{ij} S_{Aj}} \tag{59c}$$

When the periods between functions are well separated, the cross-function coefficient ρ_{ij} approaches zero for all cases where $i \neq j$. For the case in which i=j, the value of ρ_{ij} becomes 1, and the CQC method degenerates into the SRSS method. Most large structures will have distinct separation between periods and will fall into this default category in which the SRSS method will apply.

Table 3 shows that the normalization factor L_n can have different algebraic signs for different shape functions. When the CQC method is used, those signs must be preserved throughout the calculations. Further, when combining east-west, north-south and up-down contributions to any spectral quantity, the contributions must be added algebraically before being used either in the SRSS method or the CQC method (EC 1110-2-6050).

The following example illustrates the procedure for finding the spectral response of a distributed-mass system in which Rayleigh's solution is used to find the period T.

Example Solution for a Stepped Tower

Problem statement

Calculate the forces, overturning moment, and displacements on the square step-tapered intake tower under the maximum design earthquake, using the uncracked section for computing forces and the fully cracked and rotated section for computing the displacements. The Type 1 ATC 3-06 response spectrum is to be used. Maximum ground acceleration is 0.45g, the foundation is rock, γ_{conc} = 150 lb/ft^3, and Gross E_c = 3.6 x 10^6 lb/in.^{2}

Compute

a. Natural periods of oscillation for the first three shape functions.

b. Spectral displacements, velocities, and accelerations for the first three shape functions.

c. Combined accelerations for the first three shape functions.

d. Base shear under the combined accelerations.

e. Overturning moment under the combined accelerations.

f. Displacements of the cracked and damaged tower.

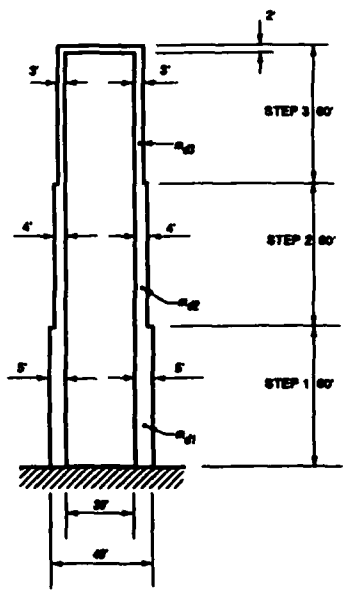

$$m_{d3} = 1984\ slugs/ft = 1.00 m_{d3}$$
$$I_3 = bh^3/12 = 72{,}470\ ft^4 = 1.000 I_3$$

$$m_{d2} = 2534\ slugs/ft = 1.28 m_{d3}$$
$$I_2 = bh^3/12 = 106{,}260\ ft^4 = 1.466 I_3$$

$$m_{d1} = 3261\ slugs/ft = 1.64 m_{d3}$$
$$I_1 = bh^3/12 = 145{,}830\ ft^4 = 2.012 I_3$$

Solution

Because the shape function is discontinuous at the steps, it is defined by three discontinuous equations:

$0 \le z \le \frac{1}{3}$: $\psi = A_1 \sin(az) + B_1 \cos(az) + C_1 \sinh(az) + D_1 \cosh(az)$

$\frac{1}{3} \le z \le \frac{2}{3}$: $\psi = A_2 \sin(az) + B_2 \cos(az) + C_2 \sinh(az) + D_2 \cosh(az)$

$\frac{2}{3} \le z \le 1$: $\psi = A_3 \sin(az) + B_3 \cos(az) + C_3 \sinh(az) + D_3 \cosh(az)$

Boundary conditions are:

At $z = 0$, $\psi_1 = 0$ and $\psi'_1 = 0$

At $z = \frac{1}{3}$, $\psi_1 = \psi_2$; $\psi'_1 = \psi'_2$; $M_1 = M_2$ and $V_1 = V_2$

At $z = \frac{2}{3}$, $\psi_2 = \psi_3$; $\psi'_2 = \psi'_3$; $M_2 = M_3$ and $V_2 = V_3$

At $z = 1$, $M_3 = 0$ and $V_3 = 0$

where:

M = moment

V = shear

These 12 boundary conditions apply to 13 unknowns. The 13th condition is obtained by setting the displacement $\psi_3 = 1$ at the top of the tower.

At $z = 1.000$, $\psi_3 = 1.000$

The three equations of the shape function are substituted into these 13 boundary conditions, producing 13 equations in 13 unknowns. The equations are independent of mass.

$$0 = B_1 + D_1$$

$$0 = A_1 + C_1$$

$$0 = (A_1 - A_2) \sin(\tfrac{1}{3}a) + (B_1 - B_2) \cos(\tfrac{1}{3}a) + (C_1 - C_2) \sinh(\tfrac{1}{3}a) + (D_1 - D_2) \cosh(\tfrac{1}{3}a)$$

$$0 = (A_1 - A_2) \cos(\tfrac{1}{3}a) - (B_1 - B_2) \sin(\tfrac{1}{3}a) + (C_1 - C_2) \cosh(\tfrac{1}{3}a) + (D_1 - D_2) \sinh(\tfrac{1}{3}a)$$

$$0 = -(I_1 A_1 - I_2 A_2) \sin(\tfrac{1}{3}a) - (I_1 B_1 - I_2 B_2) \cos(\tfrac{1}{3}a) + (I_1 C_1 - I_2 C_2) \sinh(\tfrac{1}{3}a) + (I_1 D_1 - I_2 D_2) \cosh(\tfrac{1}{3}a)$$

$$0 = -(I_1A_1-I_2A_2)\cos(\tfrac{1}{3}a) + (I_1B_1-I_2B_2)\sin(\tfrac{1}{3}a) + (I_1C_1-I_2C_2)\cosh(\tfrac{1}{3}a) + (I_1D_1-I_2D_2)\sinh(\tfrac{1}{3}a)$$

$$0 = (A_2-A_3)\sin(\tfrac{2}{3}a) + (B_2-B_3)\cos(\tfrac{2}{3}a) + (C_2-C_3)\sinh(\tfrac{2}{3}a) + (D_2-D_3)\cosh(\tfrac{2}{3}a)$$

$$0 = (A_2-A_3)\cos(\tfrac{2}{3}a) - (B_2-B_3)\sin(\tfrac{2}{3}a) + (C_2-C_3)\cosh(\tfrac{2}{3}a) + (D_2-D_3)\sinh(\tfrac{2}{3}a)$$

$$0 = -(I_2A_2-I_3A_3)\sin(\tfrac{2}{3}a) - (I_2B_2-I_3B_3)\cos(\tfrac{2}{3}a) + (I_2C_2-I_3C_3)\sinh(\tfrac{2}{3}a) + (I_2D_2-I_3D_3)\cosh(\tfrac{2}{3}a)$$

$$0 = -(I_2A_2-I_3A_3)\cos(\tfrac{2}{3}a) + (I_2B_2-I_3B_3)\sin(\tfrac{2}{3}a) + (I_2C_2-I_3C_3)\cosh(\tfrac{2}{3}a) + (I_2D_2-I_3D_3)\sinh(\tfrac{2}{3}a)$$

$$0 = -A_3\sin(a) - B_3\cos(a) + C_3\sinh(a) + D_3\cosh(a)$$

$$0 = -A_3\cos(a) + B_3\sin(a) + C_3\cosh(a) + D_3\sinh(a)$$

$$1 = A_3\sin(a) + B_3\cos(a) + C_3\sinh(a) + D_3\cosh(a)$$

It is well to observe at this point that the boundary conditions will always include the four end conditions (at the base and at the top) plus four conditions for each discontinuity in moment of inertia. There will be as many of these interior discontinuities as there are changes in EI. Each discontinuity will simply add four more equations to the set of simultaneous equations. Since the computer will solve forty equations as readily as four, the additional equations cause no more labor than making some additional entries in the mathematics software.

The foregoing equations also show that the shape function of any distributed-mass MDOF system is independent of the distribution of the mass. Additional masses may be added or deleted at will, but as long as the stiffness is unchanged, the shape of the deflection curve will remain the same. The mass and its distribution will affect the magnitude of the displacements (and the period T), but not the shape function.

The 13 equations of the example are solved by the mathematics software, as usual, to find the coefficients at the three steps. The coefficients are listed in Table 4. Trial entries of 2, 5, and 8 for the value of a were used in finding the three shape functions shown in Table 4.

Table 4
Shape Function Coefficients

First Shape Function a = 2.15045	Second Shape Function a = 4.83575	Third Shape Function a = 7.85376
First step, $0 \le z \le 1/3$		
$A_1 = +0.24070$	$A_1 = -0.33292$	$A_1 = +0.34856$
$B_1 = -0.35659$	$B_1 = +0.34887$	$B_1 = -0.35227$
$C_1 = -0.24070$	$C_1 = +0.33292$	$C_1 = -0.34856$
$D_1 = +0.35659$	$D_1 = -0.34887$	$D_1 = +0.35227$
Second step, $1/3 \le z \le 2/3$		
$A_2 = +0.25698$	$A_2 = -0.37461$	$A_2 = +0.40870$
$B_2 = -0.46345$	$B_2 = +0.41823$	$B_2 = -0.40996$
$C_2 = -0.39978$	$C_2 = +0.40194$	$C_2 = +0.35635$
$D_2 = +0.50951$	$D_2 = -0.39552$	$D_2 = -0.35675$
Third step, $2/3 \le z \le 1$		
$A_3 = +0.23485$	$A_3 = -0.43826$	$A_3 = +0.50011$
$B_3 = -0.55413$	$B_3 = +0.52886$	$B_3 = -0.49329$
$C_3 = -0.66003$	$C_3 = -1.82776$	$C_3 = -8.49612$
$D_3 = +0.75725$	$D_3 = +1.83547$	$D_3 = +8.49651$

The equations defining the first shape function are:

$0 \le z \le \frac{1}{3}$: $\psi = 0.241 \sin(2.150z) - 0.357 \cos(2.150z) - 0.241 \sinh(2.150z) + 0.357 \cosh(2.150z)$

$\frac{1}{3} \le z \le \frac{2}{3}$: $\psi = 0.257 \sin(2.150z) - 0.463 \cos(2.150z) - 0.400 \sinh(2.150z) + 0.510 \cosh(2.150z)$

$\frac{2}{3} \le z \le 1$: $\psi = 0.235 \sin(2.150z) - 0.554 \cos(2.150z) - 0.660 \sinh(2.150z) + 0.757 \cosh(2.150z)$

The generalized mass m* and generalized stiffness k* for the first shape function are found by evaluating the integrals of Equations 44a and b. For the uncracked section:

$$m^* = \int_0^{1/3} m_{d1}L\,[0.241 \sin(2.150z) - 0.357 \cos(2.150z) - 0.241 \sinh(2.150z) + 0.357 \cosh(2.150z)]^2\,dz$$

$$+ \int_{1/3}^{2/3} m_{d2}L\,[0.257 \sin(2.150z) - 0.463 \cos(2.150z) - 0.400 \sinh(2.150z) + 0.510 \cosh(2.150z)]^2\,dz$$

$$+ \int_{2/3}^{1} m_{d3}L\,[0.235 \sin(2.150z) - 0.554 \cos(2.150z) - 0.660 \sinh(2.150z) + 0.757 \cosh(2.150z)]^2\,dz$$

$$= 90{,}560\ slugs$$

$$k^* = \int_0^{1/3} (EI_1/L^3)\,[-1.114 \sin(2.150z) + 1.650 \cos(2.150z) - 1.114 \sinh(2.150z) + 1.650 \cosh(2.150z)]^2\,dz$$

$$+ \int_{1/3}^{2/3} (EI_2/L^3)\,[-1.188 \sin(2.150z) + 2.140 \cos(2.150z) - 1.849 \sinh(2.150z) + 2.357 \cosh(2.150z)]^2\,dz$$

$$+ \int_{2/3}^{1} (EI_3/L^3)\,[-1.086 \sin(2.150z) + 2.560 \cos(2.150z) - 3.051 \sinh(2.150z) + 3.499 \cosh(2.150z)]^2\,dz$$

$$= 36.15 \times 10^6\ lb/ft$$

$$L_n = \int_0^{1/3} m_{d1}L\,[0.241 \sin(2.150z) - 0.357 \cos(2.150z) - 0.241 \sinh(2.150z) + 0.357 \cosh(2.150z)]\,dz$$

$$+ \int_{1/3}^{2/3} m_{d2}L\,[0.257 \sin(2.150z) - 0.463 \cos(2.150z) - 0.400 \sinh(2.150z) + 0.510 \cosh(2.150z)]\,dz$$

$$+ \int_{2/3}^{1} m_{d3}L\,[0.235 \sin(2.150z) - 0.554 \cos(2.150z) - 0.660 \sinh(2.150z) + 0.757 \cosh(2.150z)]\,dz$$

$$= 151{,}215\ slugs$$

The remaining constants are calculated from the following values:

Circular frequency $\omega = \sqrt{k^*/m^*} = 19.98\ rad/sec$

Period $T = 2\pi/\omega = 0.314\ sec$

Frequency $f = 1/T = 3.186\ cps$

The values for the other shape functions are found similarly.

First Shape Function	Second Shape Function	Third Shape Function
$m^* = 90{,}560$ slugs	$m^* = 77{,}800$ slugs	$m^* = 79{,}700$ slugs
$k^* = 36.2 \times 10^6$ lb/ft	$k^* = 851 \times 10^6$ lb/ft	$k^* = 6{,}116 \times 10^6$ lb/ft
$L_n = 151{,}215$ slugs	$L_n = -79{,}480$ slugs	$L_n = 50{,}540$ slugs
$L_n/m^* = 1.670$	$L_n/m^* = -1.022$	$L_n/m^* = 0.634$
$\omega = 19.98$ rad/sec	$\omega = 105$ rad/sec	$\omega = 277$ rad/sec
$T = 0.314$ sec	$T = 0.060$ sec	$T = 0.023$ sec

The spectral accelerations are found from Figure 17 for the periods just calculated.

First Shape Function	Second Shape Function	Third Shape Function
$S_A = 1.125$ g	$S_A = 0.720$ g	$S_A = 0.554$ g

Effects of Submergence

It is again noted that the foregoing solution for the period of the example step-tapered tower is mathematically exact. The solution in common use for the period of such towers when they are used as intake structures (EM 1110-2-2401, or Goyal and Chopra 1989) includes the additional mass of water, both inside and outside the intake tower, that is being accelerated by the motion of the tower. Figure 25 shows a schematic of such added mass for two pool levels. Even though the Chopra procedure for finding the added mass of water is approximate, it indicates that the added mass that lies below the waterline can sometimes triple the effective mass. The overall result is to increase markedly the natural period T above that of a "dry" tower.

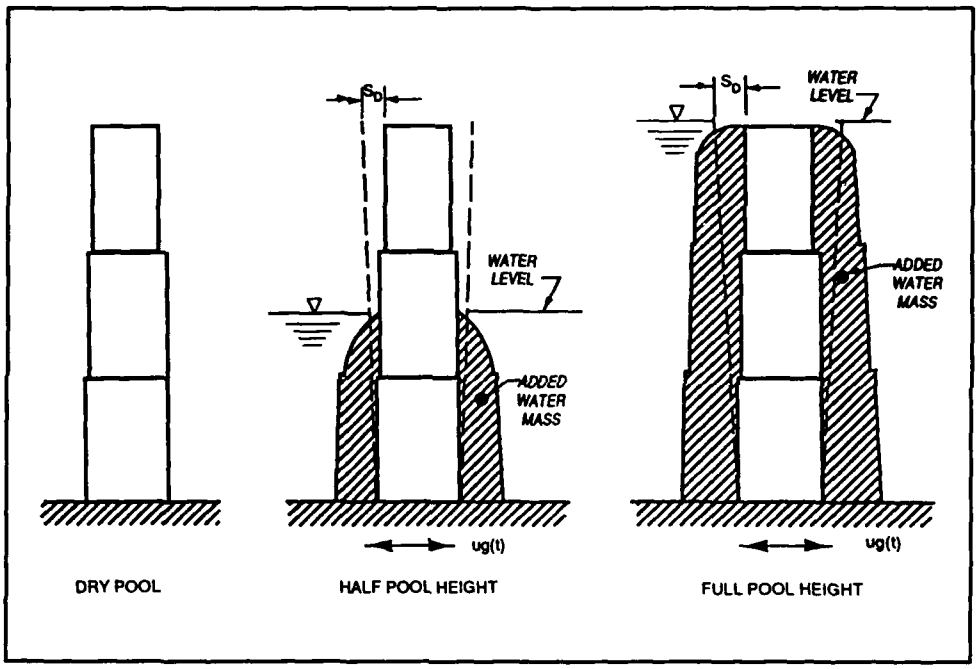

Figure 25. Added mass due to acceleration of water

The increase in mass due to the added water poses no particular problem in the Rayleigh solution. The added mass of water is computed in stepped increments as prescribed in the Chopra procedure and is then added to the mass of the tower. It is not necessary that the steps in the water mass match the steps in the tower mass. If the steps do not happen to coincide, the steps in water mass will simply create some new discontinuities in the integration for m*. As noted earlier, however, the shape function remains unchanged by the addition of hydraulic mass.

Since the added mass does not affect stiffness, the generalized stiffness k* remains constant for all levels of water both inside and outside the tower. Since the period is proportional to the square root of the mass m*

($T = 2\pi \sqrt{m^*/k^*}$), the effect of submergence is computed by evaluating m^* for various levels of submergence and then recalculating T for each of these levels. Figure 26 is a plot of the results of such calculations for the example step-tapered tower.

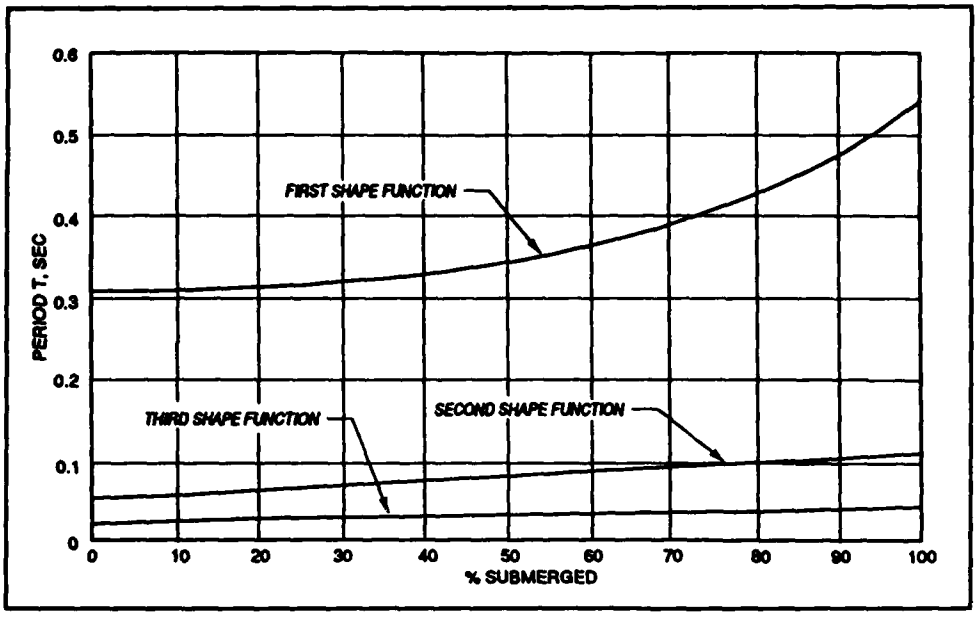

Figure 26. Effects of submergence on natural period

The magnitude of the added hydrodynamic mass is a function of the cross-sectional geometry of the tower and the depth of submergence. Gradual changes in the tower geometry produce gradual changes in effective mass and stiffness, whereas abrupt changes in the tower geometry produce abrupt changes in mass and stiffness. The effect of taper on the generalized stiffness is quite distinct. The periods will be distinctly different (as much as 50 percent different) between a tower that has a uniform cross section and one that has a tapered cross section, even when the mass is the same (EM 1110-2-2401).

Effects of Bridge Structures

Another feature of intake structures that has not been included in the previous discussions is the existence of the bridge structure that is commonly placed at the top of intake towers to permit service access. Such a bridge structure is shown in Figure 27. In an earthquake, the existence of the bridge structure can change the effective mass, and in some cases can add a restraint that must be included as a boundary condition.

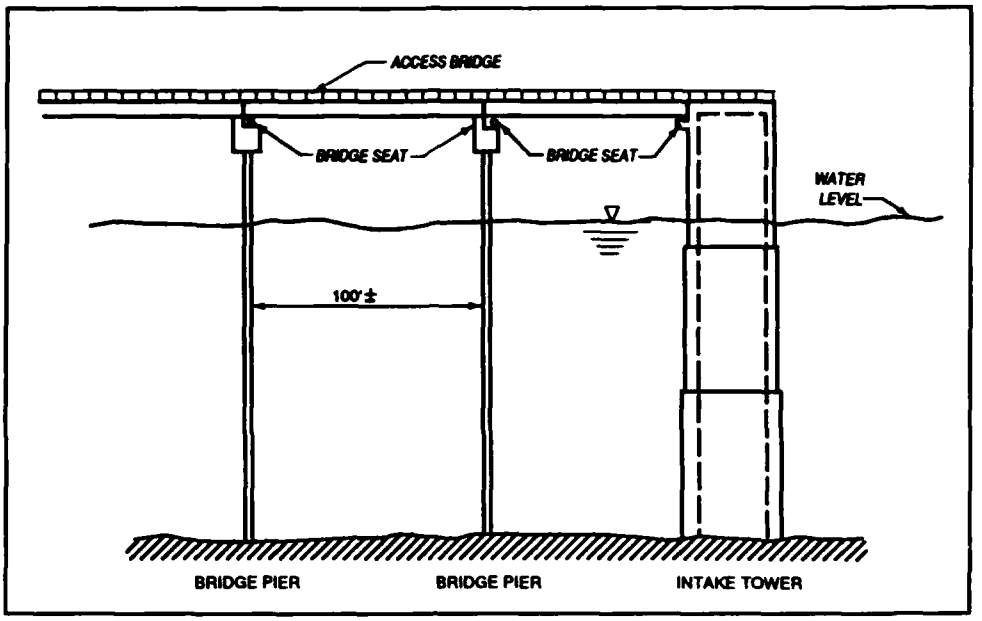

Figure 27. Bridge structure on an intake tower

Unless the bridge is anchored to the tower by pinned or fixed connections, large relative displacements between the bridge and tower can occur. These displacements, unless accounted for in the design, can lead to hammering or to a loss of the bearing support at the bridge seat. The preferred solution (not always done) is to tie the bridge and tower together, forcing the two elements to perform as a single system. The potential for damage due to hammering or to loss of support is then eliminated. The type of bearing supports at the bridge seats will determine whether the bridge can be handled simply as an added mass or whether a separate boundary condition will be necessary.

In many intake structures, the bridge beam bearings are pinned in one direction, but in many others they are pinned in two directions. Further, the bridge beams might also be pinned at their far ends at the supporting pier. The flexibility of the tall piers is enough to dissipate any thermal effects on the doubly pinned beams. With restraints such as these, lateral forces will be created at the top of the tower due to the bridge.

For earthquake motions transverse to the longitudinal axis of the bridge, the force on the pinned bearings at the tower is the inertia force of the half of the bridge supported by the tower. The additional inertial force may be included in the Rayleigh solution by converting the vertical beam reaction at the tower to an equivalent mass distributed over the height of the bridge. The step in mass thus created adds yet one more discontinuity in the distribution of mass. The integration for the generalized mass m^* is then made as usual; the extra discontinuity simply adds another term to the integration.

For motions transverse to the axis of the bridge, the addition of the bridge mass has no effect on the displacement function ψ of the tower; stiffness remains unchanged. Insofar as displacements are concerned, only the magnitudes of the displacements are changed by attaching the separate bridge mass.

For earthquake motions parallel with the longitudinal axis of the bridge, the force on the pinned bearings at the tower depends on the type of bearings used at the pier at the far end of the beams. If the far bearings are rollers, the force created at the tower would be the inertial force of the entire mass of the bridge, not just the reaction at one end. The recalculation of m* would proceed as before but with the larger added mass. If the far bearings are pinned, however, the force at the tower would be the inertial force of the entire bridge plus the force due to the spring constant k_s of the adjacent pier as it is deformed laterally by the motions of the tower. The existence of such a shear at the top of the tower can be handled readily in the Rayleigh solution by the boundary condition $\psi''' = k_s\psi$ at $z = 1$; this boundary condition would be used instead of $\psi''' = 0$.

Base Shear and Overturning Moment

There are two static loads that occur on a cantilever as a result of earthquake motions. One is the *base shear*, and the other is the *overturning moment*. These loads are shown on the distributed-mass structure of Figure 28. These two loads are computed by simple statics, and the procedure is presented in this section.

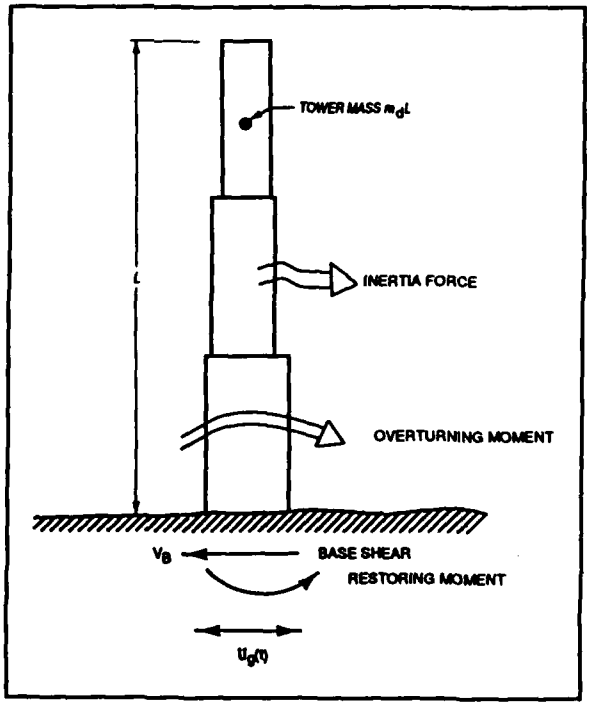

Figure 28. Base shear and overturning moment

In the Rayleigh solution for a distributed mass, the acceleration of the mass m* at the reference level r is found by multiplying the spectral acceleration S_A times the normalization ratio L_n/m^*. For any given shape function, the acceleration of the structural mass at all other points along the height of the tower is found by multiplying the acceleration at the reference level r by the shape function. The

result then becomes the *acceleration function* (Table 5). Such a calculation for the step-tapered tower of the preceding example is demonstrated in the following procedure.

Table 5
Acceleration Function Coefficients

Normalization Ratio 1.670 times S_{A1} times First Shape Function (Table 4)	Normalization Ratio -1.022 times S_{A2} times Second Shape Function (Table 4)	Normalization Ratio 0.634 times S_{A3} times Third Shape Function (Table 4)
a = 2.15045	a = 4.83575	a = 7.85376
First step, $0 \le x \le 1/3$		
A_1 = +0.45222	A_1 = +0.24498	A_1 = +0.12243
B_1 = -0.66994	B_1 = -0.25671	B_1 = -0.12373
C_1 = -0.45222	C_1 = -0.24498	C_1 = -0.12243
D_1 = +0.66994	D_1 = +0.25671	D_1 = +0.12373
Second step, $1/3 \le x \le 2/3$		
A_2 = +0.48280	A_2 = +0.27565	A_2 = +0.14355
B_2 = -0.87071	B_2 = -0.30775	B_2 = -0.14399
C_2 = -0.75109	C_2 = -0.29576	C_2 = +0.12516
D_2 = +0.95724	D_2 = +0.29104	D_2 = -0.12530
Third step, $2/3 \le x \le 1$		
A_3 = +0.44122	A_3 = +0.32249	A_3 = +0.17566
B_3 = -1.04107	B_3 = -0.38916	B_3 = -0.17326
C_3 = -1.24003	C_3 = +1.34494	C_3 = -2.98413
D_3 = +1.42268	D_3 = -1.35061	D_3 = +2.98428

With these coefficients, the accelerations are given by the following sets of three discontinuous equations, now termed the acceleration functions.

First acceleration function

$$0 \le z \le 1/3: \quad \psi = 0.45222 \sin(2.15045z) - 0.66994 \cos(2.15045z) - 0.45222 \sinh(2.15045z) + 0.66994 \cosh(2.15045z)$$

$1/3 \le z \le 2/3$: $\psi = 0.48280 \sin(2.15045z) - 0.87071 \cos(2.15045z) - 0.75109 \sinh(2.15045z) + 0.95724 \cosh(2.15045z)$

$2/3 \le z \le 1$: $\psi = 0.44122 \sin(2.15045z) - 1.04107 \cos(2.15045z) - 1.24003 \sinh(2.15045z) + 1.42268 \cosh(2.15045z)$

Second acceleration function

$0 \le z \le 1/3$: $\psi = 0.24498 \sin(4.83575z) - 0.25671 \cos(4.83575z) - 0.24498 \sinh(4.83575z) + 0.25671 \cosh(4.83575z)$

$1/3 \le z \le 2/3$: $\psi = 0.27565 \sin(4.83575z) - 0.30775 \cos(4.83575z) - 0.29576 \sinh(4.83575z) + 0.29104 \cosh(4.83575z)$

$2/3 \le z \le 1$: $\psi = 0.32249 \sin(4.83575z) - 0.38916 \cos(4.83575z) + 1.34494 \sinh(4.83575z) - 1.35061 \cosh(4.83575z)$

Third acceleration function

$0 \le z \le 1/3$: $\psi = 0.12243 \sin(7.85376z) - 0.12373 \cos(7.85376z) - 0.12243 \sinh(7.85376z) + 0.12373 \cosh(7.85376z)$

$1/3 \le z \le 2/3$: $\psi = 0.14355 \sin(7.85376z) - 0.14399 \cos(7.85376z) + 0.12516 \sinh(7.85376z) - 0.12530 \cosh(7.85376z)$

$2/3 \le z \le 1$: $\psi = 0.17566 \sin(7.85376z) - 0.17326 \cos(7.85376z) - 2.98414 \sinh(7.85376z) + 2.98428 \cosh(7.85376z)$

Figure 29 is a graph of the acceleration functions along with their SRSS combined accelerations. The CQC method of combining shape functions degenerates to the SRSS method in all of the shape functions encountered so far. The ratio T_j/T_i is so small that there is never any cross-interaction.

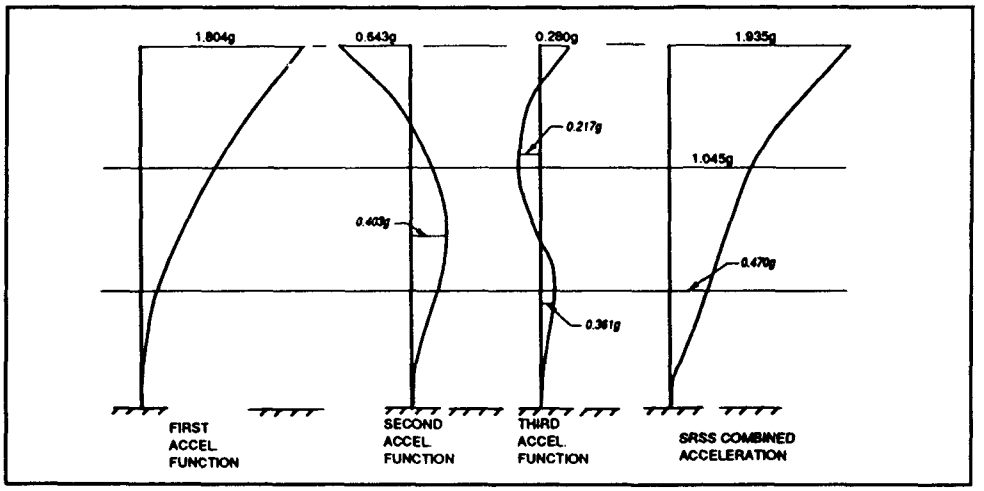

Figure 29. Acceleration functions

The acceleration is now computed each 10 ft along the height of the tower for each of the three acceleration functions. The calculations are made from the foregoing equations, again using the mathematics software. The results of these calculations are shown in the following tabulation.

Elev. From Base ft	Acceleration in g's				Incr. Mass slugs	Incr. Force kips	Cumulative Moment kip-ft
	First Accel. Function	Second Accel. Function	Third Accel. Function	SRSS Combined Accel.			
175	+1.8036	-0.6426	+0.2803	1.935	19,840	1,236[1]	7,000
165	+1.6533	-0.4572	+0.1298	1.720	19,840	1,099	14,000
155	+1.5034	-0.2757	-0.0086	1.528	19,840	976	36,000
145	+1.3547	-0.1038	-0.1210	1.364	19,840	871	69,000
135	+1.2081	+0.0514	-0.1937	1.225	19,840	783	111,000
125	+1.0650	+0.1824	-0.2174	1.102	19,840	704	160,000
115	+0.9266	+0.2823	-0.1975	0.989	25,340	807	217,000
105	+0.7930	+0.3511	-0.1351	0.878	25,340	716	282,000
95	+0.6653	+0.3916	-0.0521	0.774	25,340	632	354,000
85	+0.5452	+0.4029	+0.0372	0.679	25,340	554	432,000
75	+0.4342	+0.3863	+0.1167	0.593	25,340	484	516,000
65	+0.3342	+0.3451	+0.1715	0.510	25,340	416	604,000
55	+0.2466	+0.3030	+0.1923	0.435	32,610	457	697,000
45	+0.1703	+0.2328	+0.1824	0.341	32,610	358	794,000
35	+0.1061	+0.1595	+0.1466	0.241	32,610	253	895,000
25	+0.0557	+0.0911	+0.0947	0.143	32,610	150	999,000
15	+0.0206	+0.0363	+0.0416	0.059	32,610	62	1,104,000
5	+0.0024	+0.0044	+0.0055	0.007	32,610	7	1,209,000
0	0	0	0	0	0	0	1,246,000
						Σ = Base Shear = 10,565 kips	

[1] $1.935g \times \left(\frac{32.2\ ft/sec/sec}{1\ g}\right) \times 19{,}840\ slugs = 1{,}236{,}170\ lbs = 1{,}236\ kips$

The tabulated calculations give the three accelerations that occur at the middle of each 10-ft increment. Each of these accelerations is the maximum spectral acceleration for its particular shape function. The three maximum accelerations at each increment are then combined into a resultant acceleration using SRSS. The force at the middle of each 10-ft increment is the mass of the 10-ft segment times the combined acceleration at that level.

The sum of all the forces so obtained is the base shear. The cantilever moment at any level in the tower can be readily calculated from these forces and is included as the last column in the tabulation. Figure 30 shows a sketch of the results.

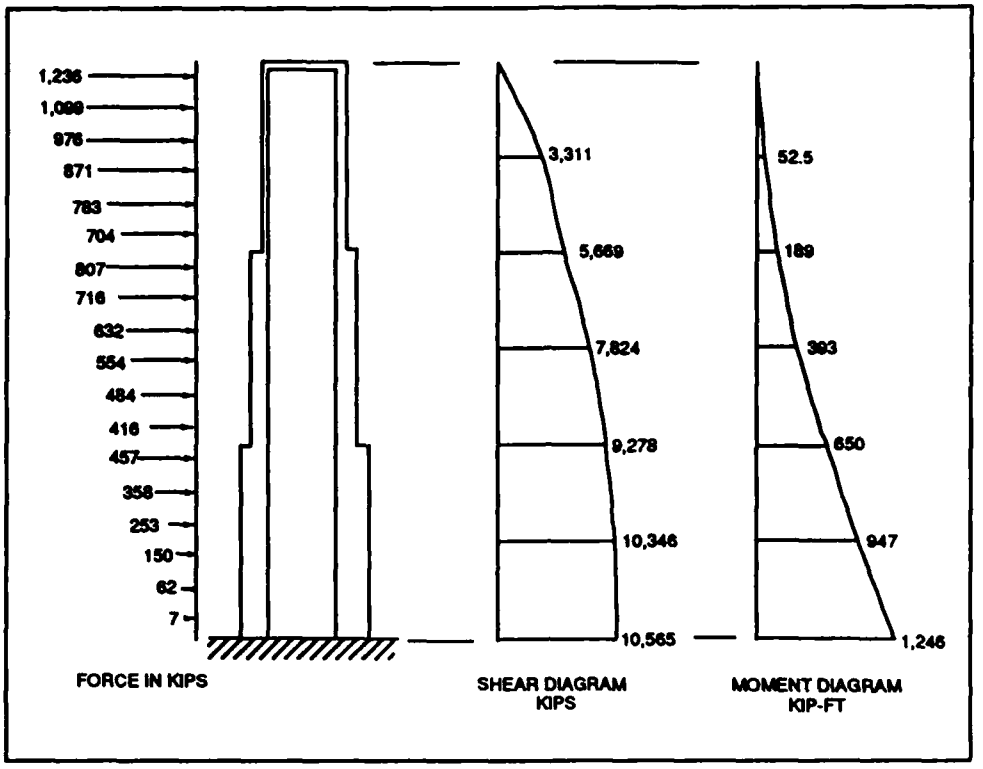

Figure 30. Forces and moments on the step-tapered tower

The remaining calculation to be made is that for the displacement of the tower after it has sustained some cracking from the maximum design earthquake (MDE). The generalized mass m* and the normalization factor L_n are unchanged in this event, but since EI is assumed to be reduced by half, the stiffness k* is reduced by $1/\sqrt{2}$. With these revisions, the Rayleigh constants and the natural frequencies become those listed in the following tabulation.

Rayleigh Constants for MDE Displacements

First Shape function	Second Shape Function	Third Shape Function
$m^* = 90{,}560$ slugs	$m^* = 77{,}800$ slugs	$m^* = 79{,}700$ slugs
$k^* = 25.6 \times 10^6$ lb/ft	$k^* = 602 \times 10^6$ lb/ft	$k^* = 4{,}325 \times 10^6$ lb/ft
$L_n = 151{,}215$ slugs	$L_n = -79{,}480$ slugs	$L_n = 50{,}540$ slugs
$L_n/m^* = 1.670$	$L_n/m^* = -1.022$	$L_n/m^* = 0.634$
$\omega = 16.81$ rad/sec	$\omega = 88.0$ rad/sec	$\omega = 233$ rad/sec
$T = 0.374$ sec	$T = 0.071$ sec	$T = 0.027$ sec

The revised spectral accelerations are found from Figure 17 for the periods just calculated.

First Shape Function, g	Second Shape Function, g	Third Shape Function, g
$S_A = 1.125$	$S_A = 0.770$	$S_A = 0.572$

With these revised values of spectral acceleration, the entire procedure introduced earlier is repeated to find the revised equations for the three acceleration functions. The new accelerations are then recomputed from the revised acceleration functions at 10-ft intervals along the tower. The displacements corresponding to these new accelerations are computed simply by dividing the accelerations by ω^2. The results of such calculations are given in the following tabulation.

Elev. Above Base ft	Displacements Under MDE, ft				Displacements Under OBE, ft
	First Function	Second Function	Third Function	SRSS Combined	Uncracked Section
175	+0.2055	-0.0029	+0.0002	0.2055	0.1455
165	+0.1884	-0.0020	+0.0001	0.1884	0.1334
155	+0.1713	-0.0012	-0.0000	0.1713	0.1213
145	+0.1544	-0.0005	-0.0001	0.1544	0.1097
135	+0.1377	+0.0002	-0.0001	0.1377	0.0975
125	+0.1214	+0.0008	-0.0001	0.1214	0.0859
115	+0.1056	+0.0013	-0.0001	0.1056	0.0747
105	+0.0904	+0.0016	-0.0001	0.0904	0.0640
95	+0.0758	+0.0018	-0.0000	0.0758	0.0537
85	+0.0621	+0.0019	+0.0000	0.0621	0.0440
75	+0.0495	+0.0018	+0.0001	0.0495	0.0350
65	+0.0381	+0.0016	+0.0001	0.0381	0.0270
55	+0.0281	+0.0014	+0.0001	0.0281	0.0200
45	+0.0194	+0.0010	+0.0001	0.0194	0.0137
35	+0.0121	+0.0007	+0.0001	0.0121	0.0086
25	+0.0064	+0.0004	+0.0001	0.0064	0.0044
15	+0.0024	+0.0002	+0.0000	0.0024	0.0017
5	+0.0003	+0.0000	+0.0000	0.0003	0.0002
0	0.0000	0.0000	0.0000	0.0000	0.0000

Note that in the tabulation, the three revised acceleration functions have been divided by ω^2 and have thus become three displacement functions. The three displacements at each elevation are combined using SRSS as shown.

The displacements for this particular tower under the MDE are completely dominated by the first displacement function. For the sake of comparison, the displacements under the OBE were calculated separately and are listed in the last column of the tabulation. The displacements under the OBE were similarly found to be completely dominated by the first displacement function.

4 Multistory Lumped-Mass Systems

Multiple Lumped-Mass Systems

The Rayleigh solution presented in th previous sections applies to systems having a distributed mass. The mass in those systems may be uniformly distributed as shown in Figure 31a; it may vary in steps as shown in Figure 31b; or it may vary continuously as shown in Figure 31c. While the computation of the generalized mass and the generalized stiffness may be quite complex, the use of mathematics software to perform the integrations makes such solutions readily possible in modern practice.

However, not all systems are distributed-mass systems. Rigid frame buildings, for example, have the building masses lumped at each floor, with comparatively slender columns and negligible masses between the floors. Such a structure is shown schematically in Figure 32. When the

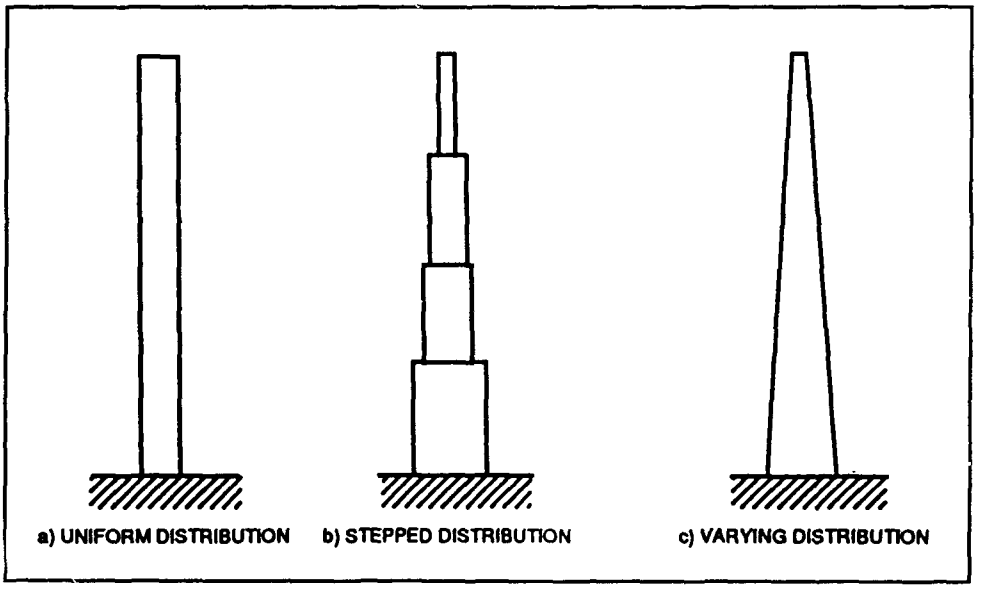

Figure 31. Distributed-mass systems

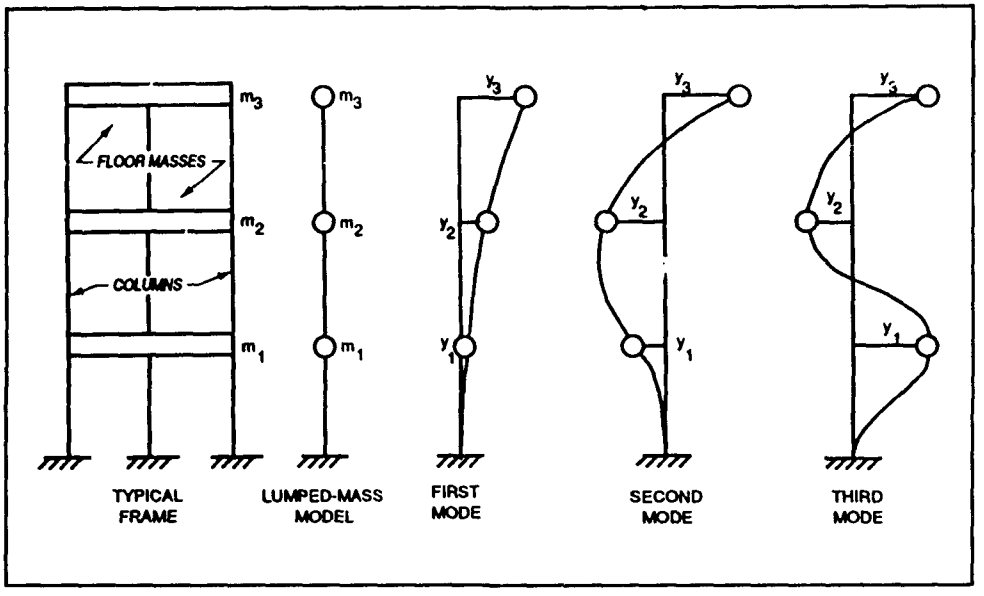

Figure 32. Lumped-mass system

building is deformed laterally, as in an earthquake, all of the restoring force is provided by flexure in the columns.

The multistory lumped-mass system shown in Figure 32 is not a single-degree-of-freedom system. Later discussions will show that this three-mass system will have three degrees of freedom, three natural frequencies, and three deformation shapes. It is classed as a multiple-degree-of-freedom (MDOF) system.

As previously stated, however, the distributed-mass systems treated in the Rayleigh solution were also MDOF systems, but it was possible to examine their dynamic responses by considering only one degree of freedom (one shape function) at a time. Therefore, the multiple lumped-mass systems may also be examined by considering only one degree of freedom (one mode shape) at a time. The shape of the deformation curve in a lumped-mass system is called the *mode shape* and is analogous to the shape function of the Rayleigh solution.

In most existing building systems, the floor beams are much stiffer in flexure than the columns. The structure will therefore deform essentially as if the columns were fixed at each floor and can be analyzed as the close-coupled system shown in Figure 32 with a deformed shape as shown in Figure 33. The structural idealization is designated as close-coupled because only the lateral displacements at each floor level are allowed to influence the distribution of inertial forces at the various floor levels. The current seismic design practice, however, is to provide columns that are stronger than the beams. The stronger column system prevents early development of plastic hinging in the columns. Plastic hinging in columns can lead to collapse of the building. When analyzing strong column/weak

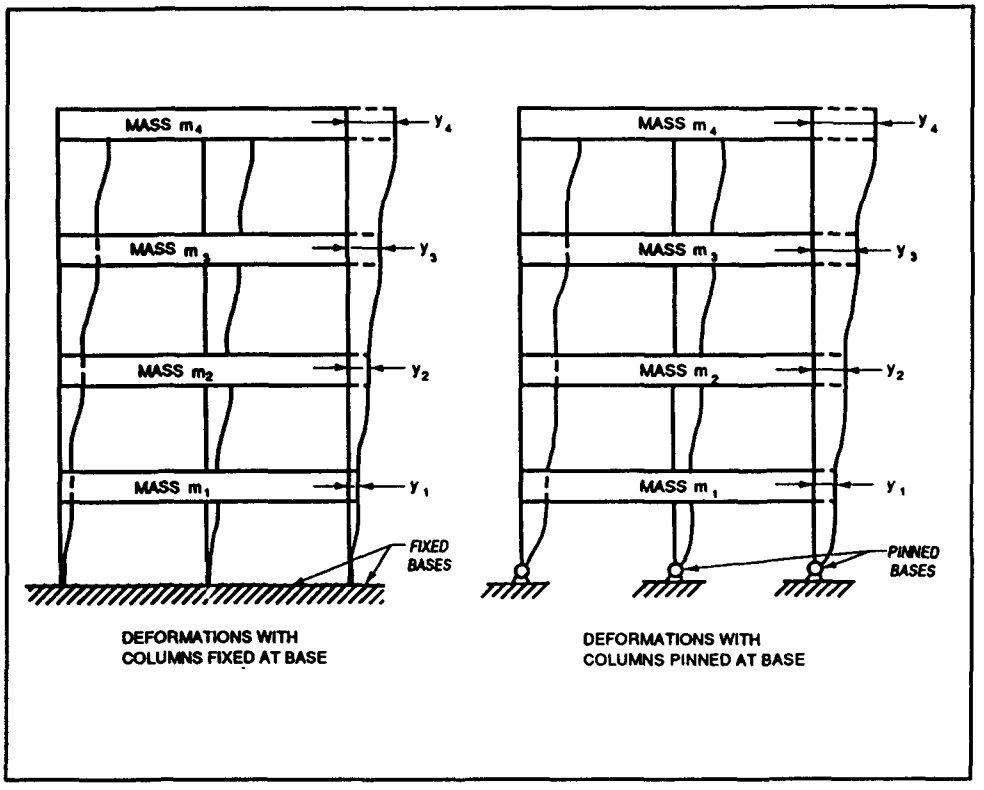

Figure 33. Lateral deformations of a lumped-mass system

beam systems for earthquake ground motions, it is desirable to use a far-coupled analysis procedure. A far-coupled structural idealization is one that includes the effects of beam/column joint rotations on the distribution of inerial forces at the various floor levels. The close-coupled system, however, is used in the following example to analyze lumped-mass building systems for earthquake ground motions.

There are two cases of deformation that occur in the columns shown in Figure 33, that of a beam fixed at both ends and that of a beam fixed at only one end. The two cases are shown in Figure 34 along with the formulas for calculating the deflections produced by a transverse load P applied at the ends. The beams depicted in Figure 34 may look more familiar if they are turned 90 deg counterclockwise.

For the beam loaded at one end only, the spring constant k is computed as the force per unit deflection,

$$k = \frac{P}{\Delta} = \frac{3EI}{L^3} \ lb/in. \tag{60}$$

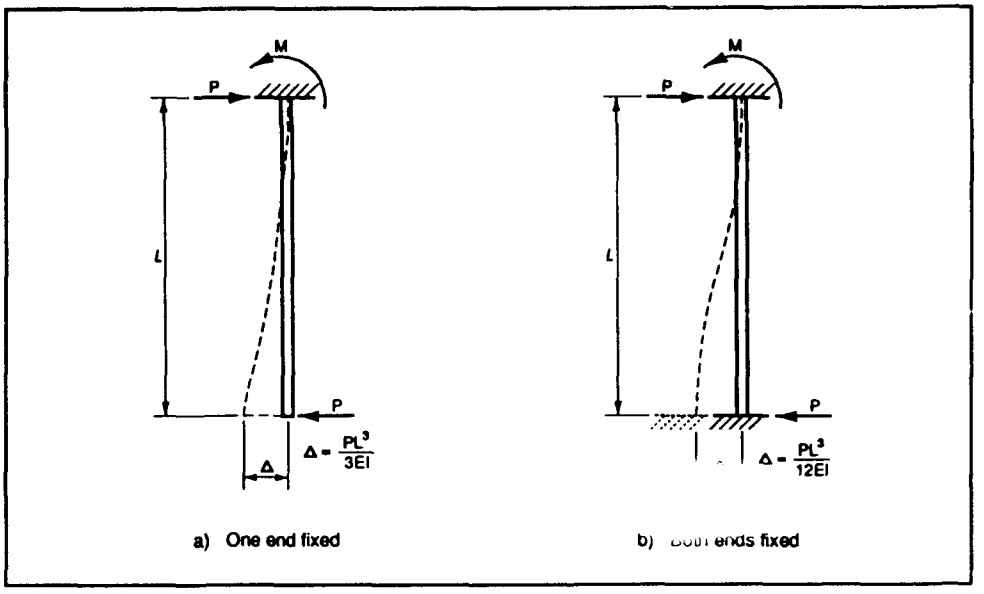

Figure 34. Force-deflection relations in beams

Similarly for the beam fixed at both ends, the spring constant k is computed as

$$k = \frac{P}{\Delta} = \frac{12EI}{L^3} \; lb/in. \tag{61}$$

The spring constant k is commonly called the *stiffness* of a member in flexure, whether a beam or a column. It is the restoring force per unit deflection that will be exerted by a beam or a column having a flexural moment of inertia I.

Modal Analysis of a Lumped-Mass System

Figure 35 shows a frame of a typical MDOF lumped-mass building. The stiffness k shown between two lumped masses is the sum of the stiffnesses of all columns that undergo the same lateral displacement. At each level i, the mass is denoted m_i, the displacement of the mass is denoted y_i, and the forcing function on the mass is denoted $F_i(t)$.

Forces are summed on the undamped free body in Figure 35 as follows:

$$-m\ddot{y}_i - k_{i-1,i}\,(y_i - y_{i-1}) + k_{i,i+1}\,(y_{i+1} - y_i) + F_i(t) = 0 \tag{62}$$

When the forcing function does not exist, the resulting mode shape at any level i will be that of free vibration of an undamped system supported laterally by the masses above and below it. The equation is:

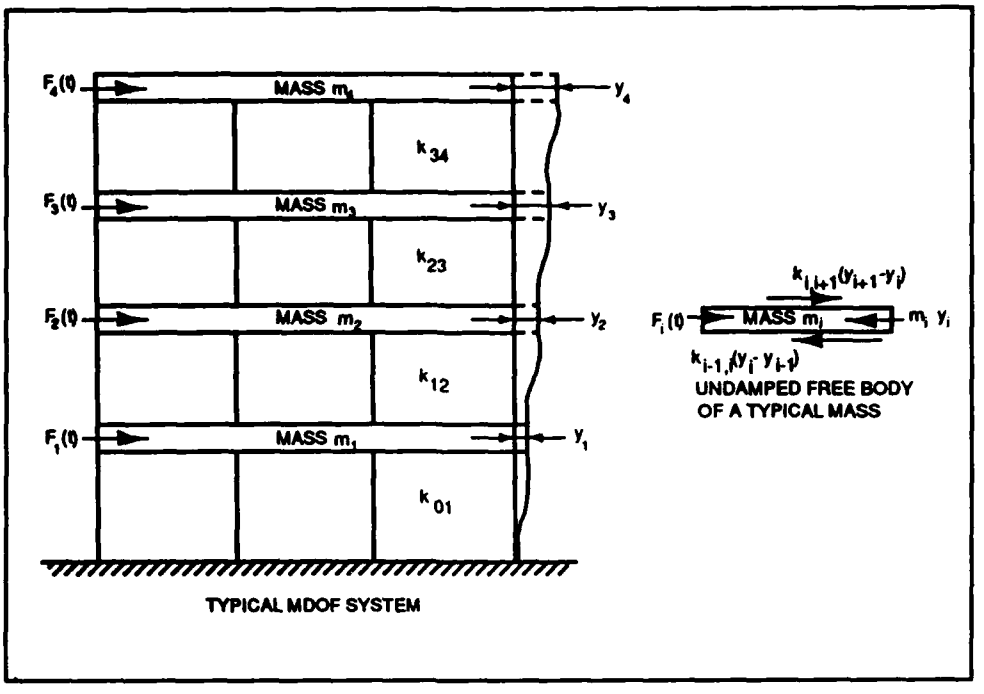

Figure 35. Forces acting on a lumped mass

$$m_i \ddot{y}_i + (\Sigma k_i) y_i = 0 \tag{63}$$

where $\Sigma k_i = k_{i-1,i} + k_{i,i+1}$

The solution to Equation 53 is, as before:

$$y_i = a_i \sin(\omega t - \alpha) \tag{64}$$

where a_i is the maximum amplitude of the displacement y_i. For this value of y_i:

$$\ddot{y}_i = -a_i \omega^2 \sin(\omega t - \alpha) = -\omega^2 y_i \tag{65}$$

These values for y_i and $\ddot{y}_i$ are substituted into Equation 53 to find, with $F_i(t) = 0$:

$$m_i \omega^2 a_i - k_{i-1,i}(a_i - a_{i-1}) + k_{i,i+1}(a_{i+1} - a_i) = 0 \tag{66}$$

In a more easily remembered form, the equation may be written:

$$k_{below} a_{below} + (m_i \omega^2 - \Sigma k_i) a_i + k_{above} a_{above} = 0 \tag{67}$$

where $\Sigma k_i = k_{below} + k_{above}$

Herein, Equation 67 is called the "three-force equation", though it might also be called the "three-amplitude equation." Combined with appropriate software for solving simultaneous equations, its use permits a very simple and direct solution for the natural frequencies and mode shapes of lumped-mass systems. The following example illustrates its use.

Example Solution for a Three-Story Building

Given: Three-story, lumped-mass system as shown below.

Find: 1) Natural periods of oscillation, and
2) Mode shapes corresponding to each period

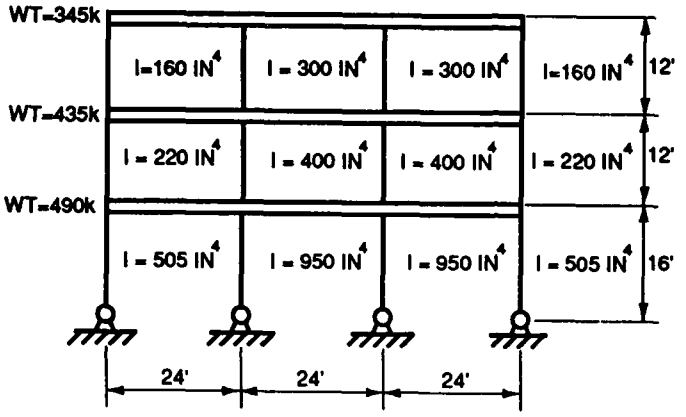

Solution:

Masses and stiffnesses are computed for each level.

$m_1 = 490{,}000/32.2x12 = 1{,}268$ lb/in/sec/sec
$m_2 = 435{,}000/32.2x12 = 1{,}126$ lb/in/sec/sec
$m_3 = 345{,}000/32.2x12 = 893$ lb/in/sec/sec

$$k_{01} = 3EI/L^3 = 3 \times 30 \times 10^6 (505 + 950 + 950 + 505)/(16 \times 12)^3 = 37{,}003 \; lb/in$$

$$k_{12} = 12EI/L^3 = 12 \times 30 \times 10^6 (220 + 400 + 400 + 220)/(12 \times 12)^3 = 149{,}498 \; lb/in$$

$$k_{23} = 12EI/L^3 = 12 \times 30 \times 10^6 (160 + 300 + 300 + 160)/(12 \times 12)^3 = 110{,}918 \; lb/in$$

The computed values are shown on a lumped-mass sketch.

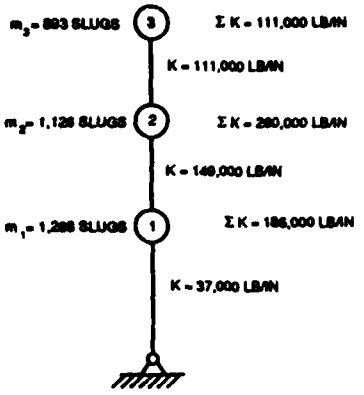

The three-force equations are written for each mass.

Mass No. 1: $0 + (1{,}268\omega^2 - 186{,}000)a_1 + 149{,}000a_2 = 0$

Mass No. 2: $149{,}000a_1 + (1{,}126\omega^2 - 260{,}000)a_2 + 111{,}000a_3 = 0$

Mass No. 3: $111{,}000a_2 + (893\omega^2 - 111{,}000)a_3 + 0 = 0$

The result at this point is three equations in four unknowns, with the variable ω^2 appearing as a coefficient. As in the distributed-mass solution, the lumped-mass solution is an eigenfunction, having one eigenvalue of ω^2 for each equation. The amplitude a_3 at the top level of the building is now set equal to unity, reducing the set of equations to three equations in three unknowns. All of the other amplitudes will then be found as multiples of amplitude a_3, termed *normalized* amplitudes.

The three simultaneous equations are solved using conventional mathematics software. No matter how the set of equations is solved, the solution for ω will always be an n^{th} degree polynomial in ω^2. Thus, there will always be n solutions for the set of n equations. This set of equations will therefore have three solutions, one for each natural frequency ω. The starting value of ω (required by the software) is varied manually until all three solutions are found. (See Appendix A for an alternate solution procedure for ω using matrix methods.)

ω_1 = 3.159 rad/sec	ω_2 = 11.602 rad/sec	ω_3 = 18.903 rad/sec
T = 1.989 sec	T = 0.542 sec	T = 0.332 sec
a_1 = +0.791	a_1 = -0.805	a_1 = +1.046
a_2 = +0.920	a_2 = -0.083	a_2 = -1.875
a_3 = +1.000	a_3 = +1.000	a_3 = +1.000

The three mode shapes are shown in the following sketches:

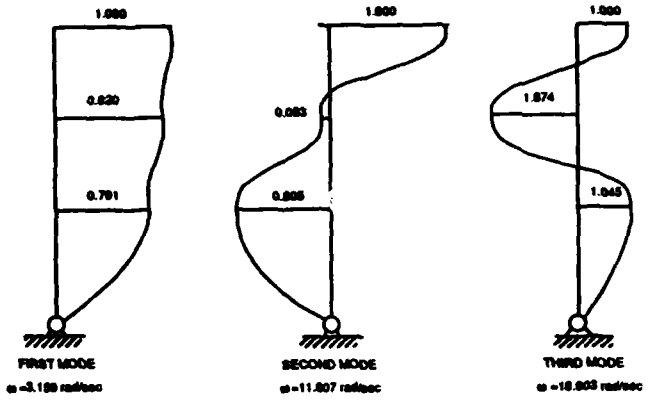

A significant feature revealed by this solution is that the lateral deflection of the first-floor mass is quite high. Almost 80 percent of the total deflection in the first mode shape occurs in the first floor. One cause of this high deflection is that the first-floor columns are longer than the other columns, a common design feature. Further, the first-floor columns are hinged at their bases rather than being fixed, making them much more flexible.

As a point of interest, if the columns at the first level could be fixed at their bases, the building would be much more rigid, and the first-floor deflections would be reduced. The following calculations show why this is so.

For fixed-column bases at ground level, the stiffness factor at the first level becomes:

$$k_{01} = 12EI/L^3 = 148{,}000\ lb/in.$$

This value is used in the three-force equation for mass No.1,

$$\text{Mass No. 1:} \qquad 0 \qquad + (1{,}268\omega^2 - 297{,}000)a_1 + 149{,}000a_2 = 0$$

With this change in the set of three-force equations, the computer solution now yields:

ω_1 = 5.302 rad/sec	ω_2 = 13.358 rad/sec	ω_3 = 19.568 rad/sec
T = 1.185 sec	T = 0.470 sec	T = 0.321 sec
a_1 = +0.441	a_1 = -0.918	a_1 = +1.644
a_2 = +0.774	a_2 = -0.436	a_2 = -2.080
a_3 = +1.000	a_3 = +1.000	a_3 = +1.000

The following sketches show the mode shapes for this more rigid structure.

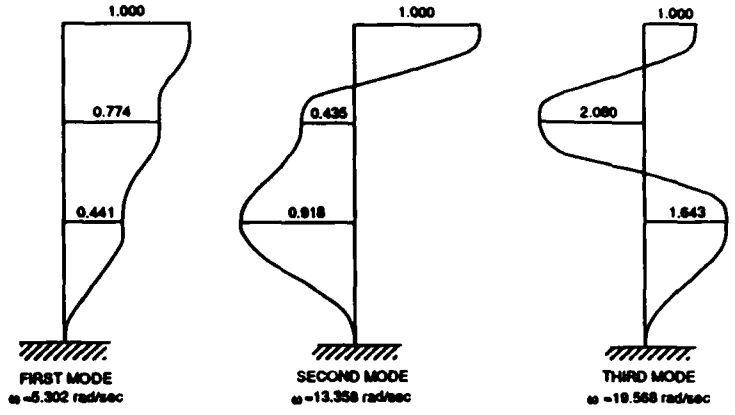

When this second (more rigid) response is compared with the first (more flexible) response, it can be seen that the deflections of the first mass are reduced considerably in the first two modes, with but little change in the third mode deflection. In the first mode, the deflection is reduced to about half of what it was. Assuming that all the upper floors deflect the same amount in both solutions, the total lateral deflection of the building has been reduced approximately 35 percent. The most striking difference, however, is in the two periods. The first-mode period of the more flexible building is almost 67 percent longer than the period of the more rigid building. This period elongation brings the response of the more flexible structure well below the peak values of spectral accelerations given by the ATC 3-06 curves shown in Figure 17. Since a further elongation of the period would reduce the spectral accelerations even more, such an alternative seems worth pursuing.

The results of the foregoing comparisons suggest that the design might be improved by base isolation. For that case, the ground floor would be raised off the foundations at each column by isolators, each having a stiffness of 5,000 lb/in. Such a base isolation system is shown in the following sketch. For best utilization of the base isolation, the ground-floor columns are fixed (rather than hinged) to the ground-floor girders.

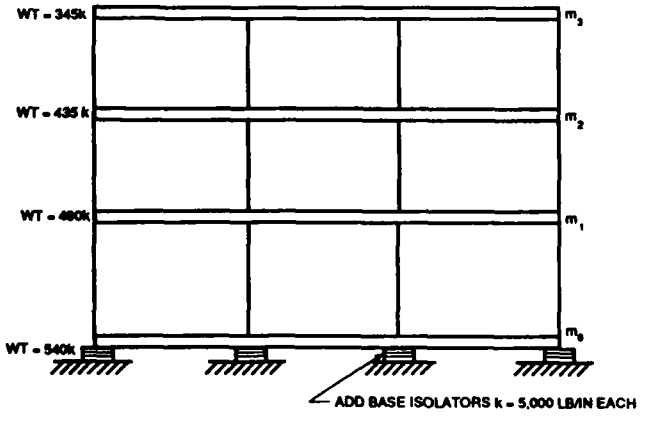

The weight of the ground floor is given as 540,000 lbs. Therefore, the ground floor mass is 1,400 lb/in/sec/sec. The stiffness of each of the four isolators is set at 5,000 lb/in, for a total stiffness at the isolator level of 20,000 lb/in. The three-force equations become:

$$\text{Mass No. 0:} \quad 0 + (1{,}400\omega^2 - 168{,}000)a_0 + 148{,}000a_1 = 0$$

$$\text{Mass No. 1:} \quad 148{,}000a_0 + (1{,}267\omega^2 - 297{,}000)a_1 + 149{,}000a_2 = 0$$

$$\text{Mass No. 2:} \quad 149{,}000a_1 + (1{,}125\omega^2 - 260{,}000)a_2 + 111{,}000a_3 = 0$$

$$\text{Mass No. 3:} \quad 111{,}000a_2 + (892\omega^2 - 111{,}000)a_3 + 0 = 0$$

The solutions of these four equations yield the following results for the three-story lumped-mass building with base isolators.

ω_1 = 1.969 rad/sec	ω_2 = 8.837 rad/sec	ω_3 = 15.038 rad/sec
T = 3.194 sec	T = 0.711 sec	T = 0.418 sec
a_0 = +0.835	a_0 = -0.797	a_0 = +0.771
a_1 = +0.917	a_1 = -0.316	a_1 = -0.774
a_2 = +0.969	a_2 = +0.372	a_2 = -0.819
a_3 = +1.000	a_3 = +1.000	a_3 = +1.000

The following sketches show the shape functions with base isolators, with ground-floor columns fixed at their bases.

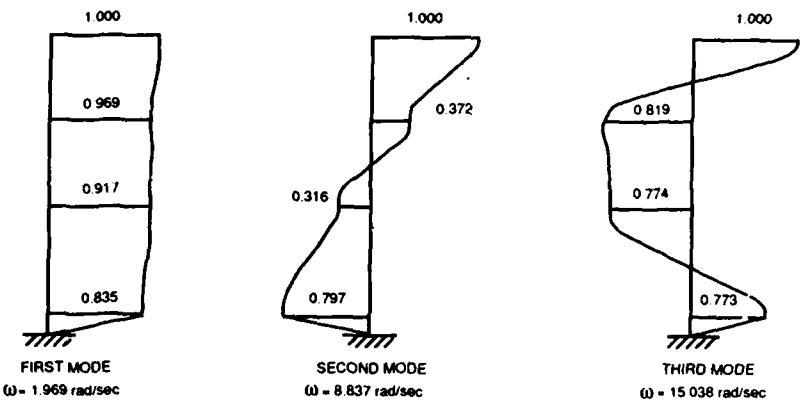

The base isolators take about 80 percent of the total lateral displacement, thereby sharply decreasing the relative displacements in the structure shown in the previous sketch. Further, the isolators significantly increase the period T, bringing the spectral response from the ATC 3-06 curves well down from the peak value.

Thus, it can be concluded that a principal advantage of base isolators is that they lengthen the natural period, thereby reducing the spectral accelerations and consequent inertial forces. One of the disadvantages is that large overall displacements must be accommodated in the building design.

Modal Participation Factor for a Lumped-Mass System

The n-story building shown in Figure 36 is subject to earthquake excitation. The equations of motion for the building are obtained by summing forces on the free body of each lumped mass.

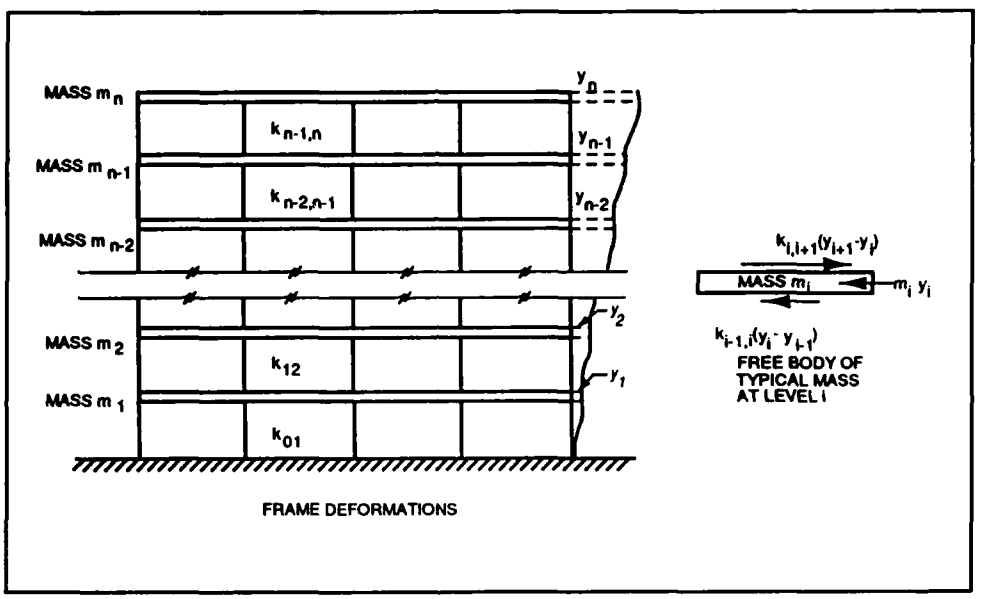

Figure 36. Typical lumped-mass building

The equations of motion are:

$$
\begin{aligned}
&m_1\ddot{y}_1 + k_{01}\,(y_1 - u_g) - k_{12}\,(y_2 - y_1) = 0\\
&m_2\ddot{y}_2 + k_{12}\,(y_2 - y_1) - k_{23}\,(y_3 - y_2) = 0\\
&\qquad\qquad \cdots\cdots\cdots\cdots\\
&\qquad\qquad \cdots\cdots\cdots\cdots\\
&m_{n-1}\ddot{y}_{n-1} + k_{n-2,n-1}\,(y_{n-1} - y_{n-2}) - k_{n-1,n}\,(y_n - y_{n-1}) = 0\\
&m_n\ddot{y}_n + k_{n-1,n}\,(y_n - y_{n-1}) = 0
\end{aligned}
\qquad (68)
$$

As was done with SDOF systems, Equation 6, the coordinate displacement y_i is transformed into the displacement relative to the ground by the transformation:

$$u_i = y_i \quad u_g(t) \tag{69}$$

where u_i is the displacement of the mass m_i relative to the ground.

Substitution into the equations of motion yields:

$$\begin{aligned}
&m_1\ddot{u}_1 + k_{01}u_1 - k_{12}(u_2 - u_1) = -m_1\ddot{u}_g(t)\\
&m_2\ddot{u}_2 + k_{12}(u_2 - u_1) - k_{23}(u_3 - u_2) = -m_2\ddot{u}_g(t)\\
&\qquad\qquad \cdots\cdots\cdots\\
&\qquad\qquad \cdots\cdots\cdots\\
&m_{n-1}\ddot{u}_{n-1} + k_{n-2,n-1}(u_{n-1} - u_{n-2}) - k_{n-1,n}(u_n - u_{n-1}) = -m_{n-1}\ddot{u}_g(t)\\
&m_n\ddot{u}_n + k_{n-1,n}(u_n - u_{n-1}) = -m_n\ddot{u}_g(t)
\end{aligned} \tag{70}$$

The system of equations is uncoupled by transforming the displacements u_i into a set of time functions $z_i(t)$ times the undamped modes, one function z_i for each mode:

$$\begin{aligned}
u_1 &= a_{11}z_1 + a_{12}z_2 + a_{13}z_3 + \cdots\cdots\\
u_2 &= a_{21}z_1 + a_{22}z_2 + a_{23}z_3 + \cdots\cdots\\
&\qquad \cdots\cdots\cdots\\
&\qquad \cdots\cdots\cdots\\
u_n &= a_{n1}z_1 + a_{n2}z_2 + a_{n3}z_3 + \cdots\cdots
\end{aligned} \tag{71}$$

where the second subscript for the amplitude a denotes the mode.

These equations are substituted back into the equations of motion. With some rather complex matrix manipulations (Paz 1991), the final solution for the time functions z_i for each mode are:

$$\begin{aligned}
&\ddot{z}_1 + \omega_1^2 z_1 = \Gamma_1\ddot{u}_g(t)\\
&\ddot{z}_2 + \omega_2^2 z_2 = \Gamma_2\ddot{u}_g(t)\\
&\qquad \cdots\cdots\cdots\\
&\qquad \cdots\cdots\cdots\\
&\ddot{z}_i + \omega_i^2 z_i = \Gamma_i\ddot{u}_g(t)
\end{aligned} \tag{72}$$

The term Γ_i for each mode i is given by:

$$\Gamma_i = -\frac{L_i}{M_i} \tag{73}$$

where $L_i = \sum_{j=1}^{n} m_j\varphi_{ji}$ and $M_i = \sum_{j=1}^{n} m_j\varphi_{ji}^2$

The symbol φ_{ji} denotes the unforced amplitude of the j^{th} mass oscillating in the i^{th} mode.

The right-hand sides of Equation 72 are the same at all levels of the building for any given mode. The factor Γ_i may therefore be viewed as a multiplier on the ground motions $\ddot{u}_g(t)$. Consequently, when ground motions are substituted into the transformation equations, Γ_i also becomes the multiplier on the relative amplitudes a_1, a_2,... a_n. The factor Γ_i is the multiplier that tranforms the relative values of modal displacements into absolute values.

Physically, the multiplier Γ_i indicates the increase or decrease of the ground motion that occurs when the various modes of the time functions z_i are summed, each of which may be positive or negative at any given instant. Γ_i is called the *modal participation factor*, and is directly analogous to the integral forms developed in the Rayleigh method, right-hand side of Equation 52.

The absolute values of displacement, velocity, and acceleration for each mass can now be expressed in terms of the spectral values of S_D, S_V, and S_A for each mode shape i.

$$\begin{aligned} u_{ji\ max} &= \Gamma_i \varphi_{ji} S_{Dj} \\ \dot{u}_{ji\ max} &= \Gamma_i \varphi_{ji} S_{Vj} \\ \ddot{u}_{ji\ max} &= \Gamma_i \varphi_{ji} S_{Aj} \end{aligned} \tag{74}$$

The values of u_j, $\dot{u}_j$, and $\ddot{u}_j$ for the various modes can be combined either by SRSS or by CQC to obtain the final combined values. If SRSS is used, the combined values are given by:

$$\begin{aligned} u_{jmax} &= \sqrt{\sum_{j=1}^{n} \left(\Gamma_i \varphi_{ji} S_{Dj}\right)^2} \\ \dot{u}_{jmax} &= \sqrt{\sum_{j=1}^{n} \left(\Gamma_i \varphi_{ji} S_{Vj}\right)^2} \\ \ddot{u}_{jmax} &= \sqrt{\sum_{j=1}^{n} \left(\Gamma_i \varphi_{ji} S_{Aj}\right)^2} \end{aligned} \tag{75}$$

The force f_j acting at any level j is simply the acceleration at that level times the mass at that level:

$$f_j = m_j \ddot{u}_{jmax} \tag{76}$$

The total shear at the base of the structure V_b is the sum of all these forces f_j over the total height of the structure:

$$V_b = \sum_{j=1}^{n} f_j \tag{77}$$

The overturning moment on a lumped-mass system can be found similarly. The force f_j acting at any level has already been found and defined by Equation 59. The overturning moment M_0 about the base of the structure caused by the forces f_j is the sum of all these forces f_j times their height y_j above the base:

$$M_0 = \sum_{j=1}^{n} f_j y_j \tag{78}$$

Equations 77 and 78 yield the design values for base shear and overturning moment for a lumped-mass system subjected to earthquake loading. From this point onward, the remainder of the analysis is one of ordinary statics. The force at any level y in the structure is given by Equation 76. The shear at any level y is then simply the static sum of forces above that level. The moment at any level y is the static sum of moments due to the forces above that level.

References

Applied Technology Council. (1978). "Tentative provisions for the development of seismic regulations for buildings," ATC 3-06, Palo Alto, CA.

Clough, R. W., Penzien, J. (1993). *Dynamics of structures.* 2nd ed., McGraw-Hill, Inc., New York, 738.

Ebeling, R. M. (1992). "Introduction to the computation of response spectrum for earthquake loading," Technical Report ITL-92-4, U.S. Army Engineer Waterways Experiment Station, Vicksburg, MS.

Goyal, A., and Chopra, A. K. (1989). "Earthquake analysis and response of intake-outlet towers," Report No. UCB/EERC-89/04, University of California, Berkeley, CA.

Headquarters, Departments of the Army, the Navy and the Air Force. (1986). "Seismic design guidelines for essential buildings," Technical Manual TM 5-809-10-1/NAVFAC P-355.1/AFM 88-3, Chap. 13, Sec A, Washington, DC.

Hudson, D. E. (1979). "Reading and interpreting strong motion accelerograms," Earthquake Engineering Research Institute, Berkeley, CA, 112.

Mohraz, B. (1976). "A study of earthquake response spectra for different geological conditions," *Bulletin of the Seismological Society of America* 66(3), 915-935.

Newmark, N. M., and Hall, W. J. (1982). "Earthquake spectra and design," Earthquake Engineering Research Institute, Berkeley, CA, 103.

Paz, M. (1991). *Structural dynamics, theory and computation.* 3rd ed., Van Nostrand Reinhold Company, Inc., New York, 626.

Seed, H. B., Ugas, C., and Lysmer, J. (1976). "Site dependent spectra for earthquake-resistance design," *Bulletin of the Seismological Society of America* 66(1), 221-244.

Seismology Committee. (1990). Recommended lateral force requirements and commentary. Structural Engineers Association of California, Sacramento, CA.

U.S. Army Corps of Engineers. (1994). "Structural analysis and design of intake structures for outlet works," Engineer Manual 1110-2-2401, Washington, DC.

_____. (1994). "Response spectra and seismic analysis for hydraulic structures," Engineer Manual 1110-2-6050, Washington, DC.

_____. (1994). "Earthquake design and analysis for Corps of Engineers projects," Engineer Regulation 1110-2-1806, Washington, DC.

Appendix A
Matrix Solution for a Three-Mass MDOF System

The general equation of motion for a lumped-mass system is given by Equation 66 in the main text. When there is no forcing function, the equation becomes:

$$k_{i-1,i}\,a_{i-1} + \left(m_i\,\omega^2 - \sum k_i\right) a_i + k_{i,i+1}\,a_{i+1} = 0 \qquad \text{(A-1)}$$

In alternate form,

$$k_{i-1,i}\,a_{i-1} - \left(k_{i-1,i} + k_{i,i+1}\right) a_i + k_{i,i+1}\,a_{i+1} = -\omega^2 m_i a_i \qquad \text{(A-2)}$$

When applied to a lumped-mass structure such as that shown in Figure A-1, the set of equations becomes:

$$\begin{aligned}
&0 - (k_{01} + k_{12})\,a_1 + k_{12}a_2 = -\omega^2 m_1 a_1 \\
&k_{12}a_1 - (k_{12} + k_{23})\,a_2 + k_{23}a_3 = -\omega^2 m_2 a_2 \\
&k_{23}a_2 - (k_{23} + k_{34})\,a_3 + k_{34}a_4 = -\omega^2 m_3 a_3 \\
&\bullet\ \bullet\ \bullet\ \bullet\ \bullet\ \bullet\ \bullet\ \bullet\ \bullet\ \bullet\ \bullet\ \bullet\ \bullet \qquad \text{(A-3)} \\
&k_{n-1,n}a_{n-1} - k_{n-1,n}a_n + 0 = -\omega^2 m_n a_n
\end{aligned}$$

In matrix notation, the set of equations is given as:

$$[K - \omega^2 M]\,a = 0 \qquad \text{(A-4)}$$

where **K** is the stiffness matrix, **M** is the mass matrix, and **a** is the amplitude matrix.

The nontrivial solution for Equation A-4 (i.e., for $\mathbf{a} \neq 0$) requires that the determinant of the coefficient matrix must be zero:

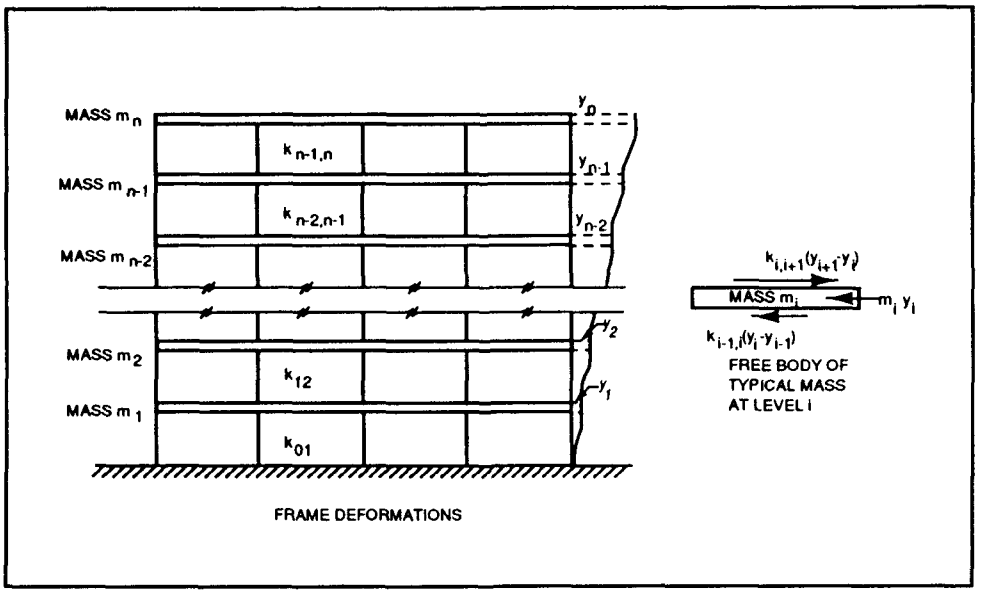

Figure A-1. General lumped-mass building

$$\boldsymbol{K} - \omega^2\boldsymbol{M} = 0 \qquad \text{(A-5)}$$

Equation A-5 defines an *eigenproblem*. The solution of the determinant yields a polynomial equation of the n^{th} degree in ω^2. The n roots of ω^2 are called the *eigenvalues* of the problem. A different set of values for the amplitudes a_1, a_2,...a_n will occur for each eigenvalue.

As an example, the solution will be applied to the three-mass structure solved earlier in Chapter 4 of the main text and shown again in Figure A-2.

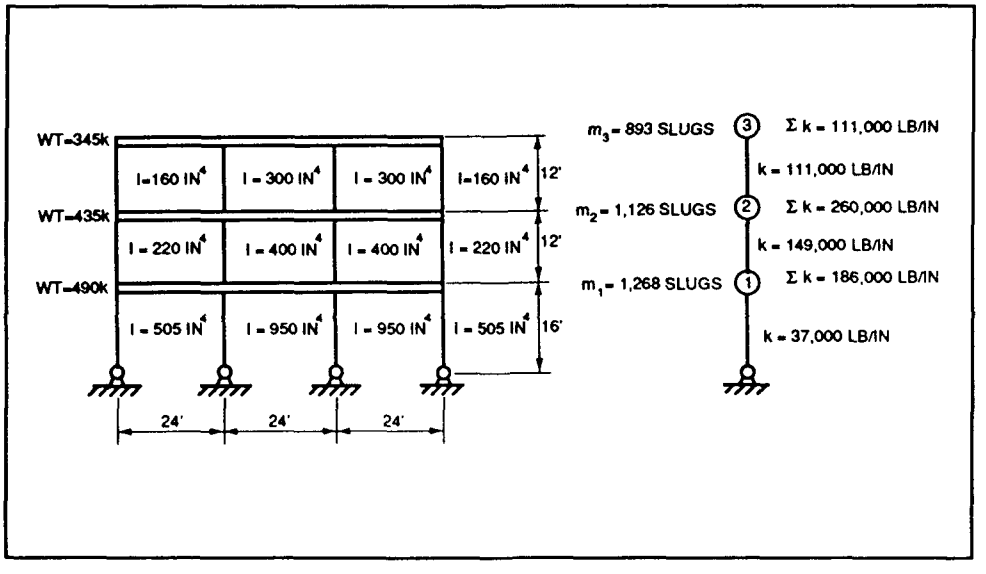

Figure A-2. Three-mass building

The stiffness matrix **K** is given by

$$\boldsymbol{K} = \begin{vmatrix} -186{,}000 & +149{,}000 & + \quad 0 \\ 149{,}000 & -260{,}000 & +111{,}000 \\ 0 & +111{,}000 & -111{,}000 \end{vmatrix} \tag{A-6}$$

The mass matrix **M** is given by

$$\boldsymbol{M} = \begin{vmatrix} -1{,}268 & 0 & 0 \\ 0 & -1{,}126 & 0 \\ 0 & 0 & -893 \end{vmatrix} \tag{A-7}$$

The coefficient matrix is found from these matrices:

$$\boldsymbol{K} - \omega^2\boldsymbol{M} = \begin{vmatrix} -186{,}000 + 1{,}268\omega^2 & +149{,}000 & 0 \\ 149{,}000 & -260{,}000 + 1{,}126\omega^2 & +111{,}000 \\ 0 & +111{,}000 & -111{,}000 + 893\omega^2 \end{vmatrix} \tag{A-8}$$

The determinant is expanded by minors to find:

$$(\omega^2)^3 - 502(\omega^2)^2 + 53{,}090(\omega^2) - 481{,}130 = 0$$

The roots of the cubic equation are found by trial and error:

$$\omega_1 = \pm 3.16 \ \textit{rad/sec} \ ; \ \omega_2 = \pm 11.61 \ \textit{rad/sec} \ ; \ \omega_3 = \pm 18.91 \ \textit{rad/sec}$$

For the first mode, $\omega = 3.16$ rad/sec and the matrix becomes:

$$[\boldsymbol{K} - \omega^2\boldsymbol{M}]\boldsymbol{a} = \begin{bmatrix} -173{,}350 & +149{,}000 & 0 \\ 149{,}000 & -248{,}770 & +111{,}000 \\ 0 & +111{,}000 & -102{,}090 \end{bmatrix} \begin{bmatrix} a_1 \\ a_2 \\ a_3 \end{bmatrix} = 0 \tag{A-9}$$

The set of equations is solved simultaneously to find:

$$a_1 = +0.791 \qquad a_2 = +0.920 \qquad a_3 = +1.000$$

The solution is repeated for the second and third eigenvalues to find the second and third mode shapes. The solutions are summarized below:

$\omega_1 = 3.16$ rad/sec	$\omega_2 = 11.61$ rad/sec	$\omega_3 = 18.91$ rad/sec
$a_1 = +0.791$	$a_1 = -0.805$	$a_1 = +1.045$
$a_2 = +0.920$	$a_2 = -0.083$	$a_2 = -1.874$
$a_3 = +1.000$	$a_3 = +1.000$	$a_3 = +1.000$

These solutions are, of course, identical with those obtained for this problem in the example given in Chapter 4 of the main text.

Appendix B
Notation

a	Peak ground acceleration
A, V, D	Constants in Chapter 2 (see Table 1 for values)
$A, B, C, \& D$	Constants of integration in Chapter 3 (Equation 56)
A'	Maximum pseudoacceleration $\omega^2 D'$ of the SDOF mass
c	Damping constant
d	Peak ground displacement
D'	Maximum relative displacement between ground and mass of an SDOF system having a natural frequency f at whatever point in time it occurs
E	Modulus of elasticity
$EI(x)$	Flexural stiffness
f	Frequency of oscillation
$f_d = c\dot{u}$	Damping force
$f_i = m\ddot{u}$	Inertial force
$f_k = ku$	Restoring force
I	Moment of inertia
k	Stiffness; also, spring constant
K	Stiffness matrix
KE	Kinetic energy

L_n/m^*	Dimensionless multiplier applied to ground acceleration
m	Mass
m_d	Mass per unit length
M	Moment on the cross section
MDE	Maximum design earthquake
OBE	Operational basis earthquake
$p(t)$	Externally applied dynamic force
$p(t)$	Harmonic force
p_{ij}	Cross-function coefficient in which i and j are any two shape functions
p_o	Maximum magnitude of the forcing function
$P(t)$	Time-dependent force of magnitude - $m \cdot \ddot{u}_g(t)$
PE	Stored potential energy
PGA	Peak ground acceleration
PGD	Peak ground displacement
PGV	Peak ground velocity
r	Reference level
SA	Absolute acceleration response spectrum
S_A	Spectral pseudoacceleration
S_D	Spectral maximum displacement
S_V	Spectral maximum pseudovelocity
t	Time
T	Undamped period of vibration
T_D	Damped period of vibration
T_u	T undamped
$u(t)$	Harmonic displacement

$u(x,t)$	Deflection
$\dot{u}(t)$	Velocity
$u_g(t)$	Earthquake ground motion
u_{max}	Maximum displacement
u_o	Initial displacement
u_{st}	Displacement that p_o would produce if applied as a static force
$ut(t)$	Total displacement of mass relative to its at-rest position
$\dot{u}_o$	Initial velocity
$\ddot{u}_t(t)$	Total acceleration
v	Peak ground velocity
V	Shear on the cross section
V'	Maximum pseudovelocity $\omega D'$ of the SDOF mass
β	Constant equal to $c/2m\omega$
β	Fraction of critical damping
Γ_i	Modal participation factor for mode i
θ	Rotation of the cross section about the neutral axis
$\bar{\theta}$	Lagging phase angle between motion of ground and motion of mass
$\upsilon(t)$	Time function
υ_o	Maximum displacement at reference level r
ψ	Displacement function
ψ	Shape function
ω	Natural circular frequency
ω	Undamped angular frequency of vibration
ω_d	Damped circular frequency

ω_D Damped angular frequency of vibration

$\tilde{\omega}$ Forcing frequency

REPORT DOCUMENTATION PAGE

Form Approved
OMB No. 0704-0188

1. AGENCY USE ONLY (Leave blank)	2. REPORT DATE	3. REPORT TYPE AND DATES COVERED
	September 1994	Final report

4. TITLE AND SUBTITLE

Dynamics of Intake Towers and Other MDOF Structures Under Earthquake Loads: A Computer-Aided Approach

5. FUNDING NUMBERS

6. AUTHOR(S)

Samuel E. French, Robert M. Ebeling, Ralph Strom

7. PERFORMING ORGANIZATION NAME(S) AND ADDRESS(ES)

See reverse.

8. PERFORMING ORGANIZATION REPORT NUMBER

Technical Report ITL-94-4

9. SPONSORING/MONITORING AGENCY NAME(S) AND ADDRE.. (ES)

U.S. Army Corps of Engineers
Washington, DC 20314-1000

10. SPONSORING/MONITORING AGENCY REPORT NUMBER

11. SUPPLEMENTARY NOTES

Available from National Technical Information Service, 5285 Port Royal Road, Springfield, VA 22161.

12a. DISTRIBUTION/AVAILABILITY STATEMENT

Approved for public release; distribution is unlimited.

12b. DISTRIBUTION CODE

13. ABSTRACT *(Maximum 200 words)*

This technical report presents an introduction to the basic dynamics of structures subject to earthquake excitation along with a brief summary of the preparation of response spectra for earthquake motions. The report is a primer on structural dynamics, specifically directed toward those engineers who have little or no formal training in dynamics beyond elementary dynamics. The report utilizes the readily understandable classical approach to structural dynamics, with standard computer software being used to evaluate the cumbersome and tedious mathematics inherent in the classical approach.

The report develops first the dynamics of structural systems having a single degree of freedom, then extends the study into systems having multiple degrees of freedom. The report is oriented toward the analysis of distributed-mass intake structures but includes the analysis of lumped-mass systems as well.

This report presents a new application of a traditional procedure for analyzing distributed-mass intake towers by using the Rayleigh method of analysis. This neoclassical approach represents an alternative to the traditional lumped-mass modeling procedure currently used for the dynamic analysis of intake towers.

14. SUBJECT TERMS

Computer-aided engineering
Dynamics of structures
Earthquake engineering
Neoclassical methods
Rayleigh solution
Response spectra

15. NUMBER OF PAGES
95

16. PRICE CODE

17. SECURITY CLASSIFICATION OF REPORT	18. SECURITY CLASSIFICATION OF THIS PAGE	19. SECURITY CLASSIFICATION OF ABSTRACT	20. LIMITATION OF ABSTRACT
UNCLASSIFIED	UNCLASSIFIED		

7. (Concluded).

University of Tennessee at Martin
Martin, TN 38237;
U.S. Army Engineer Waterways Experiment Station
3909 Halls Ferry Road, Vicksburg, MS 39180-6199;
U.S. Army Engineer Division, North Pacific
Portland, OR 97208-2870

WATERWAYS EXPERIMENT STATION REPORTS PUBLISHED UNDER THE COMPUTER-AIDED STRUCTURAL ENGINEERING (CASE) PROJECT

	Title	Date
Technical Report K-78-1	List of Computer Programs for Computer-Aided Structural Engineering	Feb 1978
Instruction Report O-79-2	User's Guide: Computer Program with Interactive Graphics for Analysis of Plane Frame Structures (CFRAME)	Mar 1979
Technical Report K-80-1	Survey of Bridge-Oriented Design Software	Jan 1980
Technical Report K-80-2	Evaluation of Computer Programs for the Design/Analysis of Highway and Railway Bridges	Jan 1980
Instruction Report K-80-1	User's Guide: Computer Program for Design/Review of Curvilinear Conduits/Culverts (CURCON)	Feb 1980
Instruction Report K-80-3	A Three-Dimensional Finite Element Data Edit Program	Mar 1980
Instruction Report K-80-4	A Three-Dimensional Stability Analysis/Design Program (3DSAD)	
	Report 1: General Geometry Module	Jun 1980
	Report 3: General Analysis Module (CGAM)	Jun 1982
	Report 4: Special-Purpose Modules for Dams (CDAMS)	Aug 1983
Instruction Report K-80-6	Basic User's Guide: Computer Program for Design and Analysis of Inverted-T Retaining Walls and Floodwalls (TWDA)	Dec 1980
Instruction Report K-80-7	User's Reference Manual: Computer Program for Design and Analysis of Inverted-T Retaining Walls and Floodwalls (TWDA)	Dec 1980
Technical Report K-80-4	Documentation of Finite Element Analyses	
	Report 1: Longview Outlet Works Conduit	Dec 1980
	Report 2: Anchored Wall Monolith, Bay Springs Lock	Dec 1980
Technical Report K-80-5	Basic Pile Group Behavior	Dec 1980
Instruction Report K-81-2	User's Guide: Computer Program for Design and Analysis of Sheet Pile Walls by Classical Methods (CSHTWAL)	
	Report 1: Computational Processes	Feb 1981
	Report 2: Interactive Graphics Options	Mar 1981
Instruction Report K-81-3	Validation Report: Computer Program for Design and Analysis of Inverted-T Retaining Walls and Floodwalls (TWDA)	Feb 1981
Instruction Report K-81-4	User's Guide: Computer Program for Design and Analysis of Cast-in-Place Tunnel Linings (NEWTUN)	Mar 1981
Instruction Report K-81-6	User's Guide: Computer Program for Optimum Nonlinear Dynamic Design of Reinforced Concrete Slabs Under Blast Loading (CBARCS)	Mar 1981
Instruction Report K-81-7	User's Guide: Computer Program for Design or Investigation of Orthogonal Culverts (CORTCUL)	Mar 1981
Instruction Report K-81-9	User's Guide: Computer Program for Three-Dimensional Analysis of Building Systems (CTABS80)	Aug 1981
Technical Report K-81-2	Theoretical Basis for CTABS80: A Computer Program for Three-Dimensional Analysis of Building Systems	Sep 1981
Instruction Report K-82-6	User's Guide: Computer Program for Analysis of Beam-Column Structures with Nonlinear Supports (CBEAMC)	Jun 1982

(Continued)

WATERWAYS EXPERIMENT STATION REPORTS PUBLISHED UNDER THE COMPUTER-AIDED STRUCTURAL ENGINEERING (CASE) PROJECT

(Continued)

	Title	Date
Instruction Report K-82-7	User's Guide: Computer Program for Bearing Capacity Analysis of Shallow Foundations (CBEAR)	Jun 1982
Instruction Report K-83-1	User's Guide: Computer Program with Interactive Graphics for Analysis of Plane Frame Structures (CFRAME)	Jan 1983
Instruction Report K-83-2	User's Guide: Computer Program for Generation of Engineering Geometry (SKETCH)	Jun 1983
Instruction Report K-83-5	User's Guide: Computer Program to Calculate Shear, Moment, and Thrust (CSMT) from Stress Results of a Two-Dimensional Finite Element Analysis	Jul 1983
Technical Report K-83-1	Basic Pile Group Behavior	Sep 1983
Technical Report K-83-3	Reference Manual: Computer Graphics Program for Generation of Engineering Geometry (SKETCH)	Sep 1983
Technical Report K-83-4	Case Study of Six Major General-Purpose Finite Element Programs	Oct 1983
Instruction Report K-84-2	User's Guide: Computer Program for Optimum Dynamic Design of Nonlinear Metal Plates Under Blast Loading (CSDOOR)	Jan 1984
Instruction Report K-84-7	User's Guide: Computer Program for Determining Induced Stresses and Consolidation Settlements (CSETT)	Aug 1984
Instruction Report K-84-8	Seepage Analysis of Confined Flow Problems by the Method of Fragments (CFRAG)	Sep 1984
Instruction Report K-84-11	User's Guide for Computer Program CGFAG, Concrete General Flexure Analysis with Graphics	Sep 1984
Technical Report K-84-3	Computer-Aided Drafting and Design for Corps Structural Engineers	Oct 1984
Technical Report ATC-86-5	Decision Logic Table Formulation of ACI 318-77, Building Code Requirements for Reinforced Concrete for Automated Constraint Processing, Volumes I and II	Jun 1986
Technical Report ITL-87-2	A Case Committee Study of Finite Element Analysis of Concrete Flat Slabs	Jan 1987
Instruction Report ITL-87-1	User's Guide: Computer Program for Two-Dimensional Analysis of U-Frame Structures (CUFRAM)	Apr 1987
Instruction Report ITL-87-2	User's Guide: For Concrete Strength Investigation and Design (CASTR) in Accordance with ACI 318-83	May 1987
Technical Report ITL-87-6	Finite-Element Method Package for Solving Steady-State Seepage Problems	May 1987
Instruction Report ITL-87-3	User's Guide: A Three Dimensional Stability Analysis/Design Program (3DSAD) Module	Jun 1987
	Report 1: Revision 1: General Geometry	Jun 1987
	Report 2: General Loads Module	Sep 1989
	Report 6: Free-Body Module	Sep 1989

(Continued)

WATERWAYS EXPERIMENT STATION REPORTS PUBLISHED UNDER THE COMPUTER-AIDED STRUCTURAL ENGINEERING (CASE) PROJECT

(Continued)

	Title	Date
Instruction Report ITL-87-4	User's Guide: 2-D Frame Analysis Link Program (LINK2D)	Jun 1987
Technical Report ITL-87-4	Finite Element Studies of a Horizontally Framed Miter Gate Report 1: Initial and Refined Finite Element Models (Phases A, B, and C), Volumes I and II Report 2: Simplified Frame Model (Phase D) Report 3: Alternate Configuration Miter Gate Finite Element Studies–Open Section Report 4: Alternate Configuration Miter Gate Finite Element Studies–Closed Sections Report 5: Alternate Configuration Miter Gate Finite Element Studies–Additional Closed Sections Report 6: Elastic Buckling of Girders in Horizontally Framed Miter Gates Report 7: Application and Summary	Aug 1987
Instruction Report GL-87-1	User's Guide: UTEXAS2 Slope-Stability Package; Volume I, User's Manual	Aug 1987
Instruction Report ITL-87-5	Sliding Stability of Concrete Structures (CSLIDE)	Oct 1987
Instruction Report ITL-87-6	Criteria Specifications for and Validation of a Computer Program for the Design or Investigation of Horizontally Framed Miter Gates (CMITER)	Dec 1987
Technical Report ITL-87-8	Procedure for Static Analysis of Gravity Dams Using the Finite Element Method – Phase 1a	Jan 1988
Instruction Report ITL-88-1	User's Guide: Computer Program for Analysis of Planar Grid Structures (CGRID)	Feb 1988
Technical Report ITL-88-1	Development of Design Formulas for Ribbed Mat Foundations on Expansive Soils	Apr 1988
Technical Report ITL-88-2	User's Guide: Pile Group Graphics Display (CPGG) Post-processor to CPGA Program	Apr 1988
Instruction Report ITL-88-2	User's Guide for Design and Investigation of Horizontally Framed Miter Gates (CMITER)	Jun 1988
Instruction Report ITL-88-4	User's Guide for Revised Computer Program to Calculate Shear, Moment, and Thrust (CSMT)	Sep 1988
Instruction Report GL-87-1	User's Guide: UTEXAS2 Slope-Stability Package; Volume II, Theory	Feb 1989
Technical Report ITL-89-3	User's Guide: Pile Group Analysis (CPGA) Computer Group	Jul 1989
Technical Report ITL-89-4	CBASIN–Structural Design of Saint Anthony Falls Stilling Basins According to Corps of Engineers Criteria for Hydraulic Structures; Computer Program X0098	Aug 1989

(Continued)

WATERWAYS EXPERIMENT STATION REPORTS PUBLISHED UNDER THE COMPUTER-AIDED STRUCTURAL ENGINEERING (CASE) PROJECT

(Continued)

	Title	Date
Technical Report ITL-89-5	CCHAN–Structural Design of Rectangular Channels According to Corps of Engineers Criteria for Hydraulic Structures; Computer Program X0097	Aug 1989
Technical Report ITL-89-6	The Response-Spectrum Dynamic Analysis of Gravity Dams Using the Finite Element Method; Phase II	Aug 1989
Contract Report ITL-89-1	State of the Art on Expert Systems Applications in Design, Construction, and Maintenance of Structures	Sep 1989
Instruction Report ITL-90-1	User's Guide: Computer Program for Design and Analysis of Sheet Pile Walls by Classical Methods (CWALSHT)	Feb 1990
Technical Report ITL-90-3	Investigation and Design of U-Frame Structures Using Program CUFRBC Volume A: Program Criteria and Documentation Volume B: User's Guide for Basins Volume C: User's Guide for Channels	May 1990
Instruction Report ITL-90-6	User's Guide: Computer Program for Two-Dimensional Analysis of U-Frame or W-Frame Structures (CWFRAM)	Sep 1990
Instruction Report ITL-90-2	User's Guide: Pile Group–Concrete Pile Analysis Program (CPGC) Preprocessor to CPGA Program	Jun 1990
Technical Report ITL-91-3	Application of Finite Element, Grid Generation, and Scientific Visualization Techniques to 2-D and 3-D Seepage and Groundwater Modeling	Sep 1990
Instruction Report ITL-91-1	User's Guide: Computer Program for Design and Analysis of Sheet-Pile Walls by Classical Methods (CWALSHT) Including Rowe's Moment Reduction	Oct 1991
Instruction Report ITL-87-2 (Revised)	User's Guide for Concrete Strength Investigation and Design (CASTR) in Accordance with ACI 318-89	Mar 1992
Technical Report ITL-92-2	Finite Element Modeling of Welded Thick Plates for Bonneville Navigation Lock	May 1992
Technical Report ITL-92-4	Introduction to the Computation of Response Spectrum for Earthquake Loading	Jun 1992
Instruction Report ITL-92-3	Concept Design Example, Computer Aided Structural Modeling (CASM) Report 1: Scheme A Report 2: Scheme B Report 3: Scheme C	 Jun 1992 Jun 1992 Jun 1992
Instruction Report ITL-92-4	User's Guide: Computer-Aided Structural Modeling (CASM) - Version 3.00	Apr 1992
Instruction Report ITL-92-5	Tutorial Guide: Computer-Aided Structural Modeling (CASM) - Version 3.00	Apr 1992

(Continued)

WATERWAYS EXPERIMENT STATION REPORTS PUBLISHED UNDER THE COMPUTER-AIDED STRUCTURAL ENGINEERING (CASE) PROJECT

(Concluded)

	Title	Date
Contract Report ITL-92-1	Optimization of Steel Pile Foundations Using Optimality Criteria	Jun 1992
Technical Report ITL-92-7	Refined Stress Analysis of Melvin Price Locks and Dam	Sep 1992
Contract Report ITL-92-2	Knowledge-Based Expert System for Selection and Design of Retaining Structures	Sep 1992
Contract Report ITL-92-3	Evaluation of Thermal and Incremental Construction Effects *for Monoliths* AL-3 and AL-5 of the Melvin Price Locks and Dam	Sep 1992
Instruction Report GL-87-1	User's Guide: UTEXAS3 Slope-Stability Package; Volume IV, User's Manual	Nov 1992
Technical Report ITL-92-11	The Seismic Design of Waterfront Retaining Structures	Nov 1992
Technical Report ITL-92-12	Computer-Aided, Field-Verified Structural Evaluation	
	Report 1: Development of Computer Modeling Techniques for Miter Lock Gates	Nov 1992
	Report 2: Field Test and Analysis Correlation at John Hollis Bankhead Lock and Dam	Dec 1992
	Report 3: Field Test and Analysis Correlation of a Vertically Framed Miter Gate at Emsworth Lock and Dam	Dec 1993
Instruction Report GL-87-1	User's Guide: UTEXAS3 Slope-Stability Package; Volume III, Example Problems	Dec 1992
Technical Report ITL-93-1	Theoretical Manual for Analysis of Arch Dams	Jul 1993
Technical Report ITL-93-2	Steel Structures for Civil Works, General Considerations for Design and Rehabilitation	Aug 1993
Technical Report ITL-93-3	Soil-Structure Interaction Study of Red River Lock and Dam No. 1 Subjected to Sediment Loading	Sep 1993
Instruction Report ITL-93-3	User's Manual—ADAP, Graphics-Based Dam Analysis Program	Aug 1993
Instruction Report ITL-93-4	Load and Resistance Factor Design for Steel Miter Gates	Oct 1993
Technical Report ITL-94-2	User's Guide for the Incremental Construction, Soil-Structure Interaction Program SOILSTRUCT with Far-Field Boundary Elements	Mar 1994
Instruction Report ITL-94-1	Tutorial Guide: Computer-Aided Structural Modeling (CASM); Version 5.00	Apr 1994
Instruction Report ITL-94-2	User's Guide: Computer-Aided Structural Modeling (CASM); Version 5.00	Apr 1994
Technical Report ITL-94-4	Dynamics of Intake Towers and Other MDOF Structures Under Earthquake Loads: A Computer-Aided Approach	Jul 1994